

METABOLOMICS: A Tool to Assess the Physiological Response of Pseudomonas Strains to Environmental Changes

Wordofa, Gossa Garedeu; Schneider, Konstantin; Kristensen, Mette

Publication date:
2017

Document Version
Publisher's PDF, also known as Version of record

[Link back to DTU Orbit](#)

Citation (APA):

Wordofa, G. G., Schneider, K., & Kristensen, M. (2017). METABOLOMICS: A Tool to Assess the Physiological Response of Pseudomonas Strains to Environmental Changes. Kgs. Lyngby: Novo Nordisk Foundation Center for Biosustainability.

DTU Library Technical Information Center of Denmark

General rights

Copyright and moral rights for the publications made accessible in the public portal are retained by the authors and/or other copyright owners and it is a condition of accessing publications that users recognise and abide by the legal requirements associated with these rights.

- Users may download and print one copy of any publication from the public portal for the purpose of private study or research.
- You may not further distribute the material or use it for any profit-making activity or commercial gain
- You may freely distribute the URL identifying the publication in the public portal

If you believe that this document breaches copyright please contact us providing details, and we will remove access to the work immediately and investigate your claim.

METABOLOMICS: A Tool to Assess the Physiological Response of *Pseudomonas* Strains to Environmental Changes

PhD Thesis

Gossa G. Wordofa

Novo Nordisk Center for Biosustainability

Technical University of Denmark

November 2017

PREFACE

This thesis is written as a partial fulfilment of the requirements to obtain a PhD degree at the Technical University of Denmark (DTU). The work was carried out from Decemberr 2014 to November 2017 at the Novo Nordisk Center for Biosustainability (DTU Biosustain). The study was conducted under the supervision of Senior Researcher Konstantin Schneider (DTU Biosustain) and Mette Kristensen (Scientist, DTU Biosustain). The work was funded by the ERA-NET SynBio, Innovations-fonden and the Novo Nordisk Foundation.



Gossa G. Wordofa

Kongens Lyngby, November 2017

ABSTRACT

Qualitative and quantitative analysis of intracellular metabolites is a valuable approach for characterizing and understanding the biochemical processes in cellular systems. Their composition and level represent the molecular phenotype of an organism in response to genetic or environmental conditions. However, analysis and quantification of intracellular metabolites is a challenging task due to their high turnover rates and chemical diversity. Thus, absolute quantification of intracellular metabolite levels requires well-validated sampling techniques that instantaneously stop the metabolic activity of the cell to avoid change in concentration of those metabolites. Furthermore, the analytical tools applied should be capable to cope with the large number of metabolites to be analyzed and the complex matrix in the samples.

The general aim of this thesis was to perform detailed physiological and omics-level characterization of *Pseudomonas taiwanensis* VLB120 and mutant strains constructed for biofuel production. In order to achieve the goal of the study, the first step was the development of a metabolomics work flow which was mainly focused on sample preparation as it is one of the fundamental and important steps in such studies. The developed technique was then applied to quantify the key intracellular metabolites of *P. taiwanensis* VLB120 in order to understand how genetic manipulations and environmental changes influence the level of intracellular metabolites in *Pseudomonas*.

In **Paper I**, new quenching/extraction techniques (cold ethanol, boiling ethanol, cold methanol: acetonitrile: water mix and hot water) were introduced that combines both quenching and extraction procedures in one single step. Their efficiency was evaluated based on energy charge (EC) ratio, recovery of the metabolites and experimental reproducibility. Based on those evaluation criteria, a fast filtration system followed by boiling ethanol quenching/extraction proved to work well for *P. taiwanensis* VLB120 metabolome analysis. Applying this technique, more than 100 intracellular metabolites were quantified for *P. taiwanensis* VLB120. These metabolites are not representative of the entire metabolome of *P. taiwanensis* VLB120, however, they have an essential role in central metabolism. The

main chemical classification of these metabolites includes sugars phosphates, amino acids, organic acids, redox cofactors, nucleosides/bases and nucleotides.

In **Paper II**, the developed metabolomics tools were applied to evaluate the metabolic response of *P. taiwanensis* VLB120 towards biomass hydrolysate derived inhibitors. *P. taiwanensis* responded to these inhibitors in various ways including detoxification, efflux, repair and tolerance to protect themselves against harsh environmental conditions. These lead the strain to go through metabolic rearrangement to generate more cellular energetics (e.g. adenosine triphosphate, ATP) and redox carrier (e.g. nicotinamide adenine dinucleotide phosphate-oxidase, NADPH) in an effort to mitigate the stress imposed by inhibitors.

The data presented in this thesis show that the method developed during this PhD study was successfully applied for multi-targeted analysis of different classes of intracellular metabolites. The best-suited method was further applied to understand and confer tolerance to stress through genetic engineering. The work presented in this PhD thesis has shown to be a valuable addition to the “omics” tools used to reveal key information regarding metabolism and regulation in biological systems.

DANSK RESUME

Kvalitativ og kvantitativ analyse af intracellulære metabolitter er en værdifuld tilgang til karakterisering og forståelse af biokemiske processer i cellen. Deres sammensætning og koncentration repræsenterer den molekulære fænotype af en organisme som reaktion på genetiske eller miljømæssige forhold. Analyse og kvantificering af intracellulære metabolitter er imidlertid en udfordrende opgave på grund af deres hurtige omsætning og kemiske forskellighed. Således kræver absolut kvantificering af intracellulære metabolitniveauer velvaliderede prøveudtagningsteknikker, der øjeblikkeligt stopper cellens metabolismeaktivitet for herved at undgå fortsat ændring i metaboliske produkter. Desuden skal de anvendte analytiske værktøjer være i stand til at analysere det store antal metabolitter og kunne håndtere prøvernes komplekse matrix.

Det generelle formål med denne afhandling har været at udføre en detaljeret fysiologisk og omics-niveau karakterisering af *Pseudomonas taiwanensis* VLB120 og mutantstammer konstrueret til produktion af biobrændstoffer. For at nå målet med undersøgelsen var det første skridt udvikling af metabolomics værktøj, der primært fokuserede på prøveforberedelse, da det er et af de grundlæggende og vigtige trin i metabolomics studier. Den udviklede prøveforberedelsesteknik blev senere anvendt til at kvantificere de vigtigste intracellulære metabolitter af *P. taiwanensis* VLB120 og til at forstå, hvordan genetiske og miljømæssige ændringer påvirker niveauet af intracellulære metabolitter i *Pseudomonas*.

I **Paper I** blev der introduceret en ny quenching/ekstraktionsteknik (kold ethanol, kogende ethanol, kold methanol:acetonitril:vand blanding og varmt vand), der kombinerer både quenching og ekstraktionsprocedurer i et enkelt trin. Effektivitet af de forskellige teknikker blev vurderet baseret på energi-ladnings ratio, genfindning af metabolitterne og eksperimentel reproducerbarhed. Baseret på evalueringskriterierne viste det hurtige filtreringssystem efterfulgt af den kogende ethanol quenching/ekstraktionsteknik at fungere bedst til metabolit analyse af *P. taiwanensis* VLB120. Ved anvendelse af denne teknik blev mere end 100 intracellulære metabolitter kvantificeret fra *P. taiwanensis* VLB120. Disse metabolitter er ikke repræsentative for hele metabolomet af *P. taiwanensis* VLB120, men de har en

afgørende rolle i den central metabolisme. Den vigtigste kemiske klassificering af disse metabolitter omfatter sukkerfosfater, aminosyrer, organiske syrer, redox co-faktorer, nukleosider/baser og nukleotider.

I **Paper II** blev de udviklede metabolomics værktøjer anvendt til at evaluere det metaboliske respons af *P. taiwanensis* VLB120 imod inhibitorer udskilt ved nedbrydning af biomasse hydrolysat. *P. taiwanensis* reagerede på disse inhibitorer på forskellige måder, f.eks. ved at øge afgiftning, udpumpning, reparation og tolerance for at beskytte sig mod de hårde miljøforhold. Disse beskyttelsesmekanismer medfører at stammen producere mere cellulært energi (f.eks. adenosintrifosfat, ATP) og redoxbærer (f.eks. nikotinamid-adenin-dinukleotid-fosfat, NADPH) i et forsøg på at afhjælpe stressresponsen der udløses af inhibitorerne.

Dataene der fremlægges i denne afhandling viser at metoden, der blev udviklet under dette PhD studie, kunne anvendes til succesfuld og målrettet analyse af forskellige klasser af intracellulære metabolitter. Den bedst egnede metode blev yderligere anvendt til at forstå og bekræfte en øget stress tolerance ved anvendelse af genteknologi. Arbejdet i denne PhD afhandling har vist at være en værdifuld tilføjelse til de nuværende "omics" -værktøjer, der bruges til at afklare vigtig information om metabolisme og regulering i biologiske systemer.

ACKNOWLEDGEMENTS

I gratefully acknowledge my supervisors, Senior Researcher Konstantin Schneider and Mette Kristensen (Scientist) for their great scientific guidance, support throughout the project. I also thank my former supervisors, Professor Jochen Förster and Senior Researcher Scott James Harrison, for giving me the opportunity to join the Novo Nordisk Center for Biosustainability as their PhD student.

I would like to thank Senior Researcher Hanne Bjerre Christensen (Head of Analytical Core Facility, DTU Biosustain) for her encouragement and motivation during the whole duration of my study. My thanks also go out to Dr. Andreas Worberg (Pre-Pilot Plant Director, DTU Biosustain) for offering me a new position in his team that allowed me to focus on writing and finishing up my thesis.

Many thanks to Lars Schrübbers, Suresh Sudarsan, Douglas McCloskey, Sailesh Malla, Alexey Dudnik and Nabin Aryal for our many scientific discussions that helped me in completing this work. I also thank my colleagues Tune, Anders, Charlotte, Lars P, Abida, Ling, Yasin, Christoffer, Rene... for their help and support. It has been my pleasure to work with them.

Since my PhD project is part of an international collaboration (SynPath), I would like to take this opportunity to thank all the project partners including iAMB (RWTH Aachen University), LCSB (École Polytechnique Fédérale de Lausanne) and JBEI (University of California) for their cooperation and valued input. I also gratefully acknowledge the financial support provided by the ERA-NET SynBio, Innovations-fonden and the Novo Nordisk Foundation.

Lastly, I deeply thank my friends and family, especially Etsehiwot and Niyana for their understanding and never-ending support during the course of this PhD.

LIST OF PUBLICATIONS

Paper I

Gossa G. Wordofa, Mette Kristensen, Lars Schrübbers, Douglas McCloskey, Jochen Forster, and Konstantin Schneider. Quantifying the Metabolome of *Pseudomonas taiwanensis* VLB120: Evaluation of Hot and Cold Combined Quenching/Extraction Approaches. *ACS: Anal. Chem.* **2017**, 89, 8738–8747. **(Published)**

Paper II

Gossa G. Wordofa, Mette Kristensen, and Konstantin Schneider. Tolerance and Metabolic Response of *Pseudomonas taiwanensis* VLB120 towards Biomass Hydrolysate Derived Inhibitors. *Biotechnology for Biofuels*. **(Submitted)**

Paper III

Investigation of alternative glucose uptake by *Pseudomonas putida* KT2440. (Manuscript in preparation)

Additional work during the PhD study but not included in this thesis

Pseudomonas taiwanensis chassis engineering: Improving redox-cofactor availability for NADH-dependent biocatalysis. (Manuscript in preparation)

TABLE OF CONTENTS

PREFACE	I
ABSTRACT	II
DANSK RESUME	IV
ACKNOWLEDGEMENTS	VI
LIST OF PUBLICATIONS	VII
TABLE OF CONTENTS	VIII
INTRODUCTION AND THESIS OUTLINE	1
I. METABOLOMICS	3
1.1 APPLICATION OF METABOLOMICS	6
1.2 METABOLOMICS APPROACH.....	6
1.3 METABOLOMICS WORKFLOW	7
II. THE GENUS <i>PSEUDOMONAS</i>	18
2.1 <i>PSEUDOMONAS PUTIDA</i>	18
2.2 <i>PSEUDOMONAS TAIWANENSIS</i>	19
III. LIGNOCELLULOSIC BIOMASS	20
3.1 PRODUCTION OF BIOMASS HYDROLYSATE.....	20
3.2 COMPOSITION OF BIOMASS HYDROLYSATE	20
3.3 BIOMASS HYDROLYSATE AS FERMENTATION SUBSTRATE	21
III. AIMS OF THE RESEARCH	23

TABLE OF CONTENTS

4.1	DEVELOPMENT OF METABOLITE PROFILING AND METABOLOMICS TOOLS FOR <i>PSEUDOMONAS TAIWANENSIS</i> VLB120.....	23
4.2	TOLERANCE AND METABOLIC RESPONSE OF <i>PSEUDOMONAS TAIWANENSIS</i> VLB120 TOWARDS INHIBITORY COMPOUNDS DERIVED FROM BIOMASS HYDROLYSATES	23
4.3	TOWARDS ELUCIDATION OF THE METABOLISM OF GLUCOSE IN <i>PSEUDOMONAS PUTIDA</i> KT2440 BY ¹³ C METABOLIC FLUX ANALYSIS.....	24
V.	METHODS.....	25
5.1	CHEMICALS AND STRAINS.....	25
5.2	MEDIA AND CULTIVATIONS	25
5.3	SAMPLING TECHNIQUES	26
5.4	ANALYTICAL TECHNIQUES	26
5.5	DATA PROCESSING	27
VI.	RESULTS AND DISCUSSION.....	28
6.1	METABOLOMICS TOOL DEVELOPMENT	28
6.2	COMPOSITION OF THE CORE <i>P. TAIWANENSIS</i> VLB120 METABOLOME.....	34
6.3	UTILIZATION OF BIOMASS HYDROLYSATE DERIVED SUGARS BY <i>P. TAIWANENSIS</i> VLB120	35
6.4	EFFECT OF INHIBITORS ON <i>P. TAIWANENSIS</i> VLB120 GROWTH	37
6.5	DETOXIFICATION MECHANISM OF INHIBITORS IN <i>P. TAIWANENSIS</i> VLB120	39
6.6	METABOLIC RESPONSE OF <i>P. TAIWANENSIS</i> VLB120 TOWARDS INHIBITORS	40
6.7	INVESTIGATION OF ALTERNATIVE GLUCOSE UPTAKE BY <i>PSEUDOMONAS PUTIDA</i> KT2440.....	45
VII.	CONCLUSION AND FUTURE PROSPECT.....	49

TABLE OF CONTENTS

VIII. REFERENCE LIST 51

LIST OF PUBLICATIONS 73

INTRODUCTION AND THESIS OUTLINE

Concentration of intracellular metabolites play a key role in driving and maintaining the cellular metabolism of living systems. The ability to quantify these intracellular metabolites can help to understand various biological and biochemical processes in the living organisms. The main aim of this thesis was to perform detailed physiological and omics-level characterization of *Pseudomonas taiwanensis* VLB120 and mutant strains constructed for biofuel production. This includes the development of metabolomics tool and the characterization of the metabolic response to genetic and environmental change.

The metabolomics tool development mainly focused on sample preparation as one of the fundamental and most important steps in such studies (**Paper I**). The metabolite profile of *P. taiwanensis* VLB120 was also investigated with the objective of providing a useful reference dataset of absolute intracellular metabolite concentrations. The absolute quantification of metabolites was mainly focused on primary metabolites that occur inside the cell. The main chemical classification of these metabolites include amino acids, sugar phosphates, organic acids, nucleotides and redox cofactors.

The developed technique was subsequently utilized in targeted approaches to quantify the changes in intracellular metabolite concentrations as a response to stress conditions (**Paper II**). The technique was further used to investigate alternative carbon uptake pathways in *Pseudomonas putida* by applying ^{13}C tracer experiments (**Paper III**). Similar, the technique was applied (with minor modification) to determine the redox state of *P. taiwanensis* VLB120 mutant strains constructed for biofuel production (**Paper IV**, not included in this thesis).

The thesis is mainly divided into two sections: i) introduction and ii) results and discussion. The introduction section describes the importance and the relevant terms in the field of metabolomics with a focus on the sample preparation challenges. Recent developments in mass spectrometry and separation techniques used in metabolomics studies are also covered. Furthermore, the general characteristics of *Pseudomonas* with emphasis on *P. putida* KT2440

and *P. taiwanensis* VLB120 strains were discussed. Similarly, the composition and utilization of biomass hydrolysate as a fermentation media was summarized and discussed. The results and discussion section covers the results from method development and the findings from application of the methods for quantification of intracellular metabolites in *P. taiwanensis* VLB120 and *P. putida* KT2440.

I. METABOLOMICS

All living cells undergo characteristic combination of enzymatic reactions to derive energy and building blocks required for growth and maintenance. All these chemical reactions taking place within a cell are known as metabolism, and the chemicals involved in metabolism are considered metabolites. Metabolites provide a direct information of cellular activity and physiological status of the cell at a given condition [1]. As shown in Figure 1, transcriptomics, proteomics and genomics can provide relevant information regarding the genotype but deliver limited information about phenotype. Metabolites are the closest link to phenotype and their concentration levels reflect a snapshot of the physiological status of the cells, which shows how the metabolic profile of a complex biological system is changed in response to stress like adverse factors and environmental alterations [2–8].

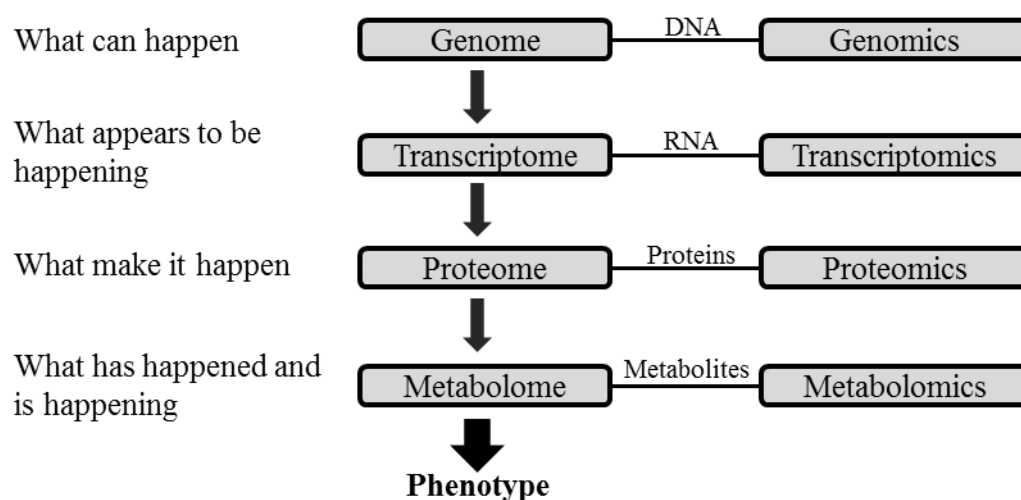


Figure 1. The '-omics' cascade. Modified from Dettmer *et al.* [9].

Metabolites are often classified as either primary or secondary metabolites. Unlike secondary metabolites, primary metabolites are directly involved in survival and existence of the organism as it provides precursors, cofactors and energy for growth [10]. The relevant primary metabolites that are involved in the central carbon metabolism include organic acids, sugar phosphates, nucleotides and redox cofactors (Figure 2) [11]. Thus, understanding how these metabolites interact will be very valuable for the microbial cell factory design process

[12]. The work in this thesis was mainly focused on intracellular metabolites that are involved in different metabolic pathways including the Embden-Meyerhof-Parnas (EMP) pathway of glycolysis, the pentose phosphate pathway (PPP), and the tricarboxylic acid cycle (TCA) (Figure 2).

Analysis and quantification of the metabolome is one of the most exciting and challenging investigations compared to other omics techniques such as genome, proteomics and transcriptome analysis. Each metabolite even from the same pathway is unique and characterized by its individual chemical structure that determines the physical and chemical properties of the metabolite [13]. These chemical and physical diversities of metabolites and the differences in abundance make it difficult to analyze the entire metabolome [14]. Therefore, a number of different approaches need to be established in order to quantify and identify as many metabolites as possible.

Metabolomics is an omics science that characterizes endogenous and exogenous metabolites produced by active and living cells. These analysis provide useful information to speed up the understanding of metabolic behaviors, characteristics of metabolic mechanisms and identification of metabolic biomarkers at a given biological conditions [8].

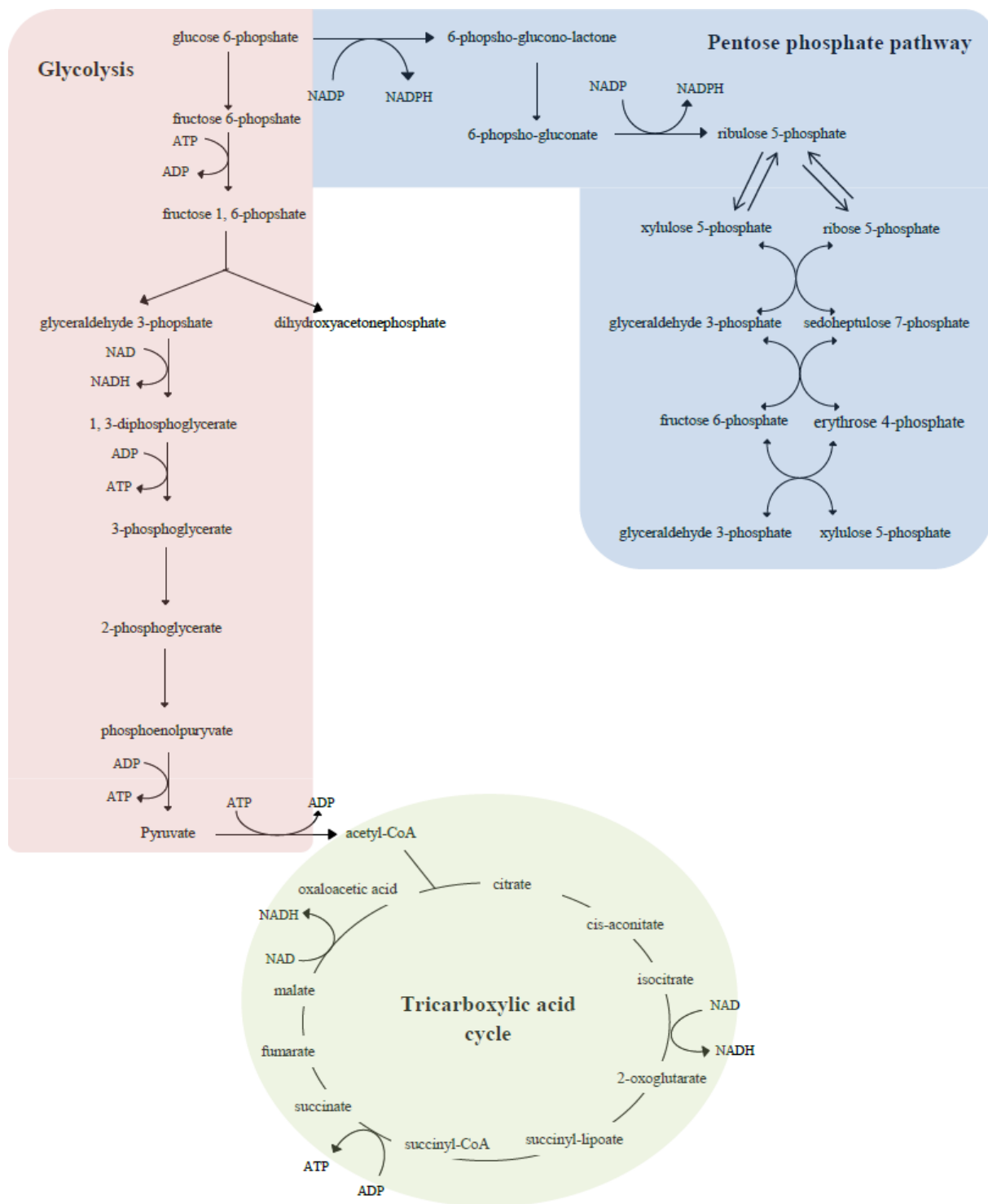


Figure 2. Key metabolites involved in central carbon metabolism. Modified from Magdenoska [10].

1.1 Application of metabolomics

Like other omics technologies such as genomics, transcriptomics and proteomics, metabolomics has been extensively used in various fields, including microbiology, plant, animal, medical and food sciences [15–17]. In microbiology, metabolomics has been used to characterize the interactions of organisms with their environment at the molecular level and [18]. It can also provide a useful information how cells function and changes in specific metabolites [18–20].

1.2 Metabolomics approach

Several approaches exist for the analysis and quantification of metabolites from different samples depending on the aim of the study. These include targeted, semi-targeted and untargeted approaches. These approaches differ in terms of sample preparation, experimental precision, number of metabolites detected, and quantification level [21] as shown in Figure 3.

Features	Targeted Approach	Semi-targeted Approach	Untargeted Approach
Effort of method development	High		Low
Metabolite coverage	Low		High
Quantitative accuracy and reproducibility	High		Low
Complexity of data processing	Low		High

Figure 3. The properties of metabolomics approaches used in metabolite quantification illustrated by four features. Modified from Zhou and Yin [22].

The untargeted metabolomics approach is a non-hypothesis driven technique and widely applied to analyze a large number of metabolites simultaneously and to investigate unknown compounds found in a biological sample [23, 24]. Since there is no single analytical technique to detect all of the metabolites in a biological system, it is necessary to combine

multiple analytical techniques to maximize the number of metabolites detected and increase coverage of the metabolome [25, 26]. Other limitations in untargeted approaches are the identification of metabolites and the necessity for complex bioinformatics tools to interpret the results [27, 28].

The targeted approach is widely used to analyze and quantify relatively small and specific number of known metabolites. The identities of these metabolites are initially established based on the available databases and confirmed by analyzing the pure compounds [29]. Quantification of the metabolites can be done through the use of internal or external standards [28]. Since the targeted approach has a greater selectivity and sensitivity than untargeted methods, it eases successful method development [30]. Furthermore, sample preparation techniques in the targeted approach can be optimized depending on metabolites of interest and downstream analysis [24]. This simplifies the analysis of the data and interpretation of the biological significance. This approach was used in the studies conducted during this PhD thesis.

The semi-targeted approach, also known as “metabolomic profiling”, falls in the middle between the untargeted and the targeted approaches. It focuses on quantifying a set of metabolites whose identity is pre-defined prior to data acquisition. This approach uses a single calibration curve for all metabolites that have similar chemical structure, rather than applying a single calibration curve for each metabolite [21, 26].

1.3 Metabolomics workflow

The metabolomics workflow can vary widely depending on the question that needs to be answered. The common procedures used in a metabolomics study are outlined in Figure 4.

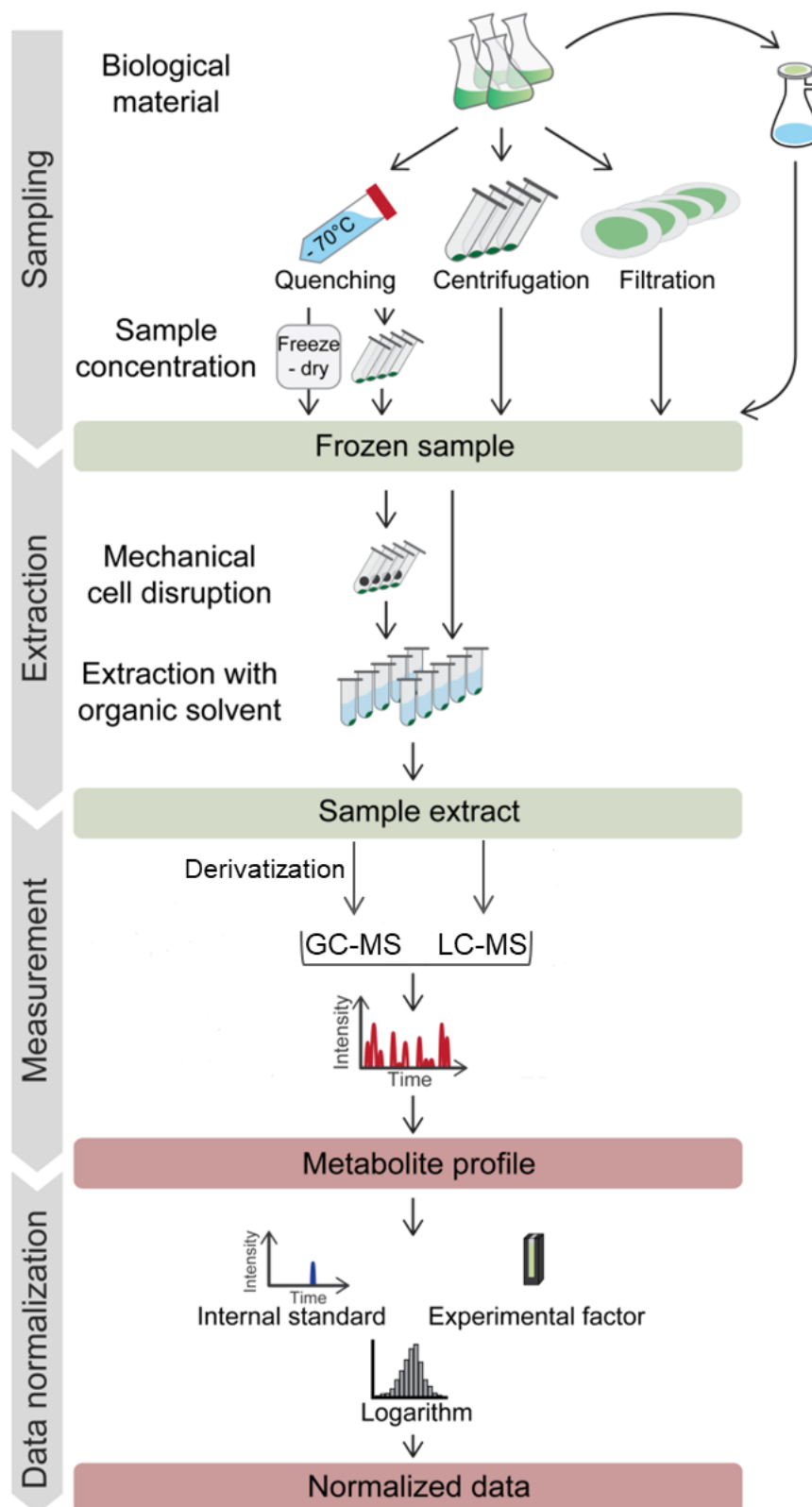


Figure 4. Commonly used metabolomics workflow. Adopted from Daniel *et al.* [31].

1.3.1 Experimental design

Experimental design is the first step in the development, validation and standardization of metabolomics studies [32]. It is one of the important steps to make sure that the samples collected reflect and represent the biology in question. Factors like sample size, quenching and extraction techniques, number of replicates, storage and randomization must be taken into account to minimize erroneous variability based on the selected model organism, types of metabolites and metabolomics approaches [33].

1.3.2 Sample preparation

Sample preparation is one of the most important steps in metabolomics studies as it influences the final composition of the analyzed extract, which can consequently influence the obtained metabolome [31, 34]. This step is generally considered as the limiting step in metabolomics studies since it is an important source of error which affect the quality of the study [13]. Sample preparation is quite different comparing different cellular systems such as e.g. eukaryotic and prokaryotic cells, and even within the eukaryotic kingdom due to the differences in cell structures. Thus, sample preparation techniques in metabolomics studies are organism-dependent or cell-structure-dependent [13] and it is not possible to establish a general method for sample preparation in metabolome analysis.

Prior to performing experiments, there are certain factors that need to be considered when selecting sample preparation techniques for metabolomics studies. These should be: non-selective, simple and rapid with a minimum number of steps, highly reproducible, incorporate metabolism quenching and metabolite extraction steps [35, 36]. The most common steps involved in sample preparation for microbial metabolome analysis include biomass cultivation, sampling, quenching of metabolic activity, metabolite extraction and sample processing [31, 37–39].

1.3.2.1 Biomass cultivation

In microbial metabolomics studies, the common methods for culturing microbial cells include batch liquid culture, continuous culture in a chemostat, and batch culture on a filter support (filter culture). Batch liquid culture is commonly used because of its simplicity and ease, whereas chemostats offer great advantage for controlling culture conditions and reproducibility. Some of the main advantages of filter culture are; the easy sampling possibility and the possibility to manipulate the cellular nutrient environment [40].

1.3.2.2 Sampling techniques

Sampling can be performed using direct quenching, centrifugation or fast filtration [41–47]. Direct quenching is usually achieved by an immediate decrease or increase in temperature or pH by subjecting the sample broth to hot, cold, acidic or alkaline solutions [13, 31]. Initially, this technique was designed to quench the cellular metabolism of eukaryotic cells using organic solvents such as methanol and ethanol at low temperature [48]. Later, the method was used to quench the metabolism of different bacteria including *Escherichia coli* [49], *Lactococcus lactis* [50] and *Lactobacillus bulgaricus* [51] as well as filamentous fungi such as *Penicillium chrysogenum* [52] and *Aspergillus niger* [53]. However, the major drawback of this technique is leakage of intracellular metabolites due to cell lysis or permeabilization of the cellular membrane during the quenching process, thus making an accurate assessment of their intracellular concentrations challenging [50, 54–58]. Direct quenching might be effective if it is used for combined intracellular and extracellular metabolite analysis; however, salts in the media might affect the subsequent analysis.

Centrifugation is another widely used harvesting technique for metabolomics studies. This technique has been used for separate quantification of intracellular and extracellular metabolites. If absolute quantification is needed, it is important that cells retain their integrity during the centrifugation process [31, 59]. Due to the uncontrolled reaction of metabolism and physiological stress during centrifugation, this technique is not that much considered for harvesting cells for absolute intracellular metabolite quantification [31, 60]. As an alternative

sampling technique, fast filtration followed by organic solvent based quenching and extraction techniques were developed [61, 62].

Fast filtration is performed either manually (using syringe) or on a vacuum filtration device to separate the cells from the medium before quenching and thus avoid the leakage of metabolites into the medium [31, 41, 46, 47, 60, 63, 64]. It can be done close to the respective experimental conditions to minimize the disturbing influences of the sampling process [31]. Fast filtration techniques were successfully employed to harvest various organisms including *E.coli* [47], *Pseudomonas taiwanensis* [46] and *Bacillus subtilis* [41] for leakage free intracellular metabolite analysis. The main drawbacks of this method are its limited suitability for high cell densities which affect the filtration speed and sometimes requires additional washing steps to remove residual medium from retained cells [65].

1.3.2.3 Quenching of metabolic activity

Following fast filtration and centrifugation, it is essential to quench cellular metabolism rapidly to minimize the reduction of unwanted variance caused by ongoing metabolic activity during sample preparation [66]. This is usually achieved by a rapid change of sample temperature to either low or high temperatures, or by applying extreme sample pH to either high (alkali, KOH or NaOH) or low (acid, perchloric acid, HCl or trichloroacetic acid) [13, 46]. Due to the high turnover rate of some of the metabolites (mainly primarily metabolites), quenching of metabolism is an extremely important step for metabolome analysis, and it should be seriously considered during establishment/development of the sample preparation method [54, 61, 67–70].

The effectiveness of the applied quenching technique is typically evaluated based on the adenylate energy charge (EC) which describes the relationship between ATP, ADP and AMP [71]. A physiological meaningful range of EC for growing cells is 0.80-0.95 depending on nutritional and environmental conditions has been described [59, 71–74].

$$EC = ([ATP] + 0.5[ADP])/([ATP] + [ADP] + [AMP])$$

Table 1. Summary of commonly used quenching and extraction protocols for intracellular metabolites analyses of different microorganisms

Quenching/Extraction techniques	Temp. °C	Microorganism	References
Quenching techniques			
60% (v/v) Methanol/water	-40	<i>L. lactis</i> , <i>S. cerevisiae</i> , <i>M. ruber</i>	[50, 63, 75–77]
60% (v/v) Methanol/water	-40/-50	<i>E. coli</i> , <i>C. glutamicum</i>	[49, 56, 78, 79]
60% (v/v) Methanol/water	-45	<i>A. niger</i>	[53]
Liquid nitrogen	-150	<i>E. coli</i> , <i>M. ruber</i>	[77, 80, 81]
Extraction techniques			
75% Ethanol	> 80	<i>S. cerevisiae</i> , <i>E. coli</i> , <i>M. ruber</i> , <i>P. chrysogenum</i>	[77, 82, 83]
Perchloric acid	-25, -80	<i>S. cerevisiae</i> , <i>M. ruber</i> , <i>E. coli</i>	[77, 78, 81, 84, 85]
Tris-H ₂ SO ₄ /EDTA	90	<i>E. coli</i>	[80, 81]
Water	100	<i>E. coli</i>	[86]
Potassium hydroxide	Ambient	<i>S. cerevisiae</i> , <i>M. ruber</i> , <i>E. coli</i> , <i>A. niger</i>	[53, 77, 81, 84, 85]
Chloroform	–	<i>M. ruber</i> , <i>L. lactis</i>	[50, 77]

1.3.2.4 Extraction of metabolites

Following quenching, the intracellular metabolites need to be extracted applying an appropriate extraction technique that lyses the cells [59]. This can be achieved by high temperature, extreme pH, organic solvents, mechanical stress, or combinations of thereof [87]. The extraction technique should not only extract metabolites, but also be able to stop all chemical and enzymatic conversions [59, 87]. As summarized in Table 1, different extraction procedures have been developed including cold and hot methanol [52, 88], boiling

ethanol [82], methanol/chloroform mix [48], hot water [86], perchloric acid and potassium hydroxide [80, 85]. However, most of these techniques were designed for specific classes of metabolites and microorganisms. This indicates that there is no universal extraction protocol available for global metabolomics studies. Thus, a proper extraction procedure will need to be developed and tested based on the goals of the experiment.

1.3.3 Analytical tools

Metabolomics studies depend on the latest advances in the field of separation sciences including high-performance liquid chromatography (HPLC) with UV detection [89], Fourier transformed infrared (FT-IR) spectroscopy [90, 91], mass spectrometry (MS) [92, 93] and nuclear magnetic resonance (NMR) (Figure 5) [94–96]. MS and NMR are the techniques utilized most commonly since both are able to detect a wide range of metabolites with relatively high specificity and reproducibility [97–101].

The development of MS techniques has provided a multitude of different platforms for the analysis of metabolites in biological samples. It provides a blend of sensitive, rapid, and selective qualitative and potentially quantitative analyses with the ability to identify metabolites [102]. Mass spectrometry can be used alone or coupled to a chromatographic technique including liquid chromatography (LC), gas chromatography (GC), or capillary electrophoresis (CE). Without chromatographic separation, direct injection mass spectrometry (DIMS) comprises the injection or continuous infusion of sample directly into the mass spectrometer with no prior separation. In this case, the MS serves as a separator and detector of the metabolites. The composition of the sample can be classified by the mass spectrum or mass list (m/z vs. detector response) [76, 103].

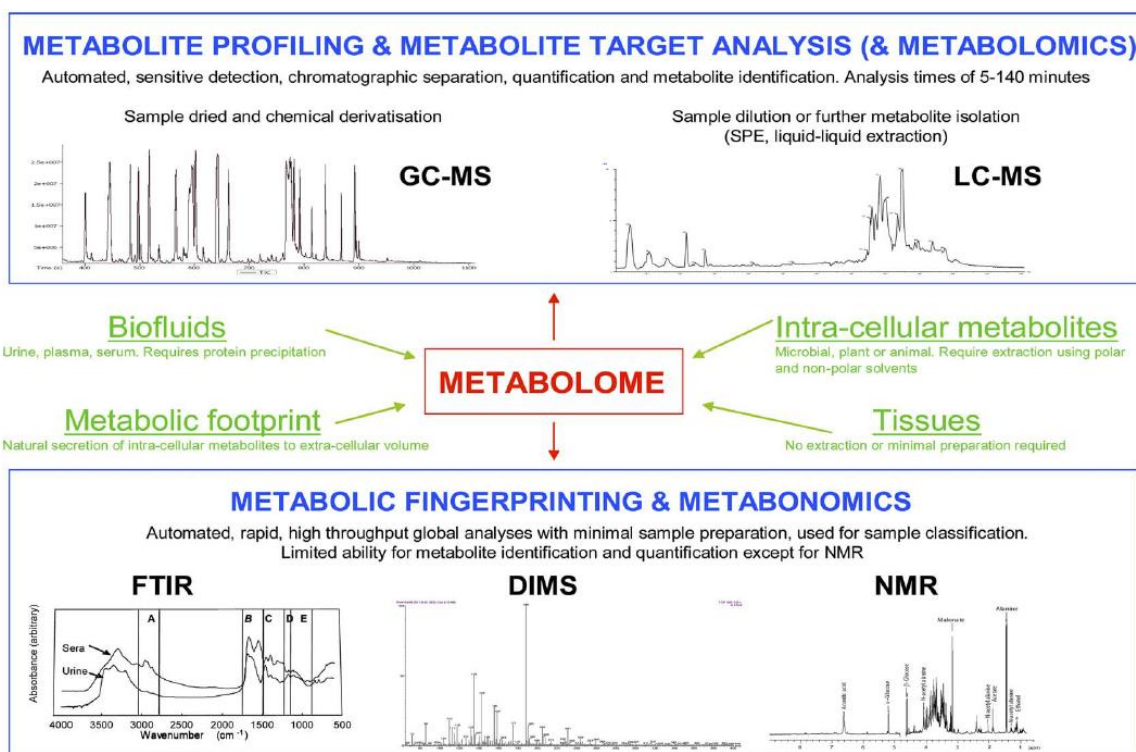


Figure 5. Summary of the analytical platform used in metabolomics studies. Adopted from Warwick *et al.* [102].

GC-MS, LC-MS and CE-MS have become a sensitive and robust analytical method in metabolomics, with specific software packages available for metabolite identification. GC-MS offers very high chromatographic resolution, but sample preparation requires significant effort, as many metabolites require derivatization prior to analysis except volatile compounds [104].

CE is another useful analytical technique that has higher separation efficiency. It is suitable to detect different classes of metabolites (mainly charged metabolites) from complex samples [105]. The major limitations associated with this technique are its relatively poor concentration sensitivity due to low volume of sample injection. The concentration detection limit of CE-MS is relatively too high for metabolomics application. Other drawbacks associated with CE-MS include the interface to combine CE with MS and limitations in electrolyte selections [106]. The use of LC-MS might overcome these drawbacks with extremely high efficiency and peak capacities [107, 108].

Although LC-MS has lower chromatographic resolution compared to GC-MS, this separation technique can be used for large-scale targeted metabolomics analysis [22, 109]. In the studies conducted during this PhD thesis, quantification of intracellular metabolites was performed using ion-pairing LC-MS operating in multiple reaction monitoring (MRM) mode. MRM allows a better identification and quantification of metabolites in a very complex matrices as it provides one or several unique fragment ion that can be easily be monitored [110]. This characteristic makes the MRM sensitive and capable of separating isomeric compounds (e.g. glucose 6-phosphate and fructose 6-phosphate) that are normally difficult to separate. However, utilization of this technique in metabolomics studies has been limited as the specific MRM transitions allow to discriminate some of the metabolites [22].

Currently, there is no single chromatographic technique suitable for all classes of metabolites, which differ in physical and chemical properties [111]. In this PhD study, ion-pairing separation technique was applied, as this technique improves the chromatographic resolution of many polar compounds (e.g. nucleotides, redox cofactors and sugar phosphates) that are generally poorly retained and exhibit poor peak shape by conventional reverse phase chromatographic techniques [112].

NMR is also one of the most commonly applied analytical tools in metabolomics studies. It can identify and quantify almost all kinds of metabolites with the same efficiency, and in this sense, NMR can be considered as a universal detector [113]. NMR is the only detection technique which does not depend on separation of the analytes, and the sample can be recovered for further analysis using GC-MS or LC-MS [114, 115]. In general the NMR technique can provide the most reliable structural and quantitative information of metabolites with simple sample preparation, but the sensitivity is lower compared to MS based assay [37, 116, 117].

1.3.4 Data analysis

Like other "omics" technologies, metabolomics studies produce large and complex datasets. This data may contain various experimental artifacts, which may require complex data processing workflows to remove systematic bias and explore biologically significant

findings. Based on the goals and designs of studies, it may be necessary to use a variety of data analysis techniques or a combination of them in order to obtain an accurate and comprehensive result [118].

Metabolomics data analysis usually consists of feature extraction, compound identification, quantification and statistical analysis [118, 119]. Feature extraction is the process of finding and extracting all relevant spectral and chromatographic information. In order to give biological or scientific meaning to these extracted spectral peaks, compound identification need to be performed using reference database (e.g. METLIN and mzCloud) for searching or spectral library matching [118]. Statistical metabolomics data analysis are most often performed using chemometrics approaches including principal components analysis (PCA) and partial least squares (PLS) regression [120, 121].

PCA is a statistical modeling technique to visualize the variance in a data set and explore the relationship between variables by reducing high dimensional dataset to lower dimensional set of variables while retaining most of the information [122, 123]. This can be done by converting a number of possibly correlated variables into a smaller number of linearly uncorrelated variables, which are known as principal component [124]. The number of principal components equals to the number of variables; however, only a limited number of principal components are interpreted [119]. In most of the cases, the first principal components explain a large proportion of the variation in the data. The data is visualized using scores or loadings plots [122]. The scores plot is mainly used to discover groupings in the data while the loadings plot is mainly used to find variables that are responsible for separating the groups [119]. This technique was applied in **Paper II** as an initial explorative method to investigate the effect of different inhibitors on *P. taiwanensis* VLB120 metabolite levels.

Partial least squares (PLS) regression is another commonly used chemometric technique that can also be considered as a dimension reduction method. It reduces the dimension of the predictors to a smaller set of uncorrelated components by constructing a sequence of linear combinations of the original predictor variables. This technique combines features from

principal component analysis (PCA) and multiple linear regression. Its main goal is to predict a set of dependent variables from a set of independent variables (or predictors) [125, 126]. However, it is not usually appropriate to use this technique for screening out factors that have a negligible effect on the response [125].

II. THE GENUS *PSEUDOMONAS*

Pseudomonas is one of the most thoroughly studied and ecologically important groups of bacteria, containing many validly described species [127–129]. These species isolated from different sources ranging from plants to contaminated soils and water to human clinical samples [128]. Its genus represents a group of Gram-negative bacteria that are non-spore-forming, motile and rod-shaped. The taxonomy of the genus *Pseudomonas* has been revised extensively on the basis of phenotypic features,[130] 16S rRNA gene sequence similarity,[131] *gyrB* and *rpoD* gene sequences [132] and chemotaxonomic data [127, 133–135].

Species from the genus *Pseudomonas* can live under a wide range of environmental conditions due to their metabolic diversity that allow them to resist to adverse conditions caused by abiotic and biotic factors [129, 136]. Furthermore, it utilizes a wide range of compounds as sole carbon and energy source, and are even able to survive in nutrients limited environment [127].

2.1 *Pseudomonas putida*

One of a commonly investigated *Pseudomonas* strain is *P. putida* KT2440, which is a TOL plasmid cured derivative of *P. putida* mt-2 [137, 138]. The sequencing of the *P. putida* KT2440 genome has revealed the genomic repertoire of the organism, provided novel insights into its inherent capabilities and facilitated genetic engineering of the organism [139]. The use of *P. putida* KT2440 is interesting in an industrial setting as the strain has been approved as safe biological strain [136]. The strain is well known for its versatile metabolism, grows fast with simple nutrient requirement and robustness against harsh environmental conditions such as high temperature, extreme pH or the presence of inhibitory compounds [127, 140]. *P. putida* KT2440 is able to grow using a number of other substrates including fatty acids, polyols such as glycerol, amino acids, and aromatic compounds [141].

Although the physiological behavior and biochemical capabilities of *P. putida* KT2440 are well known, there are still unanswered questions regarding glucose uptake/metabolism. It

has been reported that besides the direct import of glucose into the cytoplasm and subsequent phosphorylation to glucose-6-phosphate via glucokinase (glk), an oxidative pathway exists, in which glucose is oxidized in the periplasmic space to gluconate and 2-ketogluconate via glucose dehydrogenase and gluconate 2-dehydrogenase. Both gluconate and 2-ketogluconate can be transported into the cell and catabolized to 6-phosphogluconate, the initial metabolite of the Entner-Doudoroff pathway [142–144]. Even though these growth phases can be observed, the uptake fluxes of glucose, gluconate and 2-ketogluconate cannot be determined directly from their extracellular concentrations profiles. Thus, an alternative carbon uptake pathways by *P. putida* requires further investigation.

2.2 *Pseudomonas taiwanensis*

P. taiwanensis is another species of the genus *Pseudomonas* species that has been isolated from soil at the Institute of Microbiology, University of Stuttgart, Germany [145–148]. It can thrive in diverse habitats and is known for its ability to colonize soil and participate in soil biochemical processes [149, 150]. The potential of *P. taiwanensis* for the degradation and bioremediation of a wide variety of chemicals, including natural and synthetic compounds such as caprolactam [151], naphthalene [152] and toluene [152] has attracted a great research interest [148]. Furthermore, the strain can utilize a wide range of organic molecules as carbon sources including pentose/hexose sugars and aromatic hydrocarbons.[146] Thus, it has a great potential for applications in industrial biotransformation processes [146, 154–157].

In contrast to other *Pseudomonas putida* strains with an industrial potential, like *P. putida* KT2440, *P. putida* DOT-T1E and *P. putida* S12, *Pseudomonas taiwanensis* VLB120 is able to utilize xylose naturally without any genetic modifications [146]. This is the only known *Pseudomonas* strain with the ability to grow on xylose as the sole carbon and energy source [146]. Thus, the physiology of *P. taiwanensis* VLB120 matches the basic requirements for growth on biomass hydrolysate, which is the most abundant renewal resource on earth [146, 158–160]. However, the exposure of this strain to biomass hydrolysate-derived inhibitors has not yet been characterized.

III. LIGNOCELLULOSIC BIOMASS

Lignocellulosic biomass such as agricultural waste and forestry residues is considered to be the most abundant and renewable feedstock available on earth. It consists of cellulose, hemicellulose, lignin and other extractable components that are strongly bonded by non-covalent forces as well as by covalent cross-links [161–163]. Cellulose is the major structural component of lignocellulosic biomass, which is responsible for mechanical strength while, hemicellulose is a macromolecules with repeated polymers of pentoses and hexoses. Lignin mainly contains aromatic alcohols such as coniferyl alcohol, sinapyl alcohol and *p*-coumaryl alcohol [164, 165].

3.1 Production of biomass hydrolysate

The biological conversion of lignocellulosic biomass to value-added chemicals and polymers requires pretreatment and hydrolysis steps in order to break down the biomass structure to form fermentable liquid, known as biomass hydrolysate [166, 167]. These steps alter the structure of lignocellulosic biomass to release free simple sugars and make them more accessible for microorganisms [168, 169]. Several pretreatment techniques including acid/alkali treatment, hydrothermal processing, oxidative methods, ammonia explosion have been successfully employed for generating cost-effective fermentable biomass hydrolysates [170].

3.2 Composition of biomass hydrolysate

The composition of biomass hydrolysate is determined by the biomass type and pretreatment technique used [171]. Most of the biomass hydrolysates consist of simple sugars including hexoses (glucose, mannose, galactose and rhamnose) and pentoses (xylose and arabinose) and other compounds including weak acids, furan and phenolic compounds [172–174]. Pentose sugars result from hydrolysis of cellulose and hemicellulose, while hexoses can be generated from cellulose. Weak acids and phenolic compounds are released from cellulose and hemicellulose during hydrolysis while furans arise from further dehydration of pentose and hexose monomers (Figure 6) [175–179].

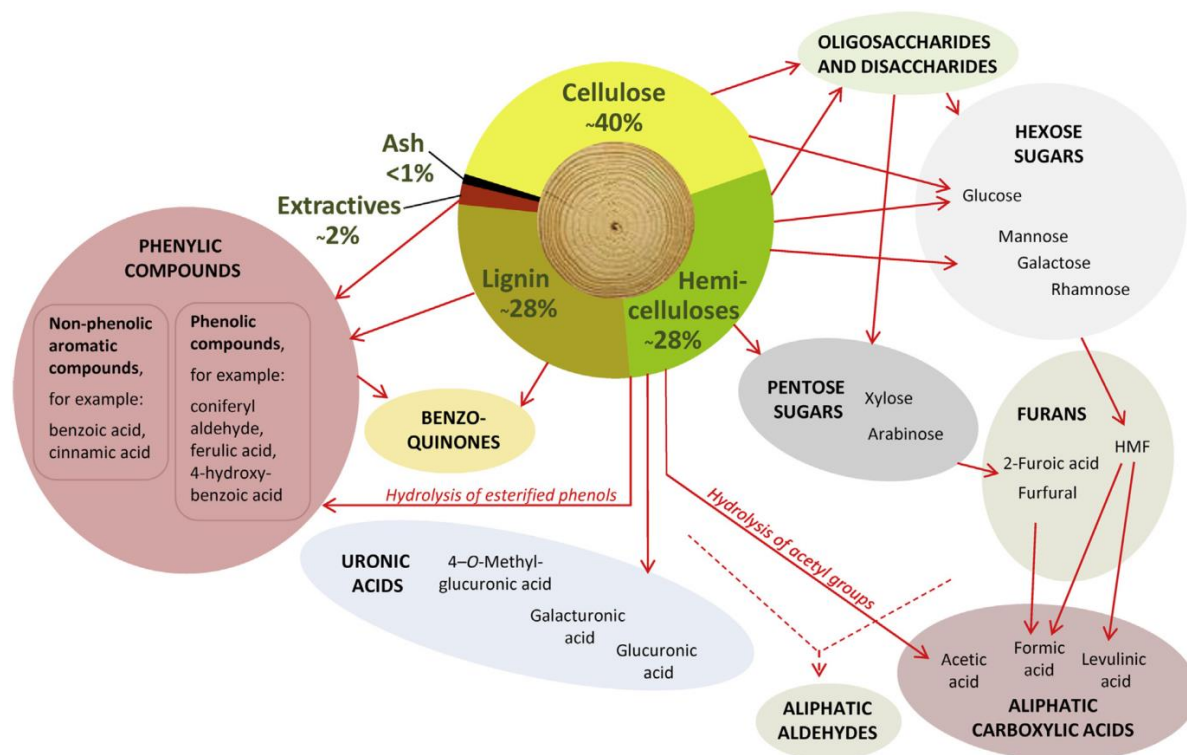


Figure 6. Degradation products from lignocellulosic biomass as a result of pretreatment. Adopted from Leif *et al.* [170].

3.3 Biomass hydrolysate as fermentation substrate

Very few microorganisms can use biomass hydrolysate directly for growth and production due to the presence of other compounds including weak acids, furan and phenolic compounds [172–174, 180]. These compounds influence the growth of microorganisms in various ways, including DNA mutation, membrane disruption, intracellular pH drop, and other cellular targets (Table 2) [170, 179]. To overcome this, various physical and chemical detoxification methods including dilution, adsorption, and precipitation have been developed. However, these techniques have substantial drawbacks in terms of cost, waste generation and loss of fermentable sugars [159]. In order to achieve high fermentation efficiency with no or minimum detoxification steps, one potential solution is the use of microbes that are highly resistant to the effects of those inhibitors in processes where biomass hydrolysates are applied [170, 172, 179]. In **Paper II**, the effects of some of these inhibitors including weak

acids (e.g. acetic acid, formic acid and levulinic acid), furans (e.g. furfural and 5-HMF) and phenolic aldehyde (e.g. vanillin) on the physiology of *P. taiwanensis* VLB120 were evaluated.

Table 2. Lignocellulose derived inhibitors and their toxicity effect [176]

Inhibitors	Mode of action
Weak acids Acetic acid, formic acid, levulinic acid	<ul style="list-style-type: none"> • Decrease cellular pH • Decreases cellular ATP • Inhibit macromolecule biosynthesis • Inhibits DNA synthesis/repair • Inhibits glycolytic enzymes
Furans Furfural, 5-hydroxymethylfurfural (5-HMF)	<ul style="list-style-type: none"> • Damages membranes • Oxidative damage • Damages nucleic acids • Damages proteins • Limits sulfur assimilation • Reduces NADH/NADPH pools • Inhibit enzymes
Phenolics Vanillin, ferulic acid, coumaric acid	<ul style="list-style-type: none"> • Damages membranes • Decrease cellular pH • Decreases cellular ATP • Inhibit translation • Oxidative damage • Denatures proteins • Damage cytoskeleton • DNA mutagenesis • Induces apoptosis

III. AIMS OF THE RESEARCH

4.1 Development of metabolite profiling and metabolomics tools for *Pseudomonas taiwanensis* VLB120

Strain development for the production of chemicals has relied on measurements of product metabolite titers to assess the performance of engineered strains [181]. The broader measurements of the cellular metabolic state are considered as the most significant contributor to assess the metabolic state of the cell, identify bottlenecks in cellular metabolism, and assess toxicity-derived impacts [181]. Nowadays, there are numerous metabolomics tools available to identify and quantify the metabolome of different microorganisms. However, the majority of these tools were designed for specific classes of metabolites and microorganisms. In many cases, these techniques are directly applied without validating them for the given conditions and the investigated organism, which might lead to highly biased results [75]. Thus, the aim of **Paper I** was to conduct a comprehensive examination of different sample preparation techniques with the objective of identifying a better quenching and extraction techniques for *P. taiwanensis* VLB120 metabolome study. Furthermore, this study was also aimed at identifying and quantifying the intracellular metabolite of *P. taiwanensis* VLB120 to provide a reference dataset that can be used for strain design.

4.2 Tolerance and metabolic response of *Pseudomonas taiwanensis* VLB120 towards inhibitory compounds derived from biomass hydrolysates

Bioconversion of lignocellulosic biomass to biofuels and other valuable chemicals involves a pretreatment step that facilitates the conversion of polysaccharides to free sugars. A major drawback of the pretreatment process is the formation of lignocellulose-derived by-products including weak acids, furans and phenolic compounds, which inhibit the downstream enzymatic hydrolysis and microbial growth during fermentation. In order to achieve high fermentation efficiency with no or minimum detoxification steps, one potential solution is to use microbes that are more resistant to those inhibitors for processes where biomass

hydrolysates are applied [172]. Thus, understanding how naturally occurring toxic tolerant microbes, like *Pseudomonas*, respond to inhibitors and identifying which metabolic pathways and metabolites are involved will help to design toxic tolerant microorganisms. Hence, the tolerance and metabolic response of *P. taiwanensis* VLB120 towards biomass hydrolysate derived inhibitory compounds was investigated in **Paper II**.

4.3 Towards elucidation of the metabolism of glucose in *Pseudomonas putida* KT2440 by ¹³C metabolic flux analysis

The bacterium *Pseudomonas putida* is a promising microbial host for industrial processes such as production of fine chemicals due to its high ability to adapt to external influences. This includes the high tolerance towards solvents and the flexible utilization of substrates. Though the physiological behavior and biochemical capabilities of *P. putida* are well known, there are still some open questions regarding glucose uptake.

P. putida growing on medium containing glucose exhibits different growth phases, which differ with respect to biomass yields and growth rates. The first phase is characterized by the conversion of glucose to gluconate as well as to 2-ketogluconate. The second phase starts, when glucose is depleted. In this phase, gluconate is consumed while the 2-ketogluconate concentration further increases. The third phase is characterized by the utilization of 2-ketogluconate [142]. In well resolved growth curves, a reduction of the growth rate is apparent simultaneous with the shift between the growth phases [182]. Even though these growth phases were observed, the uptake fluxes of glucose, gluconate and 2-ketogluconate cannot be determined directly from their extracellular concentrations profiles. Thus, ¹³C tracer experiments were performed to disclose the activity of the alternative carbon uptake pathways, **Paper III**.

V. METHODS

5.1 Chemicals and Strains

All chemicals and reagents used in this study were purchased from Sigma-Aldrich (Chemical Co., USA), unless otherwise specified.

In **Paper I** and **II**, *Pseudomonas taiwanensis* VLB120 strain was employed. This strain is a wild-type phenotype VLB120 strain isolated from soil at the Institute of Microbiology, University of Stuttgart, Germany. The strain was kindly provided by Prof. Dr. Andreas Schmid (Department of Solar Materials, The Helmholtz-Center for Environmental Research, UFZ, Germany). In **Paper III**, *Pseudomonas putida* KT2440 and mutant strains (Δ glk and Δ gcd) were used. *P. putida* KT2440_ Δ glk, and *P. putida* KT2440_ Δ gcd are a mutant deficient in glucokinase and glucodehydrogenase, respectively. In **Paper IV** (not included in this thesis), *Pseudomonas taiwanensis* VLB120 wild type strain and five mutant strains with deleted gene were employed. Prior to the experiments, all the strains were stored in glycerol (30% v/v) at -80 °C.

5.2 Media and Cultivations

The growth medium used in this study contains 2.12 g $\text{NaH}_2\text{PO}_4 \cdot 2\text{H}_2\text{O}$, 2 g $(\text{NH}_4)_2\text{SO}_4$, 10 mg EDTA, 0.1 g $\text{MgCl}_2 \cdot 6\text{H}_2\text{O}$, 2 mg $\text{ZnSO}_4 \cdot 7\text{H}_2\text{O}$, 1 mg $\text{CaCl}_2 \cdot 2\text{H}_2\text{O}$, 5 mg $\text{FeSO}_4 \cdot 7\text{H}_2\text{O}$, 0.2 mg $\text{Na}_2\text{MoO}_4 \cdot 2\text{H}_2\text{O}$, 0.2mg $\text{CuSO}_4 \cdot 5\text{H}_2\text{O}$, 0.4 mg $\text{CoCl}_2 \cdot 6\text{H}_2\text{O}$ and 1 mg $\text{MnCl}_2 \cdot 2\text{H}_2\text{O}$ per liter.

In **Paper I** and **IV**, aerobic cultivations of *P. taiwanensis* VLB120 and mutant strains were carried out from an initial optical density ($\text{OD}_{600\text{nm}}$) of 0.05 in 250 mL shake flask (working volume of 25 mL) at 30 °C with shaking at 250 rpm in minimal medium supplemented with 4.5 g L^{-1} of glucose.

In **Paper II**, cultivations were performed in growth profiler and bioreactor. Growth Profiler 960 (EnzyScreen, Heemstede, The Netherlands) was used to evaluate the threshold

concentration of the inhibitors affecting growth of *P. taiwanensis* VLB120. Once the inhibitors threshold concentration was identified, bioreactor-batch cultivations were performed to characterize the metabolic response of *P. taiwanensis* VLB120 under stress conditions. The experiments were performed in 1.3 L bioreactors (SARTORIOUS®) with 0.5 L working volume. Cultures were inoculated at OD_{600nm} of approx. 0.05 and fermentation temperature, stirrer speed and pH were set at 30 °C, 800 rpm and 7.0, respectively.

In **Paper III**, the main cultures were cultivated in 1.3 L bioreactors (Eppendorf®) with a working volume of 500 mL at 750 rpm and 30 °C. The medium was complemented with 10 mM of U-¹³C glucose and 10 mM of gluconate or 2-ketogluconate, respectively. This experiment was performed at Institute of Applied Microbiology (iAMB), RWTH Aachen University, Germany.

5.3 Sampling techniques

Samples for extracellular and intracellular metabolite analysis were collected by centrifugation and fast filtration, respectively, unless otherwise stated. Samples for extracellular metabolite analysis were spun down at 10 000g for 5 min and stored at -20 °C for further use. In **Paper I, II, and III**, fast filtration followed by combined quenching and extraction methods were employed for intracellular metabolite analysis. In **Paper IV**, direct broth quenching were performed for redox-balance analysis. The samples collected for intracellular analysis were concentrated by evaporating the extraction solvent using a vacuum concentrator (SAVANT, SpeedVac, Thermo Fisher Scientific, San Diego, CA, USA) followed by lyophilization (LABCONCO, FreeZone, Kansas City, MO, USA). All dried extracts were stored -80 °C until analysis or re-suspended in LC-MS grade water for LC-MS analysis.

5.4 Analytical techniques

Extracellular metabolites including sugars, organic acids and aldehydes were measured by high-performance liquid chromatography (HPLC). Aldehydes and their corresponding acid were measured by a Dionex Ultimate 3000 HPLC equipped with a Supelco Discovery HS

F5-3 HPLC column (150 x 2.1 mm x 3 μ m) and a UV detector (260, 277, 304 and 210 nm). Sugars and organic acids were analyzed using a Dionex Ultimate 3000 HPLC with an Aminex® HPX-87X Ion Exclusion (300 x 7.8mm) column (BioRad, Hercules, CA) and RI-150 refractive index detector. In **Paper I**, D- glucose and D-gluconate/D-glucono- δ -lactone test kits (R- BIOPHARM AG, Germany) were also used particularly to measure glucose and gluconate.

Intracellular metabolites were measured on AB SCIEX Qtrap1 5500 mass spectrometer (AB SCIEX, Framingham, MA, USA). The mass spectrometer was run in negative ion mode applying multiple reaction monitoring (MRM) An XSELECT HSS XP (150 mm \times 2.1 mm \times 2.5 μ m) (Waters, Milford, MA, USA) column with ion-pairing technique was used for the chromatography separation.

5.5 Data Processing

Peak integration of HPLC and LC-MS data were performed using Chromeleon™ 7.1.3 (Thermo Scientific™) and Multi-Quant™ 3.0.2 (AB SCIEX™), respectively. For absolute quantification of intracellular metabolites, isotope-ratio based approach was used. This approach was performed using cell extracts grown in fully U ¹³C-labeled glucose as internal standard for quantifying the intracellular metabolites of the strain grown on naturally labeled glucose. The calibration curve was also prepared by adding fully U ¹³C-labeled cell extract as internal standard to the unlabeled calibration standards, and linear calibration curves were obtained by plotting the height ratios between the U ¹³C and ¹²C metabolites against the known concentrations of ¹²C metabolites in the calibration standard. All statistical analyses were performed using R (R Development Core Team [183]) and SIMCA (Umetrics, Umea, Sweden).

VI. RESULTS AND DISCUSSION

In **Paper I**, a combined quenching/extraction technique was introduced. The idea was to stop the biological reactions in a cell and, at the same time, to extract as many metabolites as possible in an unbiased and non-destructive manner. A comprehensive examination of different hot and cold combined quenching/extraction approaches was performed to extract and quantify the metabolome of *P. taiwanensis* VLB120. In of the remaining publications, this developed tool was used to study the physiology of *P. taiwanensis* VLB120 under different stress conditions (**Paper II**). The method was further applied to analyze glucose uptake by *P. putida* KT2440 (**Paper III**) and redox balance of *P. taiwanensis* VLB120 and mutant strains (**Paper IV**, not included in this thesis) with minor modification.

6.1 Metabolomics tool development

The suitability of a pressure driven fast filtration system followed by cold ethanol (CE) extraction, cold methanol/acetonitrile/water mix (MeOH:ACN:H₂O) extraction, boiling ethanol (BE) extraction, and hot water (HW) extraction were assessed for *P. taiwanensis* VLB120 metabolome analysis (Table 3). The suitability of each approach was evaluated based on quenching efficiency, intracellular metabolite concentrations and experimental reproducibility. For all quenching/extraction approaches, cells were obtained from the same shake flask and each quenching/extraction procedure was performed using five independent shake flasks as biological replicates.

Table 3. Combined quenching and extraction techniques for *P. taiwanensis* VLB120 metabolome analysis.

Quenching/ extraction techniques	Concentration in water	Temperature °C
Ethanol	75% (v/v)	– 40 and +70
Methanol:Acetonitrile:Water	40:40:20% (v/v/v)	– 40
Water	100%	+90

6.1.1 Quenching of metabolic activity

Quenching procedures must be able to rapidly stop the cellular metabolism of the cells to retain a valid snapshot of the metabolism at the point of harvest. The quenching effectiveness of cold ethanol, boiling ethanol, cold methanol: acetonitrile: water mix, and hot water techniques was evaluated based on the adenylate energy charge (EC) ratio. As indicated in Figure 7, the tested quenching/extraction techniques have a considerable effect on the proper quenching of cellular metabolism. Organic solvent based quenching/extraction techniques were found to be highly effective in deactivating cellular metabolism since the EC was within a physiological meaningful range. The highest energy charge was obtained for the BE quenching/extraction procedure (0.93 ± 0.01).

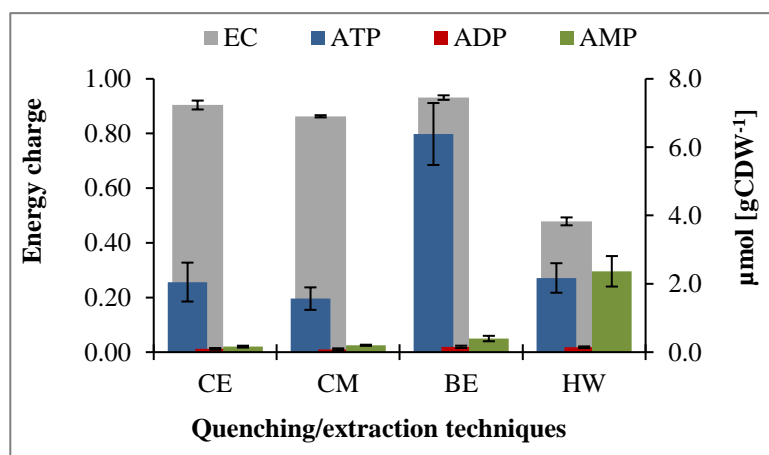


Figure 7 (**Paper I**). Effect of different quenching/ extraction techniques on adenylate concentrations and energy charge ratio of *P. taiwanensis* VLB120 grown in minimal media supplemented with 4.5 g L^{-1} of glucose. CE: cold ethanol/water (75:25, v/v); CM: cold methanol/acetonitrile/water (40:40:20, v/v/v); BE: boiling ethanol/water (75:25, v/v); HW: hot water. The error bars indicate standard deviations from five biological replicates.

In contrast to other organic solvent based quenching/extraction techniques such as CE, CM and BE, HW-based quenching/extraction resulted in a low EC (0.48 ± 0.014) which implies that this method was not efficient in deactivating cellular metabolism.

6.1.2 Extraction of metabolites

The efficacy of the quenching/extraction approaches was also evaluated based on the intracellular concentrations of key metabolites including sugar phosphates, organic acids, amino acids, nucleotides, redox cofactors and nucleosides/bases. The hot extraction methods appeared to extract high quantities of metabolites (molar basis) compared to the cold extraction techniques. The statistically most significant changes were found in the metabolite classes comprising redox-cofactors, nucleotides, nucleosides and bases as shown in Figure 7.

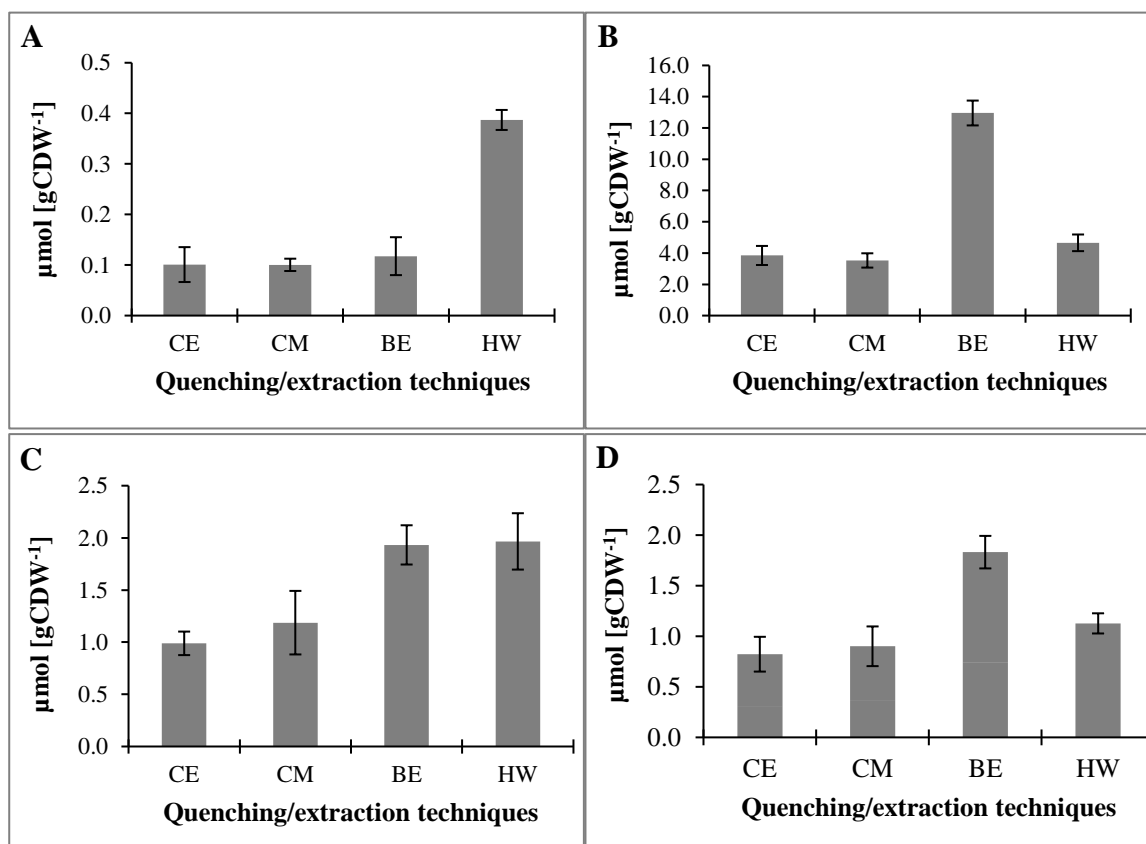


Figure 8. Classes of metabolites that separate the tested quenching/extraction techniques. (A) nucleosides/bases (adenine, adenosine, cytidine, guanine, guanosine and uracil), (B) nucleotide triphosphates (UTP, ITP, dATP, GTP, CTP and ATP), (C) NAD(P)(H) (NAD, NADH, NADP and NADPH) and (D) co-enzymes (acetyl CoA and co-enzyme A). Abbreviations: CE, cold ethanol/water (75/25, v/v); CM, cold methanol/acetonitrile/water (40:40:20, v/v); BE, boiling ethanol/water (75/25, v/v) and HW, hot water. The error bars indicate standard deviations from five biological replicates.

Some of these metabolites were changed more than threefold between hot and cold quenching/extraction techniques. This suggests that temperature is an important factor in the metabolite extraction for *P.taiwanensis* VLB120. This could be related to the strain's intrinsic solvent resistance compared to other less resistant organisms such as *E. coli* where cold quenching/extraction methods turned out to be favorable [47, 184, 185].

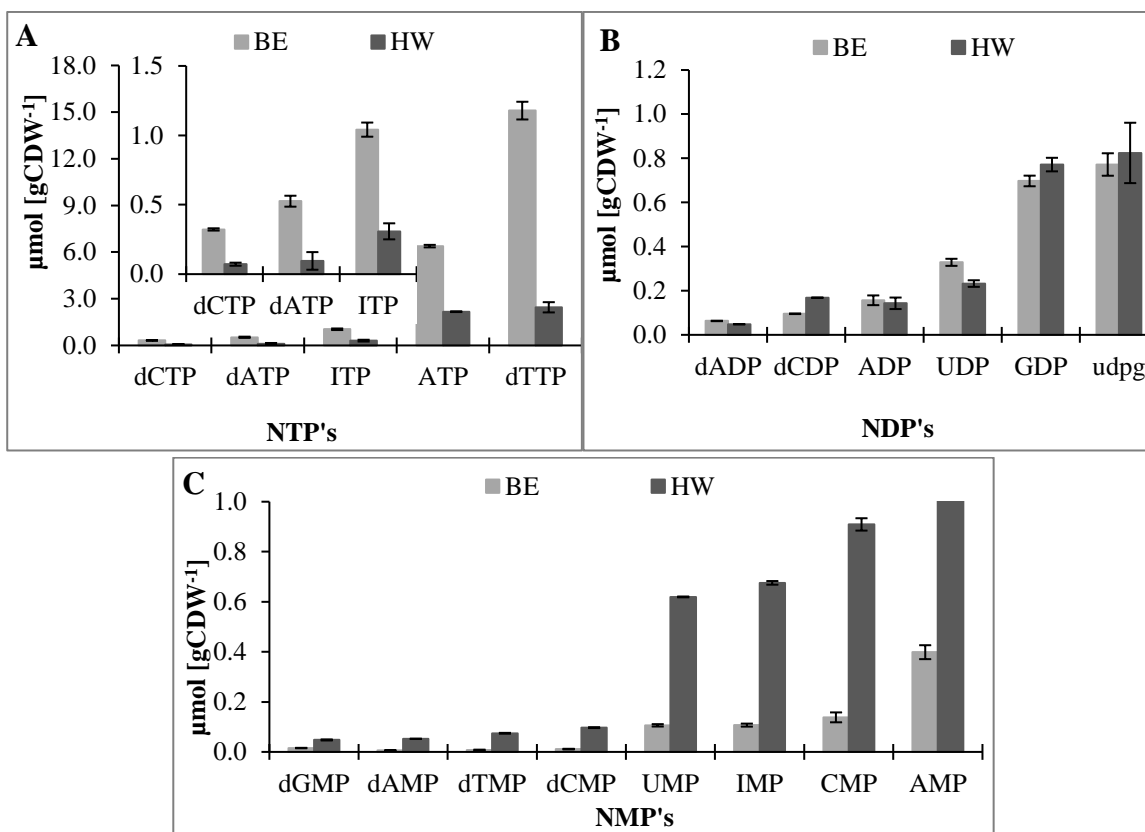


Figure 9. Effect of hot water (HW) and boiling ethanol (BE) on nucleotide extraction. (A) Nucleotide tri-phosphates (NTP's), (B) Nucleotide di-phosphates (NDP's) and (C) Nucleotide mono-phosphates (NMP's). BE, boiling ethanol; HW, hot water. The error bars indicate standard deviations from five biological replicates.

There was also a remarkable difference between the two tested hot quenching/extraction techniques (boiling ethanol and hot water). The boiling ethanol based quenching/extraction technique appeared to extract more nucleotide triphosphate and redox-cofactors whereas nucleosides/bases were better extracted by hot water, as shown in Figure 8. Furthermore, the hot water quenching/extraction approach appeared to be more efficient in extracting nucleotide monophosphates (NMPs) than nucleotide triphosphates (NTPs) compared to other

evaluated quenching/extraction techniques (Figure 9). This is not directly related to the efficiency of the extraction technique but to the incomplete quenching of cellular metabolism resulting in increased amounts of lower-grade phosphorylated nucleotides as also observed from the energy charge evaluation. This pattern of metabolite losses and gains is detrimental in metabolome studies, leading to underestimation of triphosphate levels and overestimation of less phosphorylated nucleotides.

6.1.3 Experimental reproducibility

The reproducibility of each of the techniques was evaluated based on percent relative standard deviation (RSD, %). The mean RSDs of the quantified metabolites for CE, CM, BE and HW were 30, 27, 20 and 28% respectively, implying the highest reproducibility for BE (Figure 10). The majority of extracted classes of metabolite by the BE method possess low RSDs (below 20%) compared to the other three quenching/extraction methods applied. Based on those findings, BE is the most robust method applied amongst the used quenching/extraction techniques which is likely due to a more complete extraction of metabolites.

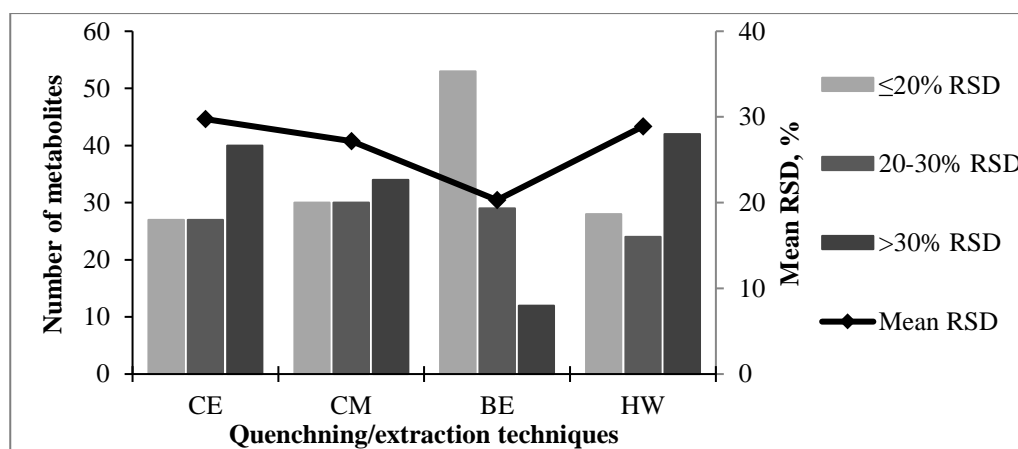


Figure 10 (Paper I). Reproducibility of tested quenching/extraction techniques. The bars show total number of metabolites that have a RSD below 20%, between 20 and 30% and above 30%; solid line represents the mean RSD (%) of all quantified metabolites for each quenching/extraction technique. Abbreviations: CE, cold ethanol/water (75/25, v/v); CM, cold methanol/acetonitrile/water (40:40:20, v/v); BE, boiling ethanol/water (75/25, v/v); HW, hot water; RSD, relative standard deviation (n=5, biological replicates).

Table 4. Summary of tested combined quenching/ extraction techniques

Quenching/ extraction	Concentration (v/v)	Temp. °C	Energy Charge (0.80-0.95)	Overall yield ($\mu\text{mol/gCDW}$)	Median RSD (%)
Ethanol	75% in H ₂ O	-40	0.90	165	28.19
MeOH:ACN:H₂O	40:40:20%	-40	0.86	170	24.05
Ethanol	75% in H ₂ O	+70	0.93	187	19.50
Hot water	100%	+90	0.48	163	27.72

The results from this study indicate that each method has its own advantage and disadvantage, depending on their physical properties. For *P. taiwanensis* VLB120 metabolome analysis, a pressure driven fast filtration approach followed by boiling ethanol quenching/extraction seems to be an adequate technique based on quenching efficiency, extraction yields of metabolites, and experimental reproducibility.

6.1.4 Thermal degradation of metabolites

In **Paper I**, the negative effect of the applied quenching/extraction temperature was also addressed by estimating the recovery of the ¹³C-labeled internal standard. Compared to both cold quenching/ extraction techniques, the peak height of ATP in the ¹³C labeled internal standard was reduced in both hot extraction/quenching procedures while both ADP and AMP increased under the same conditions (Figure 11). This suggests degradation of ATP to lower-grade phosphorylated compounds during the hot quenching/extraction process. However, this thermal degradation has no contribution to the overall results presented in **Paper I** as the added ¹³C-labeled internal standard accounts for all possible losses including thermal degradation.

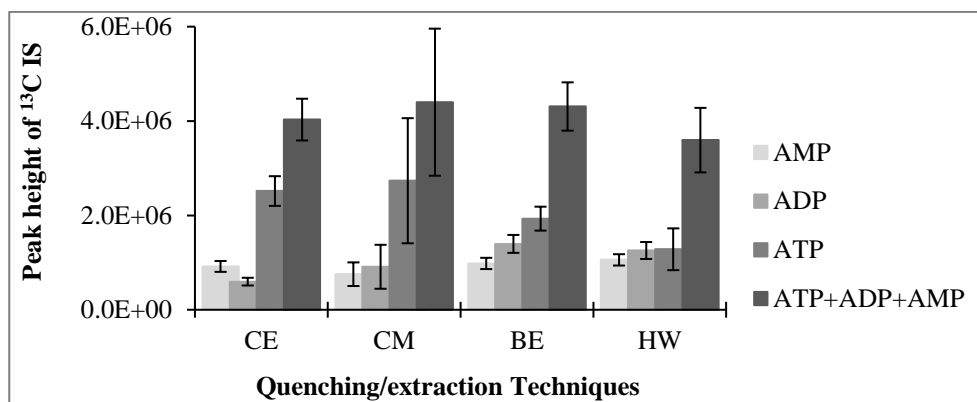


Figure 11 (**Paper I**). Effect of quenching/extraction temperatures on ATP, ADP and AMP of ^{13}C -labeled internal standard (IS) which was added to quenching/extraction solution prior to the quenching/extraction process. Abbreviations: CE, cold ethanol/water (75:25, v/v); CM, cold methanol/acetonitrile/water (40:40:20, v/v); BE, boiling ethanol/water (75:25, v/v); HW, hot water. The error bars indicate standard deviations from five biological replicates.

6.2 Composition of the core *P. taiwanensis* VLB120 metabolome

Knowledge of concentration levels of intracellular metabolites along with information about kinetic properties of the enzymes involved in specific pathways is of fundamental importance for the characterization of microbial metabolism [186, 187]. In **Paper I**, metabolite profiling of *P. taiwanensis* VLB120 was performed to provide a reference dataset of absolute intracellular metabolite concentrations. More than 100 metabolites were quantified mainly from the Embden-Meyerhof-Parnas (EMP) pathway, the pentose phosphate pathway (PPP), and the tricarboxylic acid cycle (TCA). These metabolites may not be representative of the entire metabolome of *P. taiwanensis* VLB120, however, they cover all the highly abundant metabolites on a molar basis. Among the quantified intracellular metabolites, most are related to the central carbon metabolism, energy and redox metabolism as well as amino acid metabolism.

The metabolome of *P. taiwanensis* VLB120 was dominated by a small number of highly abundant compound classes on a concentration basis: amino acids (52%), central carbon intermediates including sugar phosphates and organic acids (22%), nucleotides (13%) and redox cofactors (9%). The fifteen most abundant compounds (Figure 12) comprised 81% of

the total content of the quantified metabolome, whereas the less abundant half of the quantified metabolites includes metabolites of all classes together comprised only 2.5%.

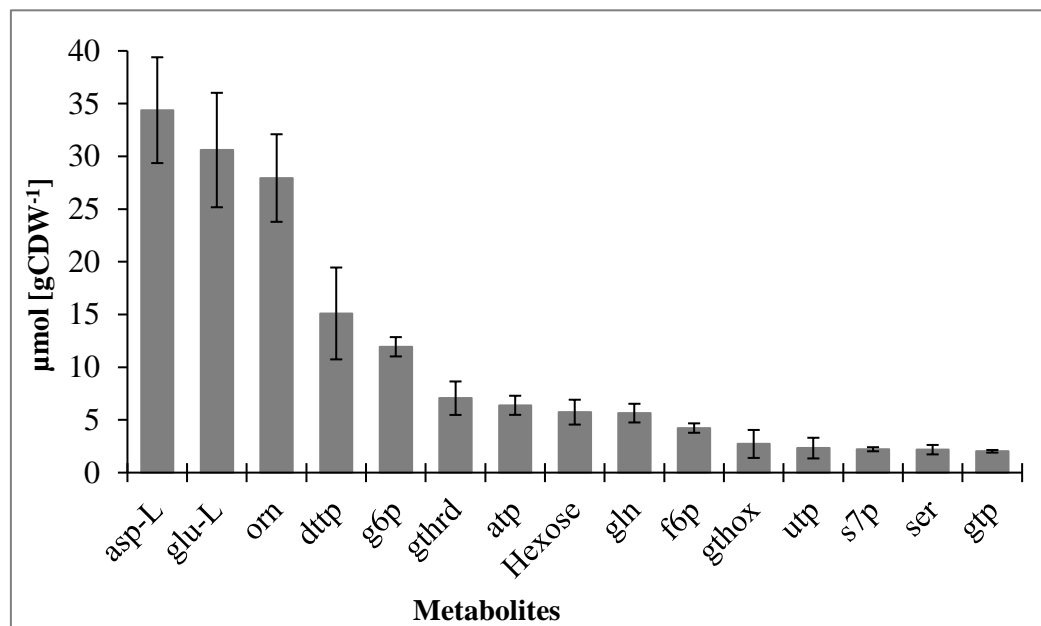


Figure 12. Top fifteen abundant metabolites of *P. taiwanensis* VLB120 growing in minimal media supplemented by 4.5 g L⁻¹. Abbreviations: aspartate (asp), glutamate (glu), ornithine (orn), 6-phosphogluconate (6pgc), glucose 6-phosphate (g6p), reduced glutathione (gthrd), adenosine triphosphate (ATP), hexose pool (fructose and glucose-D), glutamine, fructose 6-phosphate (f6p), oxidized glutathione (gthox), uridine triphosphate (UTP), sedoheptulose 7-phosphate (s7p), serine (ser), guanosine triphosphate (GTP).

6.3 Utilization of biomass hydrolysate derived sugars by *P. taiwanensis* VLB120

Biomass hydrolysates consist of complex mixtures of hexose and pentose sugars, as well as organic acids, aldehydes and phenolic compounds. In most cases, these mixtures can only be metabolized partly or sequentially and require organisms that utilize them and are tolerant to the inhibitory compounds. In **Paper II**, the utilization of the most abundant biomass hydrolysate sugars by *P. taiwanensis* VLB120 was evaluated. Cultivations were performed in 24-well clear bottom microplate (EnzyScreen, Heemstede, The Netherlands) working volume 750 μL at 30 °C, 225 rpm.

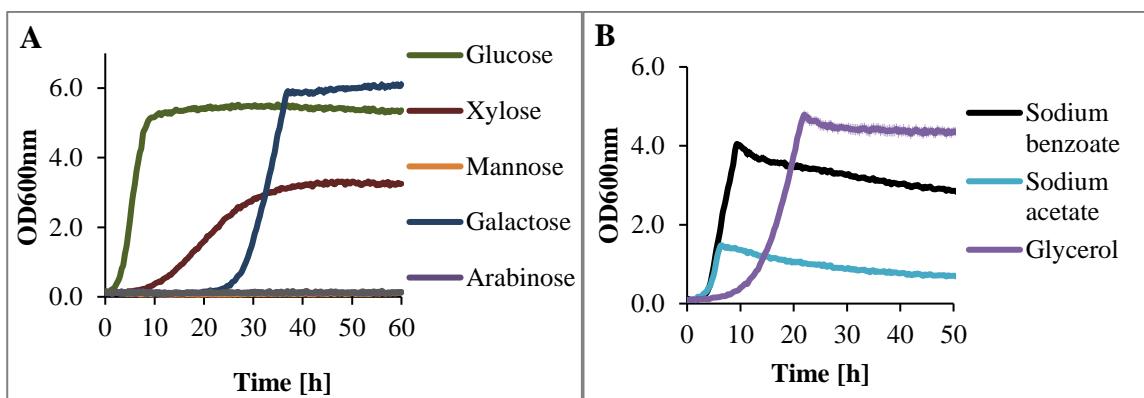


Figure 13 (**Paper II**). Growth profiles of *P. taiwanensis* VLB120 in biomass derived (A) and non-biomass derived (B) carbon sources. Error bars are the standard deviation of three biological replicate cultures.

As described in **Paper II**, *P. taiwanensis* VLB120 has shown the potential to efficiently utilize glucose, xylose and galactose regardless of a longer lag phase in case of galactose (Figure 13A). However, no growth of *P. taiwanensis* VLB120 was observed when using mannose, arabinose and rhamnose as sole carbon source. Other carbon sources including sodium acetate, sodium benzoate, glycerol were assessed for their effectiveness in growth of *P. taiwanensis* VLB120. The study showed that *P. taiwanensis* VLB120 was able to grow on these compounds as sole source of carbon and energy (Figure 13B). Mixing those carbon sources improved the specific growth rate of *P. taiwanensis* VLB120 (Figure 14).

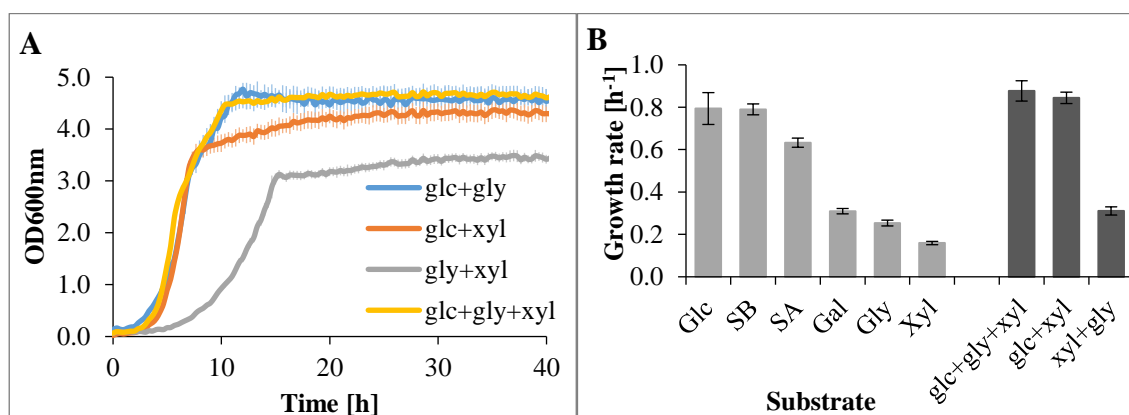


Figure 14. Growth profile of *P. taiwanensis* VLB120 in mixed carbon sources (A) and the specific growth rates (B). Error bars are the standard deviation of three biological replicate cultures. Abbreviations: glucose (glc), sodium benzoate (SB), sodium acetate (SA), galactose (gal), glycerol (gly) and xylose (xyl).

6.4 Effect of inhibitors on *P. taiwanensis* VLB120 growth

As it is explained in (**Paper II**), the inhibitory effect of the tested compounds varied with respect to lag-phase, specific growth rate, and biomass yield compared to the control sample. Furfural and 5-HMF resulted in mainly longer lag-phase and lower final cell densities, respectively. It was also observed that both furfural and 5-HMF significantly reduced the specific growth rate compared to the reference medium not containing inhibitors. Acetic acid and formic acid slightly increased the final biomass of *P. taiwanensis* VLB120 (Figure 15), but reduced the growth rate as their concentration increased. The main difference of acetic acid and formic acid was observed as the concentration of acetic acid exceeded 6 g L^{-1} where after the lag-phase was clearly elongated compared to formic acid.

In similar study (**Paper II**), the inhibitory threshold concentrations that reduce the growth of *P. taiwanensis* VLB120 by 50% (IC50) after 24 hours of cultivation were examined. Based on these values, 5-HMF provided the strongest inhibition followed by furfural and vanillin, respectively. Surprisingly, IC50 values for acetic acid and formic acid were above the highest tested values (10 g L^{-1}), which means this concentration was not sufficiently high to reduce the growth of *P. taiwanensis* VLB120 by 50%.

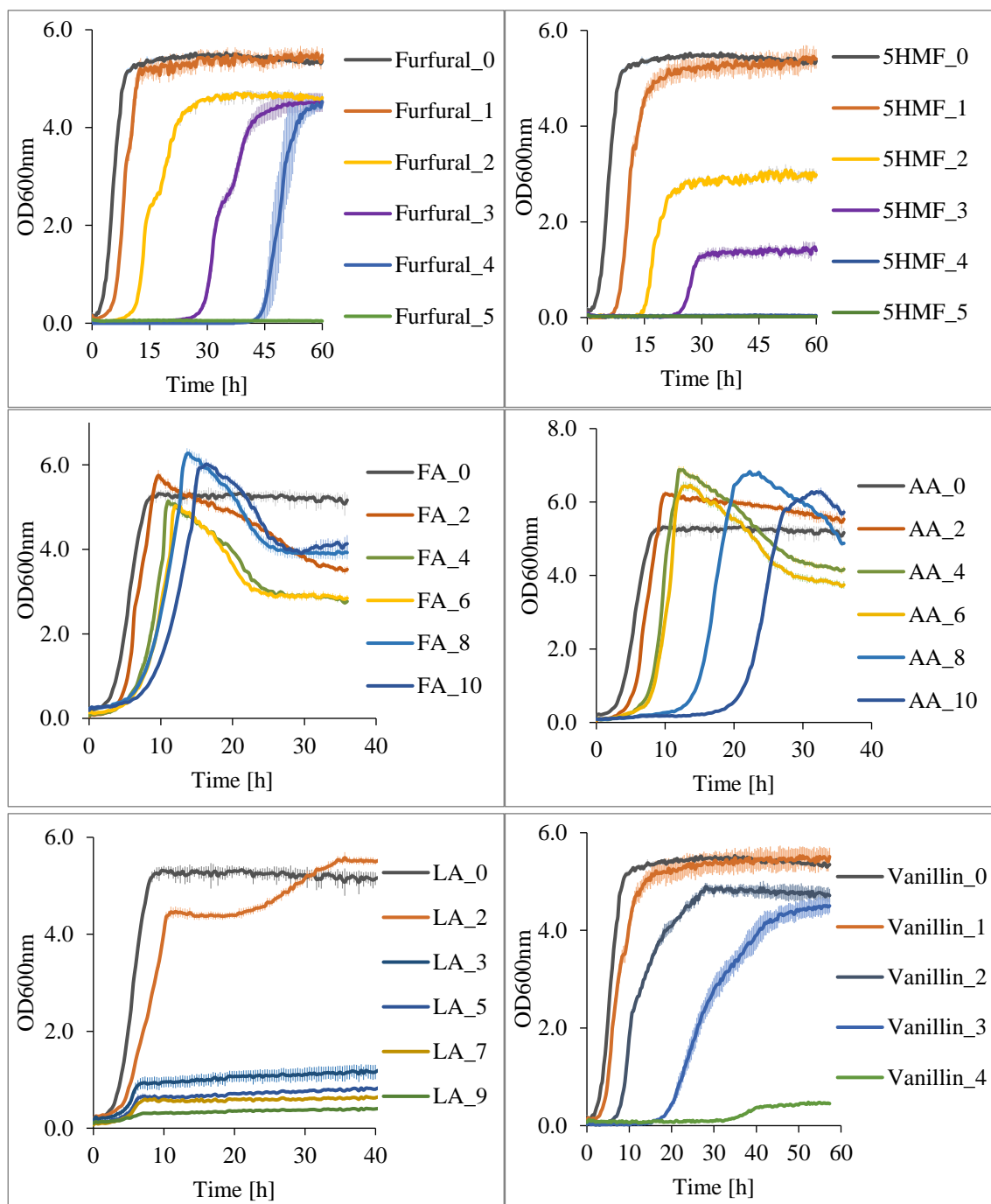


Figure 15. Growth curves of *P. taiwanensis* VLB120 in the presence of furfural, 5-HMF, levulinic acid (LA), formic acid (FA), acetic acid (AA) and vanillin. Aerobic cultivations were carried out in 24-well clear bottom microplate (EnzyScreen, Heemstede, The Netherlands) working volume 750 μL at 30 $^{\circ}\text{C}$, 225 rpm. Concentration: [g L^{-1}]. Error bars are the standard deviation of three biological replicate cultures.

6.5 Detoxification mechanism of inhibitors in *P. taiwanensis* VLB120

In order to evaluate the degradation capacity of inhibitory compounds by *P. taiwanensis* the extracellular metabolome study was performed as described in **Paper II**. Since some of the biomass hydrolysate inhibitors have structural similarity and share the same degradation pathway, only acetic acid, levulinic acid, furfural and vanillin were considered. For both extracellular and intracellular metabolite analysis, cultivations were performed in 1.3 L bioreactor (working volume 0.5 L) as described in chapter V.

P. taiwanensis VLB120 responded to the tested inhibitors in various ways including detoxification, tolerance and efflux to protect themselves against hostile environmental conditions. Inhibitors such as furfural and vanillin were oxidized to their corresponding acids, while acetic acid was directly utilized as an additional carbon and energy source. Levulinic acid was neither consumed nor converted and remained at constant levels in the broth throughout the fermentation process.

There was no noticeable growth of cells observed during the conversion of vanillin and furfural to vanillic acid and 2-furoic acid, respectively. This indicates that the presence of these inhibitors in the media obstructed the growth of *P. taiwanensis* VLB120, but their corresponding acids seem to be less toxic which is also in agreement with previous studies showing that aldehyde is the most toxic compounds for microorganisms, whereas the corresponding acids were less toxic [171, 188–190].

The specific glucose uptake rate was substantially reduced when vanillin and furfural were added to the cultivation medium (Figure 16). In contrast, when growing *P. taiwanensis* VLB120 with acetic acid and levulinic acid added to the medium, the specific glucose uptake rate was increased approx. by 40% and 9%, respectively, compared to that of the control condition. The decreased specific growth rates and increased specific glucose uptake rate possibly reflects the additional energy required to export inhibitors that enter the cells through the plasma membrane [191].

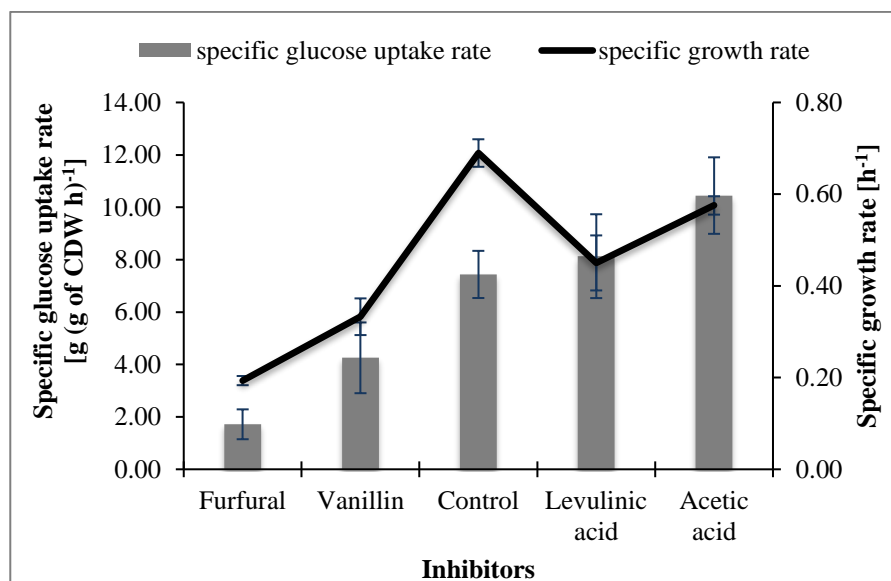


Figure 16. Effect of inhibitory compounds on specific growth and glucose uptake rates of *P. taiwanensis* VLB120 grown on minimal medium supplemented with 4.5 and 2 g L⁻¹ of glucose and inhibitory compound, respectively, at stirrer speed of 800 rpm, temperature 30 °C and pH 7. Specific growth and glucose uptake rates were calculated during the glucose phase as *P. taiwanensis* VLB120 exhibits biphasic growth (glucose and gluconate phase). Error bars indicate standard deviations of three independent cultures. CDW, cell dry weight.

6.6 Metabolic response of *P. taiwanensis* VLB120 towards inhibitors

In this part of the study (**Paper II**), the developed metabolomics tools (**Paper I**) was applied to study the relationship between the change of intracellular metabolite levels of *P. taiwanensis* VLB120. Since the mechanism of detoxification, energy and co-factor requirement for cells are different while being exposed to different inhibitors, the intracellular metabolite response of the microorganism may also vary greatly depending on the chemistry of these inhibitors [176, 192–194]. In order to investigate change of intracellular metabolite levels between treated and untreated samples, principal component analysis (PCA) (Figure 17) and heatmap analysis (Figure 18) were performed.

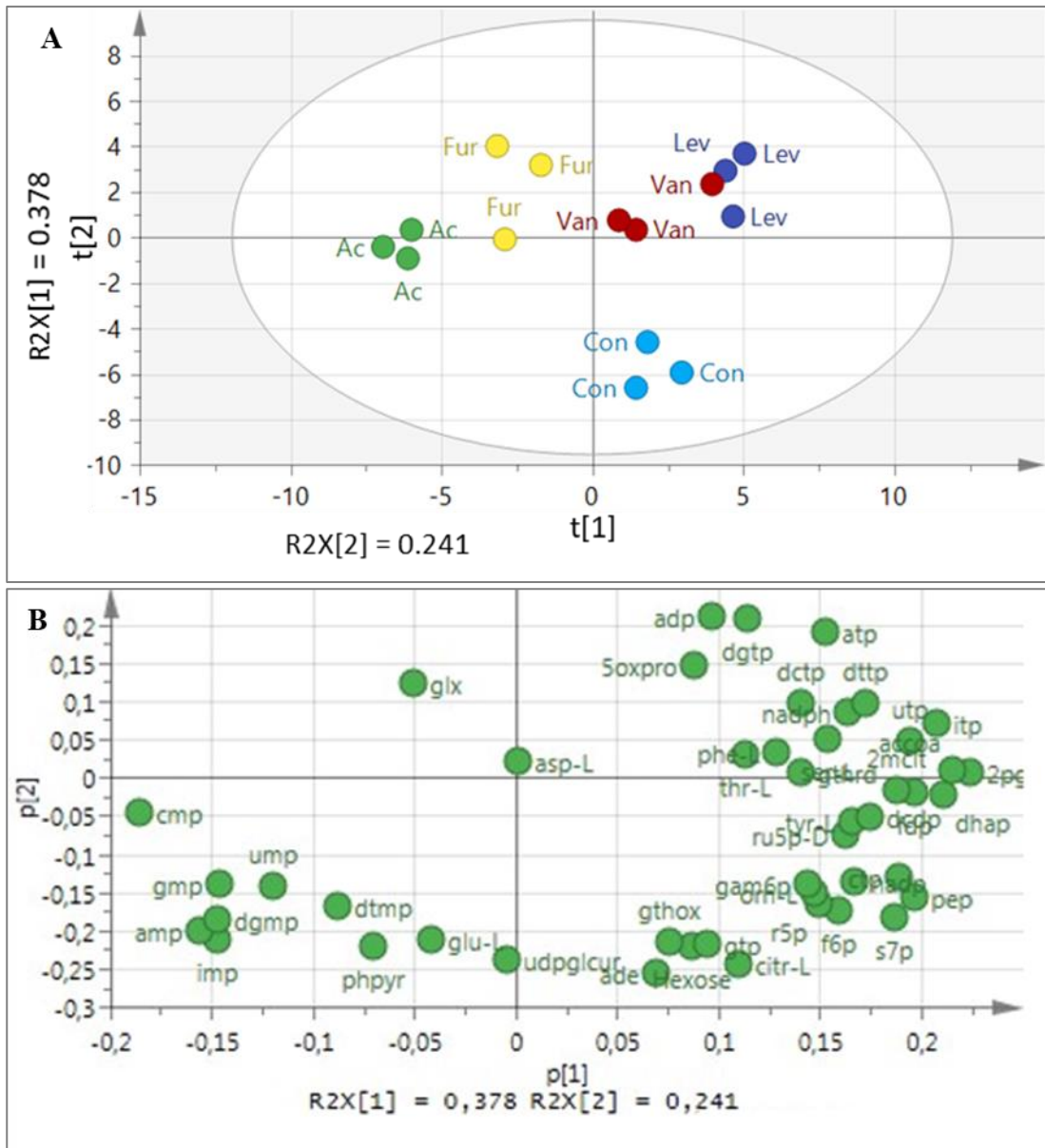


Figure 17 (**Paper II**). Principal component analysis (PCA) of metabolic profiles of *P. taiwanensis* VLB120 treated under different conditions including acetic acid, levulinic acid, vanillin and furfural. (A) Score plot shows the statistical discrimination between the tested conditions. (B) Loading plot illustrates the metabolites that contribute strongly to statistical separation between the conditions. Abbreviations: furfural (Fur), vanillin (Van), levulinic acid (Lev), acetic acid (Ac) and control (Con).

The principal component analysis model (PCA) generated from intracellular metabolite data showed a clear separation between the control and treated groups (Figure 17A), indicating an adjustment of intracellular metabolism of the *P. taiwanensis* strain in response to

inhibitors. The changes in concentration levels of nucleotides, redox-cofactors and sugar phosphates particularly contributed to separate the groups (Figure 17B). Samples treated with vanillin, furfural and levulinic acid are located on the upper part of PC(1), indicating relative similarity of their effect on metabolite levels. This is corroborated by a heatmap cluster analysis based on the degree of similarity of metabolite abundance profiles (Figure 18). Levulinic acid and vanillin were positioned closer together, indicating their effect on metabolite level was comparable.

Nucleotide monophosphates and acetyl-CoA seemed to have high influence in separating the samples treated with acetic acid from the rest of the groups. This could be related to the conversion of acetic acid to acetyl-CoA that requires adenosine triphosphate, which results in production of adenosine monophosphate [195, 196].

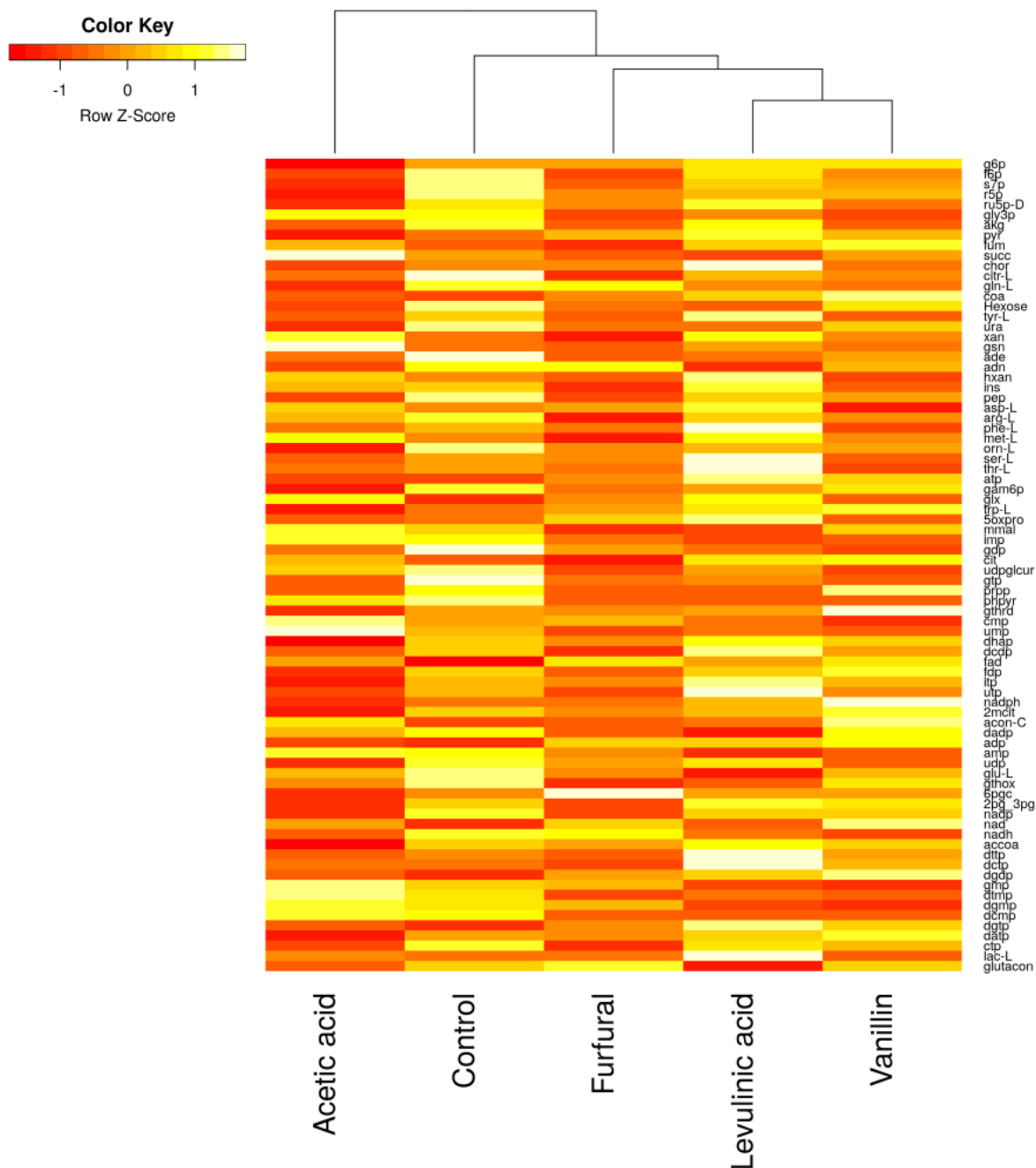


Figure 18. Heatmap of metabolites extracted from *P. taiwanensis* VLB120 under different stress conditions. Metabolites abundance differences were clustered according to trends measured across all biological replicates (n = 3).

Intracellular metabolites analysis revealed that the concentrations of most of the quantified metabolites in *P. taiwanensis* VLB120 exposed to inhibitors were changed with respect to the control group, (**Paper II**). This can be the consequence of changes in cellular energy

content (e.g. ATP) and redox balance (e.g. NADPH), because they involve in many important metabolic reactions. It has also reported that these metabolites have key functions in the survival of microorganisms in a stressful environment [197].

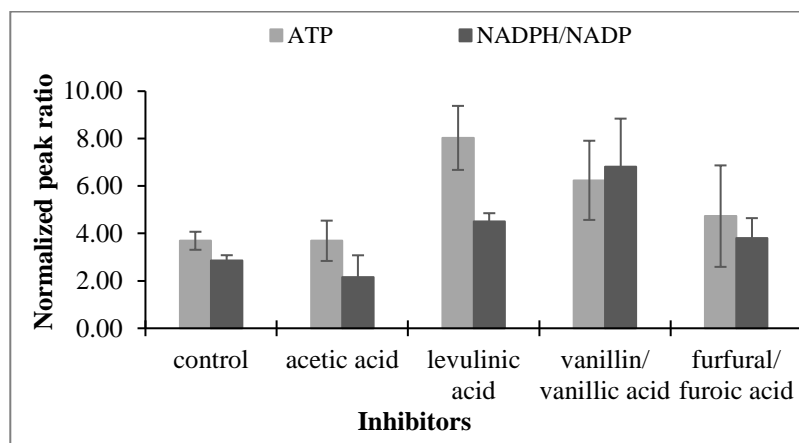


Figure 19 (**Paper II**). Effect of inhibitors on energy state and redox-carrier of glucose-utilizing *P. taiwanensis* VLB120. The bars indicate the peak ratio of ATP and NADPH/NAD; the line represents the concentration of acetic acid, levulinic acid, vanillic acid and 2-furoic acid at the time of sampling. Peak ratio is the height ratio between the U ^{13}C and ^{12}C metabolites normalized to biomass. Error bars indicate standard deviations of three independent cultures.

As indicated in Figure 18, the levels of ATP and the NADPH/NADP ratio were markedly increased in the cells subjected to oxidative stress compared to that of the control. This indicates *P. taiwanensis* VLB120 requires both NADPH dependent detoxification and ATP-dependent efflux to cope with the inhibitors. ATP was mainly used to pump out the inhibitors from the cells, whereas NADPH provides reducing power to deal with the oxidative stress [176, 198, 199]. Under acetic acid stress, the NADPH/NADP ratio was slightly impaired, while the concentration of remained ATP unchanged, which is in reasonable agreement with a previous study [200].

Overall, there appeared to be a metabolic shift in *P. taiwanensis* to generate more ATP and NADPH in order to cope with the stress imposed by inhibitors. Thus, adequate supplies of these metabolites are essential for the survival and reproduction of *P. taiwanensis* in the presence of biomass derived inhibitors

6.7 Investigation of alternative glucose uptake by *Pseudomonas putida* KT2440

Glucose uptake in *P. putida* KT2440 was investigated using KT2440 wild type strain and two KT2440 mutant strains including KT2440 Δglk (a mutant deficient in glucokinase) and KT2440 Δgdc (a mutant deficient in glucose dehydrogenase). As indicated in Figure 20, the investigated strains were fed with equimolar amounts of U- ^{13}C glucose and naturally labelled gluconate. Extracellular metabolite analysis revealed that both KT2440 and KT2440 Δglk oxidized labelled glucose to gluconate and 2-ketogluconate via glucose dehydrogenase (*gcd*) and gluconate dehydrogenase (*gad*), respectively. The labelling was incorporated into the resulting compounds. On the other side, *P. putida* KT2440 Δgdc can only transport the labelled glucose to the cytosol via an ABC uptake system, indicating there are more options for glucose uptake in the wild type KT2440 strain.

In order to determine the activity of the alternative carbon uptake pathways by *P. putida* KT2440, labelling changes in intracellular metabolites resulting directly from labelled glucose were investigated. Thus, the labelling of glucose 6-phosphate (g6p), fructose 6-phosphate (f6p) and 6-phosphogluconate (6pg) was determined and compared for all tested strains. Since this part of the work is not fully completed, the results presented in this section is based on the preliminary data obtained.

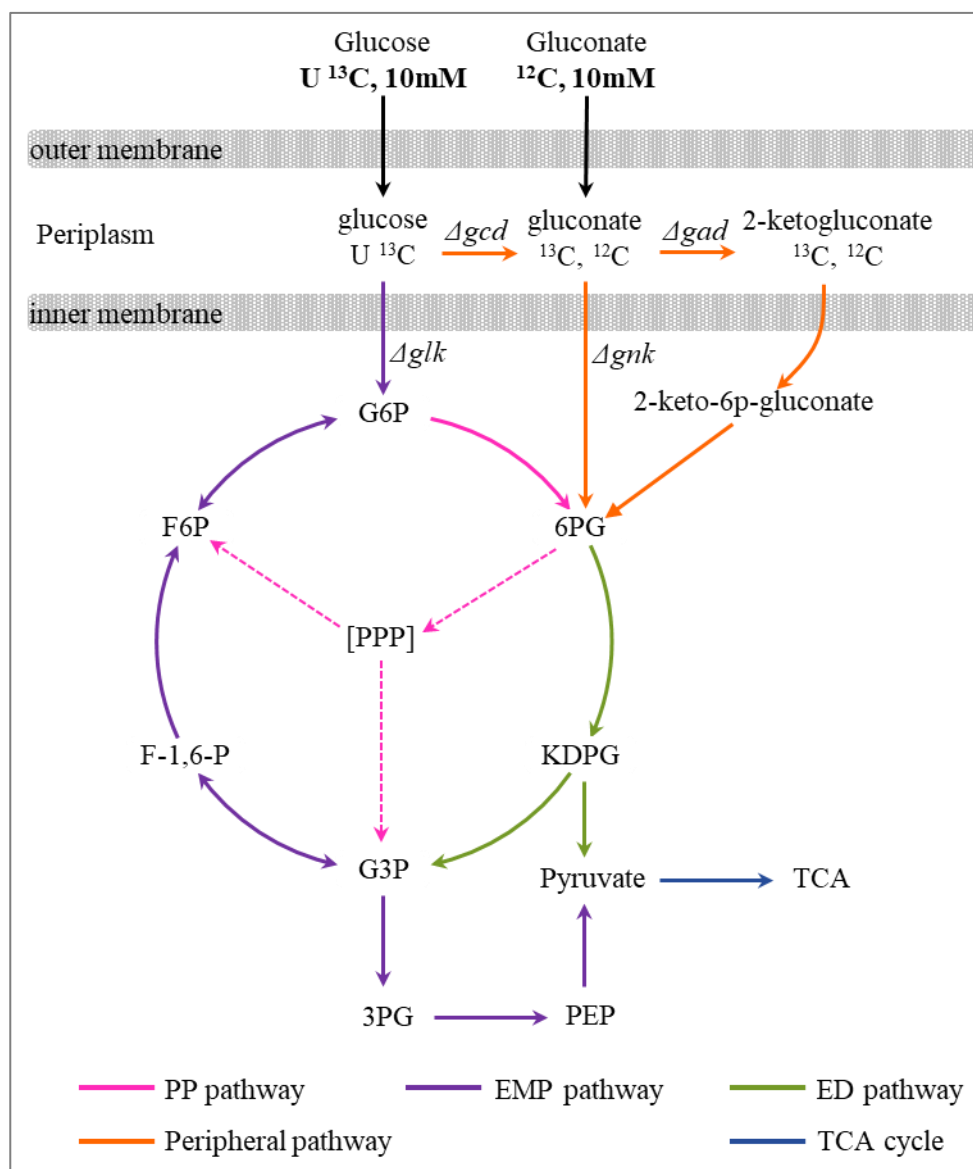


Figure 20. Metabolic pathways involved in the utilization of substrate by *P. putida* KT2440, modified from Nikel *et al.* [142]. The routes consist of the peripheral pathway, the pentose phosphate pathway (PPP), the Entner-Doudoroff (ED) pathway, the Embden-Meyerhof-Parnas Pathway (EMP) and the tricarboxylic acid (TCA) cycle. Abbreviations: glucose 6-phosphate (G6P), fructose 6-phosphate (F6P), 6-phosphogluconate (6PG), 2-keto-3-deoxy-6phospho-gluconate (KDPG), glyceraldehyde 3-phosphate (G3P), fructose 1,6-bisphosphate (F-1,6-P), phosphoenolpyruvate (PEP), 3-phosphoglycerate (3PG).

The fractional labelling of g6p and f6p in *P. putida* KT2440 Δglk was below 25% after 2 hours of cultivation and gradually increased to 63% after 5 hours of the growth experiment (Figure 21A). This is an indication of more pronounced uptake of naturally labelled gluconate

and/or 2-ketogluconate by KT2440 Δglk during the first phase of growth. Furthermore, the observed equal labelling pattern of g6p and f6p in case of KT2440 Δglk indicates that g6p can only originate from f6p, which was derived from either from the PP pathway or a cyclic ED pathway activity.

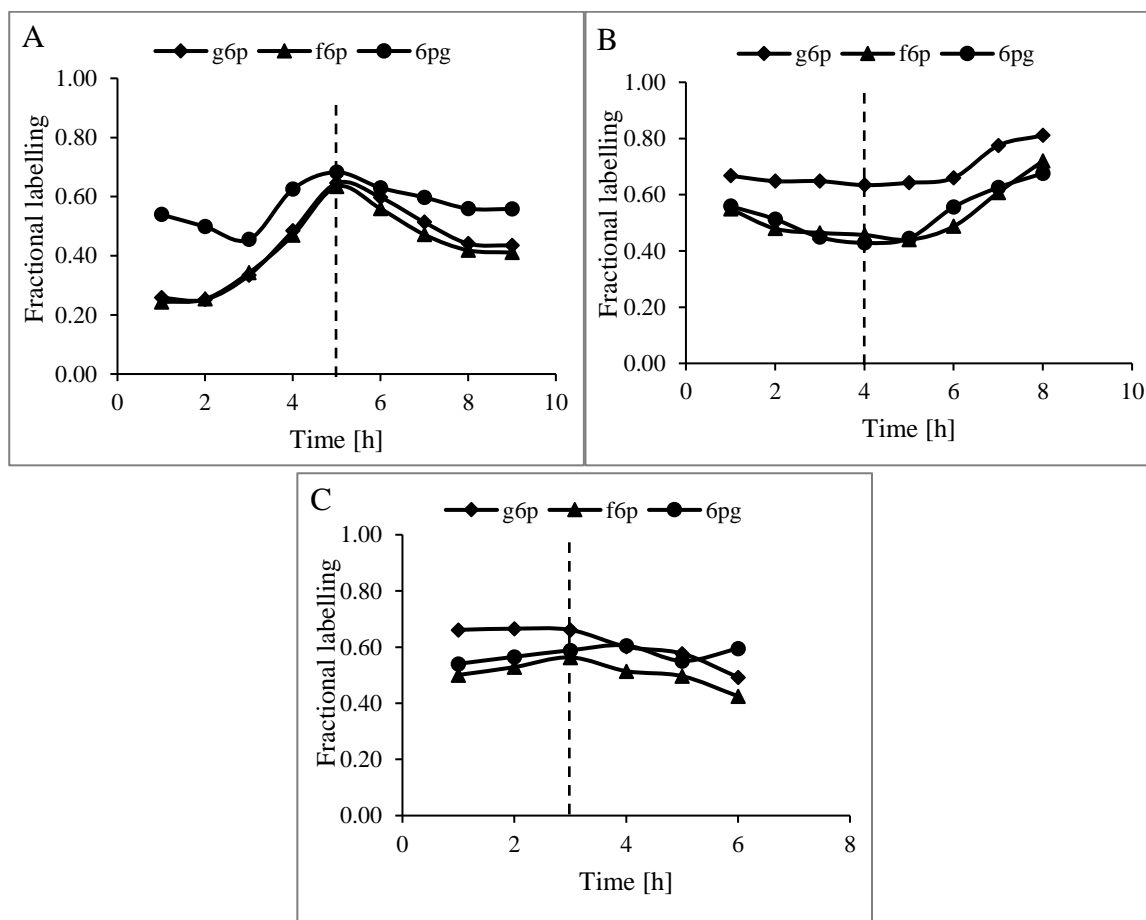


Figure 21. Time course of fractional labelling pattern of glucose 6-phosphate (g6p), fructose 6-phosphate (f6p) and 6-phosphogluconate (6pg) in case of KT2440 Δglk (A), KT2440 Δgcd (B) and KT2440 (C) using U ^{13}C glucose and ^{12}C gluconate as initial carbon sources. The broken lines indicate the turning point of labelling pattern.

In case of KT2440 Δgcd , the fractional labelling of f6p was lower than that of g6p (Figure 21B) indicating f6p was produced from both g6p via phosphoglucose isomerase and the PP pathway, hence can originate from both glucose and gluconate. A partially cyclic ED pathway flux is also conceivable, in which the formed glyceraldehyde-3-phosphate (g3p) is recycled back to f6p, enabling formation of g6p and 6pg from gluconate, as well. The

fractional labelling of 6pg and f6p in case KT2440 Δgcd was reduced during the first 4 hours of growth. This reduction indicates the strain uptake more gluconate than labelled glucose until gluconate almost depleted from the medium.

The fractional labelling of g6p in wild type KT2440 strain was identical with that of KT2440 Δgcd for the first 3 hours of growth (Figure 21B and 21C). In the second phase of growth, when labelled glucose was almost completely oxidized to gluconate and 2-ketogluconate, the fractional labelling of both g6p and f6p was reduced. This indicates that g6p was mainly generated from glucose during the first phase of growth. Furthermore, a co-utilization of labelled glucose and naturally labelled gluconate was observed in all tested strains.

Since the evaluation of g6p, f6p and 6pg labelling did only allow for few statements concerning the uptake of differently labelled substrates, the labelling of the remaining intracellular metabolites including r5p, g3p and pyruvate must be considered for gaining more information. This information will help to investigate the labelling pattern of ED-Pathway and PP-Pathway metabolites.

VII. CONCLUSION AND FUTURE PROSPECT

The importance of sample preparation in metabolomics studies was demonstrated in **Paper I**. The tested quenching and extraction techniques significantly affected the performance of intracellular metabolite profiling. Fast filtration followed by organic solvent-based quenching/extraction techniques proved to be a good quenching method for *P. taiwanensis*. In contrast, the hot water based quenching/extraction technique resulted in a low EC ratio (0.48 ± 0.014), which implies that this method was less effective in deactivating the cellular metabolism of *P. taiwanensis*. The different outcome seen with different quenching/extraction techniques indicates that there is no universal technique that is suitable for all types of microorganisms and metabolites. Applying fast filtration system followed by boiling ethanol quenching/extraction technique, more than 100 intracellular metabolites of *P. taiwanensis* VLB120 were quantified with the objective of providing a reference dataset that can be used in the development of microbial cell factory.

Despite the great progress within microbial metabolomics, there are still some problems related to sample preparation, mainly quenching of the cells to stop all metabolic activity. The high turnover rate of intracellular metabolites requires a rapid quenching procedure that stops cellular metabolism in a fraction of a second. Among several existing quenching techniques, direct quenching is the fastest method for arresting metabolism of the cells. However, this method has been highly criticized due to the leakage of metabolites while quenching. The reason for this is not yet clearly understood, but it could be related to quenching solution, quenching temperature or both. Future work should test and optimize this technique in order to minimize (or prevent) leakage of intracellular metabolites into the extracellular medium during quenching process. Another approach could be measurement of metabolites in the culture supernatant as well as in total broth samples to calculate the intracellular levels by subtraction.

The study in **Paper II** has demonstrated that metabolomics is a powerful tool to characterize microbial metabolism. The developed metabolomics tool was applied to characterize the metabolic response of *P. taiwanensis* VLB120 towards biomass hydrolysate derived

inhibitors including weak acids, furan and phenolic compounds. The characterization was done with the objective of providing helpful data for further strain design steps. The tested inhibitors affected the growth of *P. taiwanensis* in various way; prolonged the lag-phase, reduced the specific growth rate and biomass yield. In order to cope with these hostile environmental conditions, *P. taiwanensis* went through metabolic rearrangement to enhance the level of cellular energy and redox balance that provides reducing power.

The natural ability of *P. taiwanensis* VLB120 to tolerate inhibitors and to utilize C5 and C6 sugars as sole carbon and energy source matches the basic requirements for growth on biomass hydrolysate. However, this strain never tested against mixed inhibitory compounds and real biomass hydrolysate. Thus, it requires further investigation to improve its fermentation performance in biomass hydrolysates.

VIII. REFERENCE LIST

1. Sun Y V., Hu Y-J. Integrative Analysis of Multi-omics Data for Discovery and Functional Studies of Complex Human Diseases. 2016. doi:10.1016/bs.adgen.2015.11.004.
2. Khoomrung S, Wanichthanarak K, Nookaew I, Thamsermsang O, Seubnooch P, Laohapand T, et al. Metabolomics and integrative omics for the development of Thai traditional medicine. *Front Pharmacol.* 2017;8 JUL:1–11.
3. Patel S, Ahmed S. Emerging field of metabolomics: Big promise for cancer biomarker identification and drug discovery. *J Pharm Biomed Anal.* 2015;107:63–74. doi:10.1016/j.jpba.2014.12.020.
4. Zhang J, Shen H, Xu W, Xia Y, Barr DB, Mu X, et al. Urinary metabolomics revealed arsenic internal dose-related metabolic alterations: A proof-of-concept study in a chinese male cohort. *Environ Sci Technol.* 2014;48:12265–74.
5. Peng XX. Proteomics and its applications to aquaculture in China: Infection, immunity, and interaction of aquaculture hosts with pathogens. *Dev Comp Immunol.* 2012;39:63–71. doi:10.1016/j.dci.2012.03.017.
6. Robertson DG. Metabonomics in toxicology: A review. *Toxicol Sci.* 2005;85:809–22.
7. Fuhrer T, Zamboni N. High-throughput discovery metabolomics. *Curr Opin Biotechnol.* 2015;31:73–8. doi:10.1016/j.copbio.2014.08.006.
8. Peng B, Li H, Peng XX. Functional metabolomics: from biomarker discovery to metabolome reprogramming. *Protein Cell.* 2015;6:628–37.
9. Dettmer K, Aronov PA, Hammock BD. Mass spectrometry-based metabolomics. *Mass Spectrom Rev.* 2007;26:51–78.
10. Magdenoska O. LC-MS based metabolomics. Tech Univ Denmark. 2015.

11. Wentzel A, Sletta H, Consortium S, Ellingsen TE, Bruheim P. Intracellular Metabolite Pool Changes in Response to Nutrient Depletion Induced Metabolic Switching in *Streptomyces coelicolor*. *Metabolites*. 2012;2:178–94. doi:10.3390/metabo2010178.
12. Miyamoto Y, Mukai T, Matsuoka M, Kai M, Maeda Y, Makino M. Profiling of Intracellular Metabolites: An Approach to Understanding the Characteristic Physiology of *Mycobacterium leprae*. *PLoS Negl Trop Dis*. 2016;10:1–11.
13. Villas-Bôas SG, Roessner U, Hansen MAE, Smedsgaard J, Nielsen J. *Metabolome Analysis: An Introduction*. 2006.
14. Imperlini E, Santorelli L, Orrù S, Scolamiero E, Ruoppolo M, Caterino M. Mass spectrometry-based metabolomic and proteomic strategies in organic acidemias. *Biomed Res Int*. 2016;2016.
15. Putri SP, Nakayama Y, Matsuda F, Uchikata T, Kobayashi S, Matsubara A, et al. Current metabolomics: Practical applications. *J Biosci Bioeng*. 2013;115:579–89. doi:10.1016/j.jbiosc.2012.12.007.
16. Dumas M-E. Metabolome 2.0: quantitative genetics and network biology of metabolic phenotypes. *Mol Biosyst*. 2012;8:2494. doi:10.1039/c2mb25167a.
17. Castro-Santos P, Laborde CM, Diaz-Peña R. Genomics, proteomics and metabolomics: their emerging roles in the discovery and validation of rheumatoid arthritis biomarkers. *Clin Exp Rheumatol*. 2015;33:279–86.
18. Bundy JG, Davey MP, Viant MR. Environmental metabolomics: A critical review and future perspectives. *Metabolomics*. 2009;5:3–21.
19. Griffin JL, Nicholls AW, Daykin CA, Heald S, Keun HC, Schuppe-Koistinen I, et al. Standard reporting requirements for biological samples in metabolomics experiments: Mammalian/in vivo experiments. *Metabolomics*. 2007;3:179–88.
20. Lankadurai BP, Nagato EG, Simpson MJ. Environmental metabolomics: an emerging

approach to study organism responses to environmental stressors. *Environ Rev.* 2013;21:180–205. doi:10.1139/er-2013-0011.

21. Rangel-Huerta OD, Gil A. Nutrimetabolomics: An update on analytical approaches to investigate the role of plant-based foods and their bioactive compounds in non-communicable chronic diseases. *Int J Mol Sci.* 2016;17.

22. Zhou J, Yin Y. Strategies for large-scale targeted metabolomics quantification by liquid chromatography-mass spectrometry. *Analyst.* 2016;141:6362–73. doi:10.1039/C6AN01753C.

23. Issaq HJ, Abbott E, Veenstra TD. Utility of separation science in metabolomic studies. *J Sep Sci.* 2008;31:1936–47.

24. Zhang X, Zhu X, Wang C, Zhang H, Cai Z, Zhang X, et al. Non-targeted and targeted metabolomics approaches to diagnosing lung cancer and predicting patient prognosis. *Oncotarget.* 2016;7:63437–48. doi:10.18632/oncotarget.11521.

25. Vinayavekhin N, Saghatelian A. Untargeted metabolomics. *Curr Protoc Mol Biol.* 2010; SUPPL. 90:1–24.

26. Untargeted, semi-targeted and targeted analytical approaches - Metabolomics - University of Birmingham.
<https://www.futurelearn.com/courses/metabolomics/0/steps/10688>. Accessed 6 Nov 2017.

27. Roberts L.D., Amanda L. Souza A.L., Gerszten R.E. and CCB. Targeted Metabolomics. *Curr Protoc Mol Biol.* 2013;:1–34.

28. Roberts LD, Souza AL, Gerszten RE, Clish CB. Targeted metabolomics. *Curr Protoc Mol Biol.* 2012;1 SUPPL.98:1–24.

29. Vrhovsek U, Masuero D, Gasperotti M, Franceschi P, Caputi L, Viola R, et al. A versatile targeted metabolomics method for the rapid quantification of multiple classes of phenolics in fruits and beverages. *J Agric Food Chem.* 2012;60:8831–40.

30. Johnson CH, Ivanisevic J, Siuzdak G. Metabolomics: beyond biomarkers and towards mechanisms. *Nat Rev Mol Cell Biol.* 2016;17:451–9. doi:10.1038/nrm.2016.25.
31. Veyel D, Erban A, Fehrle I, Kopka J, Schroda M. Rationales and approaches for studying metabolism in eukaryotic microalgae. 2014. doi:10.3390/metabo4020184.
32. Hayton S, Maker GL, Mullaney I, Trengove RD. Experimental design and reporting standards for metabolomics studies of mammalian cell lines. *Cell Mol Life Sci.* 2017;;1–21.
33. Martano G, Delmotte N, Kiefer P, Christen P, Kentner D, Bumann D, et al. Fast sampling method for mammalian cell metabolic analyses using liquid chromatography–mass spectrometry. *Nat Protoc.* 2014;10:1–11. doi:10.1038/nprot.2014.198.
34. Mousavi F, Bojko B, Bessonneau V, Pawliszyn J. Cinnamaldehyde Characterization as an Antibacterial Agent toward *E. coli* Metabolic Profile Using 96-Blade Solid-Phase Microextraction Coupled to Liquid Chromatography–Mass Spectrometry. *J Proteome Res.* 2016;15:963–75. doi:10.1021/acs.jproteome.5b00992.
35. Mousavi F. Optimization of SPME coating characteristics for metabolomics and targeted analysis with LC / MS. 2015;;209.
36. Vuckovic D. Current trends and challenges in sample preparation for global metabolomics using liquid chromatography-mass spectrometry. *Anal Bioanal Chem.* 2012;403:1523–48.
37. Beckonert O, Keun HC, Ebbels TMD, Bundy J, Holmes E, Lindon JC, et al. Metabolic profiling, metabolomic and metabonomic procedures for NMR spectroscopy of urine, plasma, serum and tissue extracts. *Nat Protoc.* 2007;2:2692–703. doi:10.1038/nprot.2007.376.
38. Mashego MR, Rumbold K, De Mey M, Vandamme E, Soetaert W, Heijnen JJ. Microbial metabolomics: Past, present and future methodologies. *Biotechnol Lett.* 2007;29:1–16.
39. Winder CL, Dunn WB, Schuler S, Broadhurst D, Jarvis R, Stephens GM, et al. Global

metabolic profiling of *Escherichia coli* cultures: An evaluation of methods for quenching and extraction of intracellular metabolites. *Anal Chem.* 2008;80:2939–48.

40. Najafpour GD. CHAPTER 5 - Growth Kinetics. *Biochem Eng Biotechnol.* 2007;:81–141. doi:http://dx.doi.org/10.1016/B978-044452845-2/50005-7.

41. Meyer H, Weidmann H, Lalk M. Methodological approaches to help unravel the intracellular metabolome of *Bacillus subtilis*. *Microb Cell Fact.* 2013;12:69. doi:10.1186/1475-2859-12-69.

42. Kim S, Lee DY, Wohlgemuth G, Park HS, Fiehn O, Kim KH. Evaluation and optimization of metabolome sample preparation methods for *Saccharomyces cerevisiae*. *Anal Chem.* 2013;85:2169–76.

43. Hans MA, Heinzle E, Wittmann C. Quantification of intracellular amino acids in batch cultures of *Saccharomyces cerevisiae*. *Appl Microbiol Biotechnol.* 2001;56:776–9.

44. Villas-Bôas SG, Noel S, Lane GA, Attwood G, Cookson A. Extracellular metabolomics: A metabolic footprinting approach to assess fiber degradation in complex media. *Anal Biochem.* 2006;349:297–305.

45. Sáez MJ, Lagunas R. Determination of intermediary metabolites in yeast. Critical examination of the effect of sampling conditions and recommendations for obtaining true levels. *Mol Cell Biochem.* 1976;13:73–8.

46. Wordofa GG, Kristensen M, Schrübbers L, McCloskey D, Forster J, Schneider K. Quantifying the metabolome of *Pseudomonas taiwanensis* VLB120: Evaluation of hot and cold combined quenching/extraction approaches. *Anal Chem.* 2017;:acs.analchem.7b00793. doi:10.1021/acs.analchem.7b00793.

47. McCloskey D, Utrilla J, Naviaux RK, Palsson BO, Feist AM. Fast Swinnex filtration (FSF): a fast and robust sampling and extraction method suitable for metabolomics analysis of cultures grown in complex media. *Metabolomics.* 2014;:198–209.

48. Koning W de, Dam K van. A method for the determination of changes of glycolytic metabolites in yeast on a subsecond time scale using extraction at neutral pH. *Anal Biochem.* 1992;204:118–23.
49. Buchholz a, Takors R, Wandrey C. Quantification of intracellular metabolites in *Escherichia coli* K12 using liquid chromatographic-electrospray ionization tandem mass spectrometric techniques. *Anal Biochem.* 2001;295:129–37.
50. Jensen NB, Jokumsen K V, Villadsen J. Determination of the phosphorylated sugars of the Embden-Meyerhoff-Parnas pathway in *Lactococcus lactis* using a fast sampling technique and solid phase extraction. *Biotechnol Bioeng.* 1999;63:356–62.
51. Chen M, Li A, Sun M, Feng Z, Meng X, Wang Y. Optimization of the quenching method for metabolomics analysis of *Lactobacillus bulgaricus*. *J Zhejiang Univ Sci B.* 2014;15:333–42. doi:10.1631/jzus.B1300149.
52. de Jonge LP, Douma RD, Heijnen JJ, van Gulik WM. Optimization of cold methanol quenching for quantitative metabolomics of *Penicillium chrysogenum*. *Metabolomics.* 2012;8:727–35.
53. Ruijter GJG, Visser J. Determination of intermediary metabolites in *Aspergillus niger*. *J Microbiol Methods.* 1996;25:295–302.
54. Bolten CJ, Kiefer P, Letisse F, Portais JC, Wittmann C. Sampling for metabolome analysis of microorganisms. *Anal Chem.* 2007;79:3843–9.
55. Ewald JC, Heux S, Zamboni N. High-throughput quantitative metabolomics: Workflow for cultivation, quenching, and analysis of yeast in a multiwell format. *Anal Chem.* 2009;81:3623–9.
56. Wittmann C, Krömer JO, Kiefer P, Binz T, Heinzle E. Impact of the cold shock phenomenon on quantification of intracellular metabolites in bacteria. *Anal Biochem.* 2004;327:135–9.

57. Letisse F, Lindley ND. An intracellular metabolite quantification technique applicable to polysaccharide-producing bacteria. *Biotechnol Lett.* 2000;22:1673–7.
58. Link H, Anselment B, Weuster-Botz D. Leakage of adenylates during cold methanol/glycerol quenching of *Escherichia coli*. *Metabolomics.* 2008;4:240–7.
59. Faijes M, Mars AE, Smid EJ. Comparison of quenching and extraction methodologies for metabolome analysis of *Lactobacillus plantarum*. *Microb Cell Fact.* 2007;6:27. doi:10.1186/1475-2859-6-27.
60. Meyer H, Liebeke M, Lalk M. A protocol for the investigation of the intracellular *Staphylococcus aureus* metabolome. *Anal Biochem.* 2010;401:250–9.
61. Krall L, Huege J, Catchpole G, Steinhauser D, Willmitzer L. Assessment of sampling strategies for gas chromatography-mass spectrometry (GC-MS) based metabolomics of cyanobacteria. *J Chromatogr B Anal Technol Biomed Life Sci.* 2009;877:2952–60.
62. Jozefczuk S, Klie S, Catchpole G, Szymanski J, Cuadros-Inostroza A, Steinhauser D, et al. Metabolomic and transcriptomic stress response of *Escherichia coli*. *Mol Syst Biol.* 2010;6:1–16. doi:10.1038/msb.2010.18.
63. Villas-Bôas SG, Højer-Pedersen J, Åkesson M, Smedsgaard J, Nielsen J. Global metabolite analysis of yeast: Evaluation of sample preparation methods. *Yeast.* 2005;22:1155–69.
64. Wu L, Mashego MR, Van Dam JC, Proell AM, Vinke JL, Ras C, et al. Quantitative analysis of the microbial metabolome by isotope dilution mass spectrometry using uniformly ¹³C-labeled cell extracts as internal standards. *Anal Biochem.* 2005;336:164–71.
65. da Luz JA, Hans E, Zeng AP. Automated fast filtration and on-filter quenching improve the intracellular metabolite analysis of microorganisms. *Eng Life Sci.* 2014;14:135–42.
66. Lin CY, Viant MR, Tjeerdema RS. Metabolomics: Methodologies and applications in the environmental sciences. *J Pestic Sci.* 2006;31:245–51. doi:10.1584/jpestics.31.245.

67. Jäpelt KB, Christensen JH, Villas-Bôas SG. Metabolic fingerprinting of *Lactobacillus paracasei*: the optimal quenching strategy. *Microb Cell Fact.* 2015;14:132. doi:10.1186/s12934-015-0322-5.
68. Volmer M, Northoff S, Scholz S, Thüte T, Büntemeyer H, Noll T. Fast filtration for metabolome sampling of suspended animal cells. *Biotechnol Lett.* 2011;33:495–502.
69. Hernández Bort JA, Shanmukam V, Pabst M, Windwarder M, Neumann L, Alchalabi A, et al. Reduced quenching and extraction time for mammalian cells using filtration and syringe extraction. *J Biotechnol.* 2014;182–183:97–103.
70. Kapoore RV, Coyle R, Staton CA, Brown NJ, Vaidyanathan S. Influence of washing and quenching in profiling the metabolome of adherent mammalian cells: a case study with the metastatic breast cancer cell line MDA-MB-231. *Analyst.* 2017;142:2038–49. doi:10.1039/C7AN00207F.
71. Atkinson DE, Walton GM. Adenosine Metabolic. *Enzyme.* 1967;:3239–41.
72. Lester RT and Talwalkar RL. The response of diphosphoinositide and triphosphoinositide to perturbations of the adenylate energy charge in cells of *Saccharomyces cerevisiae*. *Biochim Biophys Acta.* 1973;306:412–21.
73. Poolman B, Konings WN. Relation of growth of *Streptococcus lactis* and *Streptococcus cremoris* to amino acid transport. *J Bacteriol.* 1988;170:700–7.
74. Coulier L, Bas R, Jespersen S, Verheij E, Van Der Werf MJ, Hankemeier T. Simultaneous quantitative analysis of metabolites using ion-pair liquid chromatography-electrospray ionization mass spectrometry. *Anal Chem.* 2006;78:6573–82.
75. Mashego MR, Wu L, Van Dam JC, Ras C, Vinke JL, Van Winden WA, et al. MIRACLE: Mass Isotopomer Ratio Analysis of U-13C-Labeled Extracts. A New Method for Accurate Quantification of Changes in Concentrations of Intracellular Metabolites. *Biotechnol Bioeng.* 2004;85:620–8.

76. Castrillo JI, Hayes A, Mohammed S, Gaskell SJ, Oliver SG. An optimized protocol for metabolome analysis in yeast using direct infusion electrospray mass spectrometry. *Phytochemistry*. 2003;62:929–37.
77. Hajjaj H, Blanc PJ, Goma G, Franc J. Sampling techniques and comparative extraction procedures for quantitative determination of intra- and extracellular metabolites in ϕ filamentous fungi. *FEMS Microbiol Lett*. 1998;164:1–6.
78. Oldiges M, Kunze M, Degenring D, Sprenger GA, Takors R. L05 : 1 : 370 . Stimulation , monitoring and analysis of pathway dynamics by metabolic profiling in the aromatic amino acid pathway. 2004;:2006.
79. Al Zaid Siddiquee K, Arauzo-Bravo MJ, Shimizu K. Metabolic flux analysis of pykF gene knockout *Escherichia coli* based on ^{13}C -labeling experiments together with measurements of enzyme activities and intracellular metabolite concentrations. *Appl Microbiol Biotechnol*. 2004;63:407–17.
80. Buziol S, Bashir I, Baumeister A, Claaben W, Noisommit-Rizzi N, Mailinger W, et al. New bioreactor-coupled rapid stopped-flow sampling technique for measurements of metabolite dynamics on a subsecond time scale. *Biotechnol Bioeng*. 2002;80:632–6.
81. Chassagnole C, Noisommit-Rizzi N, Schmid JW, Mauch K, Reuss M. Dynamic modeling of the central carbon metabolism of *Escherichia coli*. *Biotechnol Bioeng*. 2002;79:53–73.
82. Gonzalez B, François J, Renaud M. A rapid and reliable method for metabolite extraction in yeast using boiling buffered ethanol. *Yeast*. 1997;13:1347–56.
83. Visser D, Van Zuylen GA, Van Dam JC, Oudshoorn A, Eman MR, Ras C, et al. Rapid sampling for analysis of in vivo kinetics using the BioScope: A system for continuous-pulse experiments. *Biotechnol Bioeng*. 2002;79:674–81.
84. Theobald U, Mailinger W, Baltes M, Rizzi M. In Vivo Analysis of Metabolic Dynamics in *Saccharomyces cerevisiae*: I . Experimental Observations. 1997.

85. Theobald U, Mailinger W, Reuss M, Rizzi M. In Vivo Analysis of Glucose-Induced Fast Changes in Yeast Adenine Nucleotide Pool Applying a Rapid Sampling Technique. *Analytical Biochemistry*. 1993;214:31–7. doi:10.1006/abio.1993.1452.
86. Bhattacharya M, Fuhrman L, Ingram A, Nickerson KW, Conway T. Single-run separation and detection of multiple metabolic intermediates by anion-exchange high-performance liquid chromatography and application to cell pool extracts prepared from *Escherichia coli*. *Anal Biochem*. 1995;232:98–106. doi:10.1006/abio.1995.9954.
87. Canelas AB, Ras C, ten Pierick A, van Dam JC, Heijnen JJ, van Gulik WM. Leakage-free rapid quenching technique for yeast metabolomics. *Metabolomics*. 2008;4:226–39.
88. Shryock JC, Rubio R, Berne RM. Extraction of adenine nucleotides from cultured endothelial cells. *Anal Biochem*. 1986;159:73–81. <http://www.ncbi.nlm.nih.gov/pubmed/3028213>.
89. Defernez M, Gunning YM, Parr AJ, Shepherd LVT, Davies H V., Colquhoun IJ. NMR and HPLC-UV profiling of potatoes with genetic modifications to metabolic pathways. *J Agric Food Chem*. 2004;52:6075–85.
90. Gidman EA, Goodacre R, Emmett B, Wilson DB, Carroll JA, Caporn SJM, et al. Metabolic fingerprinting for bio-indication of nitrogen responses in *Calluna vulgaris* heath communities. *Metabolomics*. 2005;1:279–85.
91. Harrigan GG, LaPlante RH, Cosma GN, Cockerell G, Goodacre R, Maddox JF, et al. Application of high-throughput Fourier-transform infrared spectroscopy in toxicology studies: Contribution to a study on the development of an animal model for idiosyncratic toxicity. *Toxicol Lett*. 2004;146:197–205.
92. Wilson ID, Plumb R, Granger J, Major H, Williams R, Lenz EM. HPLC-MS-based methods for the study of metabonomics. *J Chromatogr B Anal Technol Biomed Life Sci*. 2005;817:67–76.

93. Theodoridis G, Gika HG, Wilson ID. LC-MS-based methodology for global metabolite profiling in metabonomics/metabolomics. *TrAC Trends Anal Chem.* 2008;27:251–60. doi:10.1016/j.trac.2008.01.008.
94. Viant MR, Rosenblum ES, Tjeerdema RS. NMR-Based Metabolomics: A Powerful Approach for Characterizing the Effects of Environmental Stressors on Organism Health. *Environ Sci Technol.* 2003;37:4982–9.
95. Lenz EM, Weeks JM, Lindon JC, Osborn D, Nicholson JK. Qualitative high field ¹H-NMR spectroscopy for the characterization of endogenous metabolites in earthworms with biochemical biomarker potential. *Metabolomics.* 2005;1:123–36.
96. Foxall PJ, Mellotte GJ, Bending MR, Lindon JC, Nicholson JK. NMR spectroscopy as a novel approach to the monitoring of renal transplant function. *Kidney Int.* 1993;43:234–45. doi:10.1038/ki.1993.37.
97. Bedair M, Sumner LW. Current and emerging mass-spectrometry technologies for metabolomics. *TrAC Trends Anal Chem.* 2008;27:238–50. doi:10.1016/j.trac.2008.01.006.
98. Breitling R, Pitt AR, Barrett MP. Precision mapping of the metabolome. *Trends Biotechnol.* 2006;24:543–8.
99. Moco S, Vervoort J, Moco S, Bino RJ, De Vos RCH, Bino R. Metabolomics technologies and metabolite identification. *TrAC - Trends Anal Chem.* 2007;26:855–66.
100. Spratlin JL, Serkova NJ, Eckhardt SG. Clinical Applications of Metabolomics in Oncology: A Review. *Clin Cancer Res.* 2009;15:431–40.
101. Madsen R, Lundstedt T, Trygg J. Chemometrics in metabolomics-A review in human disease diagnosis. *Anal Chim Acta.* 2010;659:23–33.
102. Dunn WB, Ellis DI. Metabolomics: Current analytical platforms and methodologies. *TrAC Trends Anal Chem.* 2005;24:285–94. doi:10.1016/j.trac.2004.11.021.

103. Allen J, Davey HM, Broadhurst D, Heald JK, Rowland JJ, Oliver SG, et al. High-throughput classification of yeast mutants for functional genomics using metabolic footprinting. *Nat Biotechnol.* 2003;21:692–6. doi:10.1038/nbt823.
104. Schauer N, Steinhauser D, Strelkov S, Schomburg D, Allison G, Moritz T, et al. GC-MS libraries for the rapid identification of metabolites in complex biological samples. *FEBS Lett.* 2005;579:1332–7.
105. Lapainis T, Rubakhin SS, Sweedler J V. Capillary electrophoresis with electrospray ionization mass spectrometric detection for single-cell metabolomics. *Anal Chem.* 2009;81:5858–64. doi:10.1021/ac900936g.
106. Cai J, Henion J, Toxicology A, Drive W. Capillary electrophoresis-mass spectrometry. *J Chromatogr A.* 1995;703:667–92.
107. Frank T, Engel K-H. *Metabolomic analysis of plants and crops.* Elsevier Masson SAS.; 2013. doi:10.1533/9780857098818.2.148.
108. Naz S, Moreira dos Santos DC, García A, Barbas C. Analytical protocols based on LC–MS, GC–MS and CE–MS for nontargeted metabolomics of biological tissues. *Bioanalysis.* 2014;6:1657–77. doi:10.4155/bio.14.119.
109. Gika HG, Theodoridis GA, Wingate JE, Wilson ID. Within-day reproducibility of an HPLC-MS-based method for metabonomic analysis: Application to human urine. *J Proteome Res.* 2007;6:3291–303.
110. Mass Spectrometry Quantitation. <http://www.ionsource.com/tutorial/msquan/intro.htm>. Accessed 7 Nov 2017.
111. Olsen BA, Pack BW. *Hydrophilic interaction chromatography: A guide for practitioners.* New Jersey; 2013.
112. Knee JM, Rzezniczak TZ, Barsch A, Guo KZ, Merritt TJS. A novel ion pairing LC/MS metabolomics protocol for study of a variety of biologically relevant polar metabolites. *J*

REFERENCE LIST

Chromatogr B Anal Technol Biomed Life Sci. 2013;936:63–73. doi:10.1016/j.jchromb.2013.07.027.

113. Mahrous EA, Farag MA. Two dimensional NMR spectroscopic approaches for exploring plant metabolome: A review. J Adv Res. 2015;6:3–15. doi:10.1016/j.jare.2014.10.003.

114. Putri SP, Yamamoto S, Tsugawa H, Fukusaki E. Current metabolomics: Technological advances. J Biosci Bioeng. 2013;116:9–16. doi:10.1016/j.jbiosc.2013.01.004.

115. Ashwani Pareek, S.K. Sopory, Hans J. Bohnert G. Abiotic Stress Adaptation in Plants. 2010. doi:10.1007/978-90-481-3112-9.

116. Kim HK, Choi YH, Verpoorte R. NMR-based plant metabolomics: Where do we stand, where do we go? Trends Biotechnol. 2011;29:267–75. doi:10.1016/j.tibtech.2011.02.001.

117. Griffin JL. Metabonomics: NMR spectroscopy and pattern recognition analysis of body fluids and tissues for characterisation of xenobiotic toxicity and disease diagnosis. Curr Opin Chem Biol. 2003;7:648–54.

118. ThermoFisher. Metabolomics Data Analysis.

<https://www.thermofisher.com/dk/en/home/industrial/mass-spectrometry/mass-spectrometry-learning-center/mass-spectrometry-applications-area/metabolomics-mass-spectrometry/metabolomics-data-analysis.html#>. Accessed 6 Nov 2017.

119. Ren S, Hinzman AA, Kang EL, Szczesniak RD, Lu LJ. Computational and statistical analysis of metabolomics data. Metabolomics. 2015;11:1492–513.

120. Nicholson JK, Connelly J, Lindon JC, Holmes E. INNOVATIONMetabonomics: a platform for studying drug toxicity and gene function. Nat Rev Drug Discov. 2002;1:153–61. doi:10.1038/nrd728.

121. Tyagi S, Raghvendra, Singh U, Kalra T, Munjal K. Applications of metabolomics - A systematic study of the unique chemical fingerprints: An overview. Int J Pharm Sci Rev Res.

2010;3:83–6.

122. Gunasekaran R, Kasirajan T. Principal Component Analysis (PCA) for Beginners. 2017;2:9–11.

123. Eriksson L, Andersson PL, Johansson E, Tysklind M. Megavariate analysis of environmental QSAR data. Part I - A basic framework founded on principal component analysis (PCA), partial least squares (PLS), and statistical molecular design (SMD). *Mol Divers*. 2006;10:169–86.

124. Suryanarayana TM., Mistry PB. Principal Component Regression for Crop Yield Estimation. 2016;:17–26. doi:10.1007/978-981-10-0663-0.

125. Tobias RD. An introduction to partial least squares regression. *SAS Conf Proc SAS Users Gr Int 20 (SUGI 20)*. 1995;:2–5.

126. Abdi H. Partial least squares regression and projection on latent structure regression. *Wiley Interdiscip Rev Comput* 2010;2:97–106. doi:10.1002/wics.051.

127. Novik G, Savich V, Kiseleva E. An Insight Into Beneficial *Pseudomonas* bacteria. *Microbiol Agric Hum Heal*. 2015;:73–105. doi:10.5772/60502.

128. Jensen, Lars Juhl, Marie Skovgaard, Thomas Sicheritz-Ponten NT, Hansen, Helle Johansson, Merete Kjær Jørgensen, Kristoffer Kiil PFH and DU. Comparative genomics of four *Pseudomonas* species. J. L. Ramo. Kluwer Academic/Plenum; 2004.

129. De Smet J, Hendrix H, Blasdel BG, Danis-Wlodarczyk K, Lavigne R. *Pseudomonas* predators: understanding and exploiting phage–host interactions. *Nat Rev Microbiol*. 2017;15:517–30. doi:10.1038/nrmicro.2017.61.

130. Sneath PHA, Stevens M, Sackin MJ. Numerical taxonomy of *Pseudomonas* based on published records of substrate utilization. *Antonie Van Leeuwenhoek*. 1981;47:423–48.

131. Anzai Y, Kim H, Park J, Wakabayashi H, Oyaizu H, The P. Phylogenetic affiliation of

the *pseudomonads* based on 16S rRNA sequence. *Int J Syst Evol Microbiol*. 2000;50:1563–89.

132. Yamamoto S, Kasai H, Arnold DL, Jackson RW, Vivian A, Harayama S. Phylogeny of the genus *Pseudomonas*: intrageneric structure reconstructed from the nucleotide sequences of *gyrB* and *rpoD* genes. *Microbiology*. 2000;146:2385–94.

133. Oyaizu H, Komagata K. Grouping of *Pseudomonas* species on the basis of cellular fatty acid composition and the quinone system with special reference to the existence of 3-hydroxy fatty acids. *J Gen Appl Microbiol*. 1983;29:17–40.

134. Vancanneyti M, Witt S, Abraham W-R, Kersters K, Fredrickson HL. Fatty acid Content in Whole-cell Hydrolysates and Phospholipid and Phospholipid Fractions of *Pseudomonads*: a Taxonomic Evaluation. *Syst Appl Microbiol*. 1996;19:528–40.

135. Kersters K, Ludwig W, Vancanneyt M, De Vos P, Gillis M, Schleifer K-H. Recent Changes in the Classification of the *Pseudomonads*: an Overview. *Syst Appl Microbiol*. 1996;19:465–77. doi:10.1016/S0723-2020(96)80020-8.

136. Nikel PI, Martínez-García E, de Lorenzo V. Biotechnological domestication of *pseudomonas* using synthetic biology. *Nat Rev Microbiol*. 2014;12:368–79. doi:10.1038/nrmicro3253.

137. Bayley SA, Duggleby CJ, Worsey MJ, Williams PA, Hardy KG, Broda P. Two Modes of Loss of the Tol Function from *Pseudomonas putida* mt-2. *Molec gen Genet*. 1977;154:203.

138. Bagdasarian MM, Lurz R, Rückert B, Franklin FC, Bagdasarian MM, Frey J, et al. Specific-purpose plasmid cloning vectors II. Broad host range, high copy number, RSF1010-derived vectors, and a host-vector system for gene cloning in *Pseudomonas*. *Gene*. 1981;16:237–47. doi:doi:10.1016/0378-1119(81)90080-9.

139. Nelson KE, Weinel C, Paulsen IT, Dodson RJ, Hilbert H, Martins dos Santos VAP, et al. Complete genome sequence and comparative analysis of the metabolically versatile

Pseudomonas putida KT2440. Environ Microbiol. 2002;4:799–808.

140. Yu S, Plan MR, Winter G, Krömer JO. Metabolic Engineering of *Pseudomonas putida* KT2440 for the Production of para-Hydroxy Benzoic Acid. Front Bioeng Biotechnol. 2016;4 November:1–10. doi:10.3389/fbioe.2016.00090.

141. Poblete-Castro I, Becker J, Dohnt K, Santos VM Dos, Wittmann C. Industrial biotechnology of *Pseudomonas putida* and related species. Applied Microbiology and Biotechnology. 2012;93:2279–90.

142. Nickel PI, Chavarría M, Fuhrer T, Sauer U, De Lorenzo V. *Pseudomonas putida* KT2440 strain metabolizes glucose through a cycle formed by enzymes of the Entner-Doudoroff, embden-meyerhof-parnas, and pentose phosphate pathways. J Biol Chem. 2015;290:25920–32.

143. Martins Dos Santos VAP, Heim S, Moore ERB, Stratz M, Timmis KN. Insights into the genomic basis of niche specificity of *Pseudomonas putida* KT2440. Environ Microbiol. 2004;6:1264–86.

144. Lessie TG, Phibbs PV. Alternative pathways of carbohydrate utilization in *Pseudomonads*. AnnuRevMicrobiol. 1984;38:359–87.

145. Volmer J, Neumann C, Bühler B, Schmid A. Engineering of *Pseudomonas taiwanensis* VLB120 for constitutive solvent tolerance and increased specific styrene epoxidation activity. Appl Environ Microbiol. 2014;80:6539–48.

146. Köhler KAK, Blank LM, Frick O, Schmid A. D-Xylose assimilation via the Weimberg pathway by solvent-tolerant *Pseudomonas taiwanensis* VLB120. Environ Microbiol. 2015;17:156–70.

147. Köhler KAK, Rückert C, Schatschneider S, Vorhölter FJ, Szczepanowski R, Blank LM, et al. Complete genome sequence of *Pseudomonas sp.* strain VLB120 a solvent tolerant, styrene degrading bacterium, isolated from forest soil. J Biotechnol. 2013;168:729–30.

doi:10.1016/j.jbiotec.2013.10.016.

148. Hong SJ, Park GS, Khan AR, Jung BK, Shin JH. Draft genome sequence of a caprolactam degrader bacterium: *Pseudomonas taiwanensis* strain SJ9. *Brazilian J Microbiol.* 2017;48:187–8. doi:10.1016/j.bjm.2015.09.002.

149. Thomashow LS. Frequency of Antibiotic-Producing *Pseudomonas spp.* in Natural Environments. 1997;63:881–7.

150. Dowling DN, O’Gara F. Metabolites of *Pseudomonas* involved in the biocontrol of plant disease. *Trends Biotechnol.* 1994;12:133–41.

151. Kulkarni RS, Kanekar PP. Bioremediation of ϵ -caprolactam from nylon-6 waste water by use of *Pseudomonas aeruginosa* MCM B-407. *Curr Microbiol.* 1998;37:191–4.

152. Roselló-Mora R, Lalucat J, García-Valdés E. Comparative biochemical and genetic analysis of naphthalene degradation among *Pseudomonas stutzeri* strains. *Appl Environ Microbiol.* 1994;60:966–72.

153. Zylstra GJ, McCombie WR, Gibson DT, Finette BA. Toluene degradation by *Pseudomonas putida* F1: genetic organization of the tod operon. *Appl Environ Microbiol.* 1988;54:1498–503.

154. Ridgway HF, Safarik J, Phipps D, Carl P, Clark D. Identification and catabolic activity of well-derived gasoline-degrading bacteria from a contaminated aquifer. *Appl Environ Microbiol.* 1990;56:3565–75.

155. Loh KC, Cao B. Paradigm in biodegradation using *Pseudomonas putida*-A review of proteomics studies. *Enzyme Microb Technol.* 2008;43:1–12.

156. Gross R, Lang K, Buhler K, Schmid A. Characterization of a biofilm membrane reactor and its prospects for fine chemical synthesis. *Biotechnol Bioeng.* 2010;105:705–17.

157. Halan B, Schmid A, Buehler K. Real-time solvent tolerance analysis of *Pseudomonas*

- sp.* Strain VLB120dC catalytic biofilms. *Appl Environ Microbiol.* 2011;77:1563–71.
158. Sánchez C. Lignocellulosic residues: Biodegradation and bioconversion by fungi. *Biotechnol Adv.* 2009;27:185–94. doi:10.1016/j.biotechadv.2008.11.001.
159. Almeida JRM, Modig T, Petersson A, Hähn-Hägerdal B, Lidén G, Gorwa-Grauslund MF. Increased tolerance and conversion of inhibitors in lignocellulosic hydrolysates by *Saccharomyces cerevisiae*. *J Chem Technol Biotechnol.* 2007;82:340–9.
160. Lieth H. the Major Vegetation Units. 1975;:10–1.
161. Pérez J, Muñoz-Dorado J, De La Rubia T, Martínez J. Biodegradation and biological treatments of cellulose, hemicellulose and lignin: An overview. *Int Microbiol.* 2002;5:53–63.
162. Kumar A, Gautam A, Dutt D. Biotechnological Transformation of Lignocellulosic Biomass in to Industrial Products: An Overview. *Adv Biosci Biotechnol.* 2016;7:149–68. doi:10.4236/abb.2016.73014.
163. Chen R, Wang YZ, Liao Q, Zhu X, Xu TF. Hydrolysates of lignocellulosic materials for biohydrogen production. *BMB Rep.* 2013;46:244–51.
164. Anwar Z, Gulfraz M, Irshad M. Agro-industrial lignocellulosic biomass a key to unlock the future bio-energy: A brief review. *J Radiat Res Appl Sci.* 2014;7:163–73. doi:10.1016/j.jrras.2014.02.003.
165. E. AA, D. M-C. Oyster mushrooms (*Pleurotus*) are useful for utilizing lignocellulosic biomass. *African J Biotechnol.* 2015;14:52–67. doi:10.5897/AJB2014.14249.
166. Alvira P, Tomas-Pejo E, Ballesteros M, Negro MJ. Pretreatment technologies for an efficient bioethanol production process based on enzymatic hydrolysis: A review. *Bioresour Technol.* 2010;101:4851–61. doi:10.1016/j.biortech.2009.11.093.
167. Sun Y, Cheng J. Hydrolysis of lignocellulosic materials for ethanol production : a review

- q. *Bioresour Technol.* 2002;83:1–11. doi:10.1016/S0960-8524(01)00212-7.
168. Zhu Z, Simister R, Bird S, J. McQueen-Mason S, D. Gomez L, J. Macquarrie D. Microwave assisted acid and alkali pretreatment of *Miscanthus* biomass for biorefineries. *AIMS Bioeng.* 2015;2:449–68. doi:10.3934/bioeng.2015.4.449.
169. Wordofa G. Effect of thermal pretreatment on chemical composition and biogas production from kitchen waste. 2014;:37.
170. Jansson LJ, Martin C. Pretreatment of lignocellulose: Formation of inhibitory by-products and strategies for minimizing their effects. *Bioresour Technol.* 2016;199:103–12.
171. Zha Y, Muilwijk B, Coulier L. Inhibitory Compounds in Lignocellulosic Biomass Hydrolysates during Hydrolysate Fermentation Processes. *J Bioprocess Biotech.* 2012;2:1–11.
172. Liu X, Xu W, Mao L, Zhang C, Yan P, Xu Z, et al. Lignocellulosic ethanol production by starch-base industrial yeast under PEG detoxification. *Sci Rep.* 2016;6:20361. doi:10.1038/srep20361.
173. Fillat Ú, Ibarra D, Eugenio M, Moreno A, Tomás-Pejó E, Martín-Sampedro R. Laccases as a Potential Tool for the Efficient Conversion of Lignocellulosic Biomass: A Review. *Fermentation.* 2017;3:17. doi:10.3390/fermentation3020017.
174. Moreno AD, Alvira P, Ibarra D, Tomás-pejó E. Production of Platform Chemicals from Sustainable Resources. 2017. doi:10.1007/978-981-10-4172-3.
175. Klinke HB, Thomsen AB, Ahring BK. Inhibition of ethanol-producing yeast and bacteria by degradation products produced during pre-treatment of biomass. *Appl Microbiol Biotechnol.* 2004;66:10–26.
176. Piotrowski JS, Zhang Y, Bates DM, Keating DH, Sato TK, Ong IM, et al. Death by a thousand cuts: The challenges and diverse landscape of lignocellulosic hydrolysate inhibitors. *Front Microbiol.* 2014;5 MAR:1–8.

177. Dunlop A.P. Furfural formation and behaviour. *Ind Eng Chem.* 1948;40:204–9.
178. Ulbricht RJ, Northup SJ, Thomas JA. A review of 5-hydroxymethylfurfural (HMF) in parenteral solutions. *Toxicol Sci.* 1984;4:843–53.
179. Mills TY, Sandoval NR, Gill RT. Cellulosic hydrolysate toxicity and tolerance mechanisms in *Escherichia coli*. *Biotechnol Biofuels.* 2009;2:26. doi:10.1186/1754-6834-2-26.
180. Lee J. Biological conversion of lignocellulosic biomass to ethanol. *J Biotechnol.* 1997;56:1–24.
181. Harrison SJ, Herrgård MJ. The Uses and Future Prospects of Metabolomics and Targeted Metabolite Profiling in Cell Factory Development. *Ind Biotechnol.* 2013;9:196–202. doi:10.1089/ind.2013.0008.
182. Latrach Tlemçani L, Corroler D, Barillier D, Mosrati R. Physiological states and energetic adaptation during growth of *Pseudomonas putida* mt-2 on glucose. *Arch Microbiol.* 2008;190:141–50.
183. R Development Core Team R. R: A Language and Environment for Statistical Computing. 2011. doi:10.1007/978-3-540-74686-7.
184. Rabinowitz JD, Kimball E. Acidic acetonitrile for cellular metabolome extraction from *Escherichia coli*. *Anal Chem.* 2007;79:6167–73.
185. Prasad Maharjan R, Ferenci T. Global metabolite analysis: The influence of extraction methodology on metabolome profiles of *Escherichia coli*. *Anal Biochem.* 2003;313:145–54.
186. Ramos A, Neves AR, Santos H. Metabolism of lactic acid bacteria studied by nuclear magnetic resonance. *Antonie Van Leeuwenhoek.* 2002;82:249–61. doi:10.1007/978-94-017-2029-8_15.
187. Yasid NA binti. Metabolite analysis of *Escherichia coli* in response to changes in

oxygen levels. Univ Sheff. 2013.

188. Klinke HB, Olsson L, Thomsen AB, Ahring BK. Potential inhibitors from wet oxidation of wheat straw and their effect on ethanol production of *Saccharomyces cerevisiae*: wet oxidation and fermentation by yeast. *Biotechnol Bioeng.* 2003;81:738–47. doi:10.1002/bit.10523.

189. B. H-H. Detoxification of wood hydrolysate with laccase and peroxidase from the white-rot fungus *T. versicolor*. *Appl Microb Biotechnol.* 1998;49:691.

190. Larsson S, Quintana-Sáinz A, Reimann A, Nilvebrant NO, Jönsson LJ. Influence of lignocellulose-derived aromatic compounds on oxygen-limited growth and ethanolic fermentation by *Saccharomyces cerevisiae*. *Appl Biochem Biotechnol.* 2000;84–86:617–32. doi:10.1385/ABAB:84-86:1-9:617.

191. Suko AV, Bura R. Enhanced Xylitol and Ethanol Yields by Fermentation Inhibitors in Steam-Pretreated Lignocellulosic Biomass. *Ind Biotechnol.* 2016;12:187–94.

192. Almeida JRM, Runquist D, Sánchez Nogué V, Lidén G, Gorwa-Grauslund MF. Stress-related challenges in pentose fermentation to ethanol by the yeast *Saccharomyces cerevisiae*. *Biotechnol J.* 2011;6:286–99.

193. Narayanan V, Sánchez i Nogué V, van Niel EWJ, Gorwa-Grauslund MF. Adaptation to low pH and lignocellulosic inhibitors resulting in ethanolic fermentation and growth of *Saccharomyces cerevisiae*. *AMB Express.* 2016;6:59. doi:10.1186/s13568-016-0234-8.

194. Fu S, Hu J, Li H. Inhibitory Effects of Biomass Degradation Products on Ethanol Fermentation and a Strategy to Overcome Them. *BioResources.* 2014;9 Dunlop 1948:4323–35.

195. Bräsen C, Schönheit P. Regulation of acetate and acetyl-CoA converting enzymes during growth on acetate and/or glucose in the halophilic archaeon *Haloarcula marismortui*. *FEMS Microbiol Lett.* 2004;241:21–6.

196. Liang M-H, Qv X-Y, Jin H-H, Jiang J-G. Characterization and expression of AMP-forming Acetyl-CoA Synthetase from *Dunaliella tertiolecta* and its response to nitrogen starvation stress. *Sci Rep.* 2016;6:23445. doi:10.1038/srep23445.
197. Ask M, Bettiga M, Mapelli V, Olsson L. The influence of HMF and furfural on redox-balance and energy-state of xylose-utilizing *Saccharomyces cerevisiae*. *Biotechnol Biofuels.* 2013;6:22. doi:10.1186/1754-6834-6-22.
198. Hara M, Matsuura T, Kojima S. *Innovative Medicine.* 2015. doi:10.1007/978-4-431-55651-0.
199. Singh R, Mailloux RJ, Puiseux-Dao S, Appanna VD. Oxidative stress evokes a metabolic adaptation that favors increased NADPH synthesis and decreased NADH production in *Pseudomonas fluorescens*. *J Bacteriol.* 2007;189:6665–75.
200. Guo W, Chen Y, Wei N, Feng X. Investigate the metabolic reprogramming of *Saccharomyces cerevisiae* for enhanced resistance to mixed fermentation inhibitors via ¹³C metabolic flux analysis. *PLoS One.* 2016;11:1–15.

LIST OF PUBLICATIONS

PAPER I

**Quantifying the Metabolome of *Pseudomonas taiwanensis* VLB120: Evaluation of Hot
and Cold Combined Quenching/Extraction Approaches**

Quantifying the Metabolome of *Pseudomonas taiwanensis* VLB120: Evaluation of Hot and Cold Combined Quenching/Extraction Approaches

Gossa G. Wordofa,[†] Mette Kristensen,[†] Lars Schrübbers,[†] Douglas McCloskey,[‡] Jochen Forster,[†] and Konstantin Schneider^{*,†}

[†]Novo Nordisk Foundation Center for Biosustainability, Technical University of Denmark, DK-2800 Lyngby, Denmark

[‡]Department of Bioengineering, University of California, San Diego, 9500 Gilman Drive, La Jolla, California 92093-0412, United States

Supporting Information

ABSTRACT: Absolute quantification of free intracellular metabolites is a valuable tool in both pathway discovery and metabolic engineering. In this study, we conducted a comprehensive examination of different hot and cold combined quenching/extraction approaches to extract and quantify intracellular metabolites of *Pseudomonas taiwanensis* (*P. taiwanensis*) VLB120 to provide a useful reference data set of absolute intracellular metabolite concentrations. The suitability of commonly used metabolomics tools including a pressure driven fast filtration system followed by combined quenching/extraction techniques (such as cold methanol/acetonitrile/water, hot water, and boiling ethanol/water, as well as cold ethanol/water) were tested and evaluated for *P. taiwanensis* VLB120 metabolome analysis. In total 94 out of 107 detected intracellular metabolites were quantified using an isotope-ratio-based approach. The quantified metabolites include amino acids, nucleotides, central carbon metabolism intermediates, redox cofactors, and others. The acquired data demonstrate that the pressure driven fast filtration approach followed by boiling ethanol quenching/extraction is the most adequate technique for *P. taiwanensis* VLB120 metabolome analysis based on quenching efficiency, extraction yields of metabolites, and experimental reproducibility.



Microbial cells have been used as biocatalysts for hundreds of years in the production of alcoholic beverages, fermented foods, and chemicals from naturally available carbon and energy sources. However, one factor limiting the application of whole cells as biocatalysts, especially for biofuel production, is the toxicity of the corresponding products, which typically have detrimental effects on cellular membranes.¹ This results in low product titers as well as limited process stability, both having a negative impact on overall productivity and feasibility of such processes.² Different *Pseudomonas* species are known to have an increased inherent solvent tolerance and are therefore a promising host for the biotechnological production of such solvents.^{1,2}

Pseudomonas taiwanensis (*P. taiwanensis*) VLB120 is an obligate aerobic, biofilm-forming organism that was isolated from soil at the Institute of Microbiology, University of Stuttgart, Germany.^{2–4} The strain can utilize a wide range of organic molecules as carbon sources including pentose/hexose sugars³ and aromatic hydrocarbons such as styrene.⁵ *P. taiwanensis* VLB120 is a solvent-tolerant *Pseudomonas* strain exhibiting the ability to utilize pentose sugars (mainly D-xylose)³ as carbon source which is one of the most abundant sugars in hemicellulose accounting for up to 30% of the

lignocellulosic biomass.⁶ Those two features are highly beneficial regarding bulk production of solvents and biofuels from renewable feedstocks using cell factories.

As this wild type isolate does not natively produce any high-value products, engineering native pathways leading to the desired products or expressing heterologous production pathways are therefore common means to generate high-level production strains. As most of these bioprocesses require a detailed understanding of cellular metabolism, absolute quantification of free intracellular metabolites is a meaningful tool to assess the metabolic state of the cell, identify bottlenecks in cellular metabolism, and assess toxicity derived impacts.⁷ However, analysis and quantification of intracellular metabolites is a challenging task due to their high turnover rates and chemical diversity. Reliable and accurate methods for quenching cellular metabolism and metabolite extraction to investigate the in vivo metabolic state of a cell at a given specific condition are vital in metabolome studies, as they significantly affect the number and quantity of metabolites detected.⁸

Received: March 3, 2017

Accepted: July 20, 2017

Published: July 20, 2017

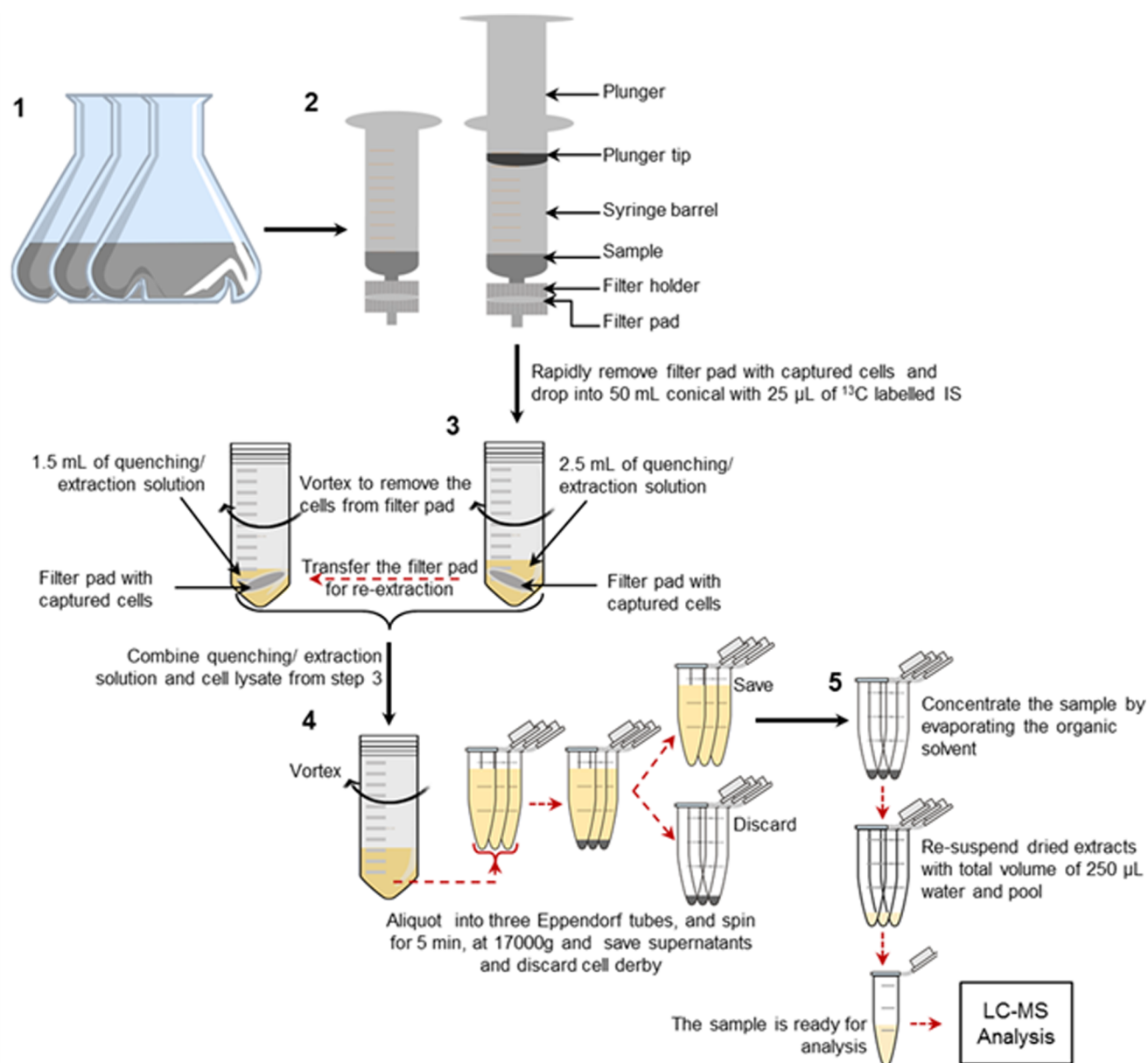


Figure 1. Work flow for cell sampling, quenching/extraction, sample processing, and analysis of the metabolites. Abbreviation: IS, internal standard. (1) Aerobic cultivations of *P. taiwanensis* VLB120 were performed in a 250 mL shake flask (working volume of 25 mL) at 30 °C with shaking at 250 rpm in Delft minimal media. (2) A 2 mL aliquot of cell broth was transferred to a 50 mL syringe barrel attached to a Swinnex filter (Merck Millipore, Hertfordshire, UK) with the plunger removed. The plunger was reinserted into the syringe barrel, and air was rapidly expelled through the filter. (3) The filter pad with captured cells was quickly removed from the filter holder (from step 2) and placed with ^{13}C -labeled IS in the 50 mL conical tube containing 2.5 mL of preheated or precooled extraction solvent and vortexed for 30 s. The filter pad was re-extracted with 1.5 mL of extraction solvent without IS. (4) The extraction solvent and cell lysate from step 3 were pooled and aliquoted into three 1.5 mL size Eppendorf tubes, and centrifuged for 5 min, at 17000g and 4 °C, after which the supernatants were stored in -80 °C and the remaining cell debris was discarded. (5) Samples from step 4 were concentrated by evaporating the organic solvent for about 5 h at 25 °C using a speed vacuum followed by freeze-drying at -40 °C (overnight). All dried extracts were resuspended in 250 μL of LC-MS grade deionized water and stored at -80 °C until analysis. The same procedure was repeated for each biological replicate.

Cold methanol quenching at -40 °C is widely used to quench the cellular metabolism of yeast cells.⁹ This method has also been applied in other studies on different bacteria including *Escherichia coli* (*E. coli*),¹⁰ *Lactococcus lactis* (*Lc. lactis*),¹¹ and *Lactobacillus bulgaricus* (*Lb. bulgaricus*)¹² as well as filamentous fungi such as *Penicillium chrysogenum* (*Pe. chrysogenum*)¹³ and *Aspergillus niger* (*A. niger*).¹⁴ In contrast to yeast cells, intracellular metabolites have been shown to leak from bacterial cells when applying this method, making an accurate assessment of their intracellular concentrations

challenging.^{11,15–17} As an alternative to cold methanol quenching, the fast filtration system followed by combined quenching/extraction proved to be effective in minimizing the losses of intracellular metabolites.^{8,18–20} The ideal combined quenching/extraction technique must stop the biological reactions in a cell and, at the same time, extract as many metabolites as possible in an unbiased and nondestructive manner.²¹ McCloskey et al.²⁰ reported on a pressure driven fast filtration system followed by cold extraction as a fast sampling and quenching method for *E. coli* cells. The authors showed

that the method excels in being fast enough to provide an accurate snapshot of intracellular metabolism while also reducing matrix effects from the media. However, this promising technique has not been tested on organisms other than *E. coli*.

Several authors proposed different solvent extraction techniques including hot methanol for endothelial cells,²² cold methanol for *Pe. chrysogenum*,¹³ boiling ethanol for *Saccharomyces cerevisiae* (*Sa. cerevisiae*),²³ *Monascus ruber* (*M. ruber*),²⁴ and *E. coli*²⁵ methanol/chloroform combinations for yeast,⁹ perchloric acid, and potassium hydroxide for *A. niger*, *S. cerevisiae*, and *E. coli*,^{14,26–28} and hot water for *E. coli*.²⁹ Although most of these techniques were designed for specific classes of metabolites and microorganisms, they are often applied directly in another context without validating them for the given conditions and the investigated organism, which can lead to highly biased results.³⁰ Thus, sampling, quenching, and extraction protocols need to be validated for each microorganism and metabolite of interest. To the best of our knowledge, no strategies were developed or tested for sampling and quantifying the central metabolites of *P. taiwanensis*.

In this study, we have conducted a comprehensive examination of different hot and cold combined quenching/extraction approaches to extract and quantify the metabolome of *P. taiwanensis* VLB120. In addition, we provide a useful reference data set of absolute intracellular metabolite concentrations for this organism. This was done by assessing commonly used metabolomics tools including a pressure driven fast filtration system and four different combined quenching/extraction approaches such as cold ethanol/water, cold methanol/acetonitrile/water, and boiling ethanol/water, as well as hot water. As far as we know, some of these techniques including hot water, cold ethanol, and boiling ethanol have never been tested or used as combined quenching/extraction techniques in metabolome studies even though they have been widely used for extraction of intracellular metabolites after quenching the cell culture either in liquid nitrogen^{19,24,31} or in cold methanol/water (60%, v/v).^{8,9,24,30,32–34}

■ EXPERIMENTAL SECTION

Chemicals and Strain. All chemicals and reagents used in this study were purchased from Sigma-Aldrich (Chemical Co., USA). *P. taiwanensis* VLB120 was obtained from the Institute of Applied Microbiology, RWTH Aachen, Germany.

Growth Conditions. Aerobic cultivations of *P. taiwanensis* VLB 120 were initiated using glycerol stocks. Single colonies were obtained after plating onto solid Luria–Bertani (LB) medium after overnight incubation at 30 °C. An isolated colony was inoculated in a 12 mL tube with 4 mL of minimal medium and grown overnight at 30 °C and 250 rpm. The main culture was carried out from an initial OD₆₀₀ of 0.05 in a 250 mL shake flask (working volume of 25 mL) at 30 °C with shaking at 250 rpm in minimal medium.³⁵ The medium contained the following (L⁻¹): 2.12 g of NaH₂PO₄·2H₂O, 2 g of (NH₄)₂SO₄, 10 mg of EDTA, 0.1 g of MgCl₂·6H₂O, 2 mg of ZnSO₄·7H₂O, 1 mg of CaCl₂·2H₂O, 5 mg of FeSO₄·7H₂O, 0.2 mg of Na₂MoO₄·2H₂O, 0.2 mg of CuSO₄·5H₂O, 0.4 mg of CoCl₂·6H₂O, 1 mg of MnCl₂·2H₂O, and 4.5 g of glucose as a carbon source.

Sampling Procedure. Cells were separated from the growth medium by pressure driven fast filtration described for *E. coli*.²⁰ Since this method was designed for cold quenching/extraction, the technique was slightly modified to

be compatible with both hot and cold quenching/extraction approaches. The complete procedure is shown in Figure 1. Briefly, the cells were grown to mid-exponential phase (CDW = 0.4 g/L, corresponding to an OD₆₀₀ of approximately 1), and 2 mL of culture broth was rapidly harvested with an electronic pipet and carefully released into a 50 mL syringe barrel attached to a Swinnex filter with the plunger removed. The plunger was carefully reinserted into the syringe barrel, and the cells were separated by manual filtration from the culture broth and retained on the filter pad (0.45 μm pore size, 25 mm diameter PVDF Durapore membrane) by rapidly expelling the culture and extra volume gas through the filter housing and into a collection vessel. Unlike the original procedure,²⁰ the filter pad with captured cells was quickly removed from the filter holder and placed in quenching/extraction solvent.

Quenching/Extraction Procedure. Four different quenching/extraction approaches were validated and assessed for *P. taiwanensis* VLB120 metabolome analysis. These include the following: (1) cold methanol/acetonitrile/water (CM; 40:40:20, v/v/v) at –40 °C; (2) hot water (HW) at 90 °C; (3) boiling ethanol/water (BE; 75:25, v/v) at 70 °C; (4) cold ethanol/water (CE; 75:25, v/v) at –40 °C. The original procedures of some of these techniques were slightly modified to make the techniques easier and straightforward to perform quantitative metabolome analysis of *P. taiwanensis* VLB120. The modifications include an exclusion of formic acid from CM³⁶ and buffer (HEPES) from BE²³ to minimize downstream steps and its potential interference in the analysis of the derived samples. The quenching/extraction temperature was also lowered (below the azeotrope boiling point of the solvent) to avoid/minimize loss of solvent or extraction solution during hot quenching/extraction procedures.

Quenching and extraction of metabolites were performed by transferring the filter pad with captured cells to 2.5 mL of preheated (BE at 70 °C and HW at 90 °C, for 3 min) or precooled (CE and CM at –40 °C, for 3 min) quenching/extraction solvents containing ¹³C-labeled internal standard (IS). The filter pad was vortexed for 30 s, followed by a second extraction step with an additional 1.5 mL of the hot or cold extraction solvent without IS added. The two solutions were pooled in a 50 mL conical tube and stored in –80 °C until further analysis.

Sample Concentration and Conditioning. Samples from –80 °C were thawed and centrifuged for 5 min, at 17000g and 4 °C, after which the supernatants were carefully collected and the remaining cell debris was discarded. The samples were concentrated by evaporating the organic solvent for 5 h at 25 °C using a vacuum concentrator (SAVANT, SpeedVac, Thermo Fisher Scientific, San Diego, CA, USA) followed by lyophilization (LABCONCO, FreeZone, Kansas City, MO, USA) overnight at –40 °C. All dried extracts were resuspended in 250 μL of LC-MS grade water (compatible with initial mobile phase of the LC-MS method) and stored at –80 °C until analysis. Prior to analyzing the samples on the LC-MS/MS instrument, a set of dilutions (1× and 10×) of the samples were prepared to cover the range of detection. Further details of the protocol are explained in Figure 1.

Cell Dry Weight Determination. Cell dry weight (CDW) was estimated by transferring 1 mL of broth sample to preweighed dry Eppendorf tubes at specified time intervals (1 h) and spun down (17000g) for 5 min at 4 °C. The sample was washed with water to remove traces of culture media in the sample. The Eppendorf tubes containing the cell pellets were

dried in a heating block at 70 °C until a constant weight was achieved. The optical density (OD) at 600 nm was measured in a spectrophotometer (VWR UV-1600PC). The correlation of optical density (OD₆₀₀) to CDW is given by $CDW = 0.4505 (OD_{600\text{ nm}}) \text{ g L}^{-1}$ for *P. taiwanensis* VLB120.

Metabolite Quantification. The concentrations of extracellular metabolites (glucose and gluconate) were analyzed by D-glucose and D-gluconate/D-glucono- δ -lactone test kits (R-BIOPHARM AG, Germany) by monitoring the increase of nicotinamide adenine dinucleotide phosphate at 340 nm in a 96-well plate format. Intracellular metabolites were determined by an AB SCIEX Qtrap1 5500 mass spectrometer (AB SCIEX, Framingham, MA, USA) operated in negative ion mode applying multiple reaction monitoring as described elsewhere.²⁰

An XSELECT HSS XP (150 mm \times 2.1 mm \times 2.5 μm) (Waters, Milford, MA, USA) column with eluent A (10 mM tributylamine, 10 mM acetic acid (pH 6.86), 5% methanol, and 2% 2-propanol) and eluent B (2-propanol) was used for the chromatography. The oven temperature was set to 40 °C and the gradient was for the following times (*t*): 0 min, 0% B; 5 min, 0% B; 9 min, 2% B; 9.5 min, 6% B; 11.5 min, 6% B; 12 min, 11% B; 13.5 min, 11% B; 15.5 min, 28% B; 16.5 min, 53% B; 22.5 min, 53% B; 23 min, 0% B; 27 min, 0% B; 33 min, 0% B. The flow rate was 0.4 mL/min (0–15.5 min), 0.15 mL/min (16.5–23 min), and 0.4 mL/min (27–33 min). Electrospray ionization parameters were optimized for 0.4 mL/min flow rate and were as follows: electrospray voltage of –4,500 V, temperature of 500 °C, curtain gas of 40, CAD gas of 12, and gases 1 and 2 of 50 and 50 psi, respectively.

Data Processing. Integration was performed using MultiQuant™ 3.0.2 (AB SCIEX), and absolute quantification of intracellular metabolites were performed using an isotope-ratio-based approach as previously described.^{18,30} Cell extracts grown in fully U-¹³C-labeled glucose were used as internal standard for quantifying the intracellular metabolites of *P. taiwanensis* VLB120 grown on naturally labeled glucose. The calibration curve was also prepared by adding fully U-¹³C-labeled cell extract as internal standard to the unlabeled calibration standards, and linear calibration curves were obtained by plotting the height ratios between the U-¹³C and ¹²C metabolites against the known concentrations of ¹²C metabolites in the calibration standard.

RESULTS AND DISCUSSION

Physiology of *P. taiwanensis* VLB120 during Batch Growth on Glucose. *P. taiwanensis* VLB120 was grown aerobically in minimal medium supplemented with 4.5 g L⁻¹ glucose. *P. taiwanensis* VLB120 exhibits biphasic growth: first, glucose was consumed (glucose phase); once glucose was exhausted, accumulated gluconate was consumed (gluconate phase), as shown in Figure 2. This observation may be compared to previous findings in *P. putida*, which have shown that this bacterium metabolizes glucose to gluconate in the periplasmic space by the activity of glucose dehydrogenase (gcd), which is then transported to the cytoplasm and subsequently converted to 6-phosphogluconate. This pathway is known as the direct oxidative pathway which takes place either under aerobic conditions or high substrate availability. The authors also suggested that the strain might convert glucose to glucose 6-phosphate in the cytoplasm, via glucokinase and further to phospho-6-gluconate by the activity of glucose-6-phosphate dehydrogenase. This alternative phosphorylative pathway predominates under oxygen or glucose

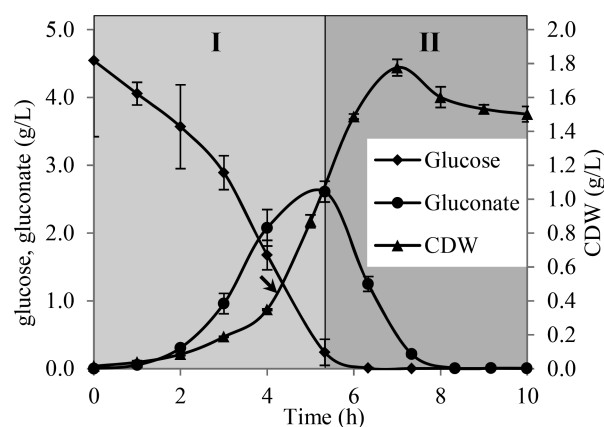


Figure 2. Growth profile of *P. taiwanensis* VLB120 in minimal media: (I) glucose phase; (II) gluconate phase. Arrow indicates the time at which samples were taken for intracellular metabolite analyses. Error bars indicate standard deviations of three independent cultures. CDW, cell dry weight. Growth conditions: 250 mL baffled shake flask, 25 mL of minimal medium, 4.5 g/L glucose, 250 rpm, 30 °C.

Table 1. Physiological Parameters of *P. taiwanensis* VLB120 during Growth on Glucose in Batch Culture (Only Glucose Phase)^a

specific growth rate, μ	h^{-1}	0.75 ± 0.03
specific glucose uptake rate	$\text{g (g of CDW h)}^{-1}$	6.27 ± 0.30
specific gluconate production rate	$\text{g (g of CDW h)}^{-1}$	5.01 ± 0.58
biomass yield on glucose	g of CDW g^{-1}	0.12 ± 0.01

^aCells were cultivated in 250 mL shake flasks (working volume, 25 mL) at 30 °C, 250 rpm in minimal medium supplemented with 4.5 g L⁻¹ glucose. Errors indicate standard deviations ($n = 3$). CDW, cell dry weight.

limiting conditions.^{2,37–39} In contrast to *P. putida* no further oxidation of gluconate to 2-ketogluconate is observed in *P. taiwanensis* but rather the conversion to 6-phosphogluconate which enters the pentose phosphate pathway.

The observed low biomass yield in the glucose phase was the consequence of the high conversion rate of glucose to gluconate, which was accumulated in the culture medium (Table 1). This result is in agreement to the previous study which found that *P. putida* mt-2 converts the major part of glucose to gluconate and 2-ketogluconate due to the saturation of one or more biosynthesis key steps and availability of excess substrate to membrane dehydrogenases.³⁹

Understanding the physiological state of the investigated organism is important prior to sampling in metabolomics studies for a representative sample during the desired growth phase. For this study, cells were harvested during the mid-exponential growth phase (CDW = 0.4 g/L) on glucose.

Comparison of Quenching/Extraction Approaches. The suitability of a pressure driven fast filtration system followed by cold ethanol extraction, cold methanol/acetonitrile/water extraction, boiling ethanol extraction, and hot water extraction was assessed for *P. taiwanensis* VLB120 metabolome analysis. The suitability of each approach was evaluated based on quenching efficiency, intracellular metabolite concentrations, and experimental reproducibility. For all quenching/extraction approaches, cells were obtained from the same shake flask and each quenching/extraction procedure was performed using five independent shake flasks as biological replicates.

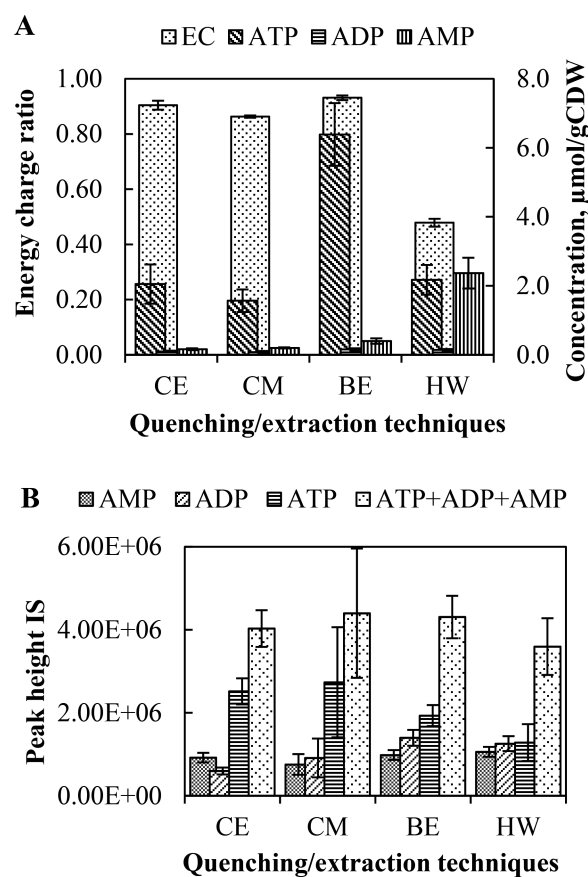


Figure 3. (A) Comparison of intracellular ATP, ADP, and AMP and the energy charge ratio ($EC = (ATP + 0.5ADP)/(ATP + ADP + AMP)$) of *P. taiwanensis* VLB120 grown on glucose. (B) Effect of quenching/extraction temperatures on ATP, ADP, and AMP of ^{13}C -labeled internal standard which was added to the quenching/extraction solution prior to the quenching/extraction process (where, for example, $6.0E+06$ represents 6.0×10^6). Abbreviations: CE, cold ethanol/water (75:25, v/v); CM, cold methanol/acetonitrile/water (40:40:20, v/v); BE, boiling ethanol/water (75:25, v/v); HW, hot water. The error bars indicate standard deviations from five biological replicates.

Quenching Efficiency. The effectiveness of the applied quenching methods was evaluated based on the adenylate energy charge (EC) to assess whether inactivation of cellular metabolism was achieved in a reasonable time scale. This parameter describes the relationship between ATP, ADP, and AMP (as shown below).⁴⁰ A physiological meaningful range of 0.80–0.95 for growing cells depending on nutritional and environmental conditions has been described.^{34,40–43}

$$EC = \frac{[ATP] + 0.5[ADP]}{[ATP] + [ADP] + [AMP]}$$

The obtained results (Figure 3A) demonstrate that the quenching/extraction solution has a considerable effect on the proper quenching of cellular metabolism. CE, CM, and BE quenching/extraction techniques were found to be highly effective in deactivating cellular metabolism since the EC was within a physiological meaningful range. The highest energy charge was obtained for the BE quenching/extraction procedure (0.93 ± 0.01).

In contrast to other organic-solvent-based quenching/extraction techniques such as CE, CM, and BE, HW-based

quenching/extraction resulted in a low EC (0.48 ± 0.014), which implies that this method was less effective in deactivating cellular metabolism. This finding is in good agreement with results obtained in a previous work performed by Meyer et al.,¹⁹ suggesting that this method is not effective in deactivating the metabolism of *Staphylococcus aureus* (*St. aureus*; EC, 0.43 ± 0.13). Instead, the method presumably causes reversible inactivation of the enzymes hydrolyzing ATP to the corresponding less phosphorylated metabolites ADP and AMP.³¹ The same effect was observed for other quantified triphosphate nucleotides that get hydrolyzed to the corresponding monophosphate nucleotides (Figure 4). This pattern of metabolite losses and gains is detrimental in metabolome studies, leading to underestimation of triphosphate levels and overestimation of less phosphorylated nucleotides.

Intracellular Metabolite Concentrations. The efficacy of the quenching/extraction approaches was also evaluated based on the intracellular concentrations of the identified metabolites. With respect to metabolite concentration changes between quenching/extraction techniques, no statistically significant difference was found for the two applied cold quenching/extraction approaches (i.e., CE and CM) at a p -value < 0.05 , except for NADPH and chorismate (Figure 4A).

On the other hand, a significant number of quantified metabolites (p -value ≤ 0.05) were present at significantly different concentrations between hot and cold quenching/extraction techniques (Figure 4B–E). The hot quenching/extraction techniques were found to be superior to cold quenching/extraction techniques when using a 2-fold change (\log_2 fold change ≥ 1 or ≤ -1) and p -value ≤ 0.05 as a significance threshold. These significant differences were found in the metabolite classes comprising redox cofactors, nucleotides, nucleosides, and bases. Some of these metabolites changed more than 3-fold between hot and cold quenching/extraction techniques (Figure S1). This indicates that temperature is one important factor (e.g., CE vs BE, Figure 4B) in the metabolite extraction for *P. taiwanensis* VLB120. This is most likely due to the strain's intrinsic solvent resistance compared to other less resistant organisms such as *E. coli* where cold quenching/extraction methods turned out to be favorable.^{20,36,44}

There was also a significant difference between the two tested hot quenching/extraction techniques (BE and HW). For instance, nucleotide triphosphates such as ATP, dATP, dCTP, CTP, ITP, UTP, and dTTP as well as redox cofactors (NADH and NADPH) were better extracted by the BE-based quenching/extraction technique whereas adenine, uracil, cytidine, and guanosine were better extracted by HW, as shown in Figure 4F. Furthermore, hot water quenching/extraction approach appeared to be more efficient in extracting nucleotide monophosphates (NMPs) than nucleotide triphosphates (NTPs) compared to other evaluated quenching/extraction techniques (Figure 4). This is not directly related to the efficiency of the extraction technique but to the incomplete quenching of cellular metabolism resulting in increased amounts of lower grade phosphorylated nucleotides as also observed during the EC evaluation.

A possible degradation of metabolites due to high temperatures during the quenching and extraction process was addressed by estimating the recovery of the ^{13}C -labeled IS. The combined peak height of ATP, ADP, and AMP was within the variation observed for CE, CM, and BE and slightly reduced for the HW quenching/extraction procedure (Figure 3B).

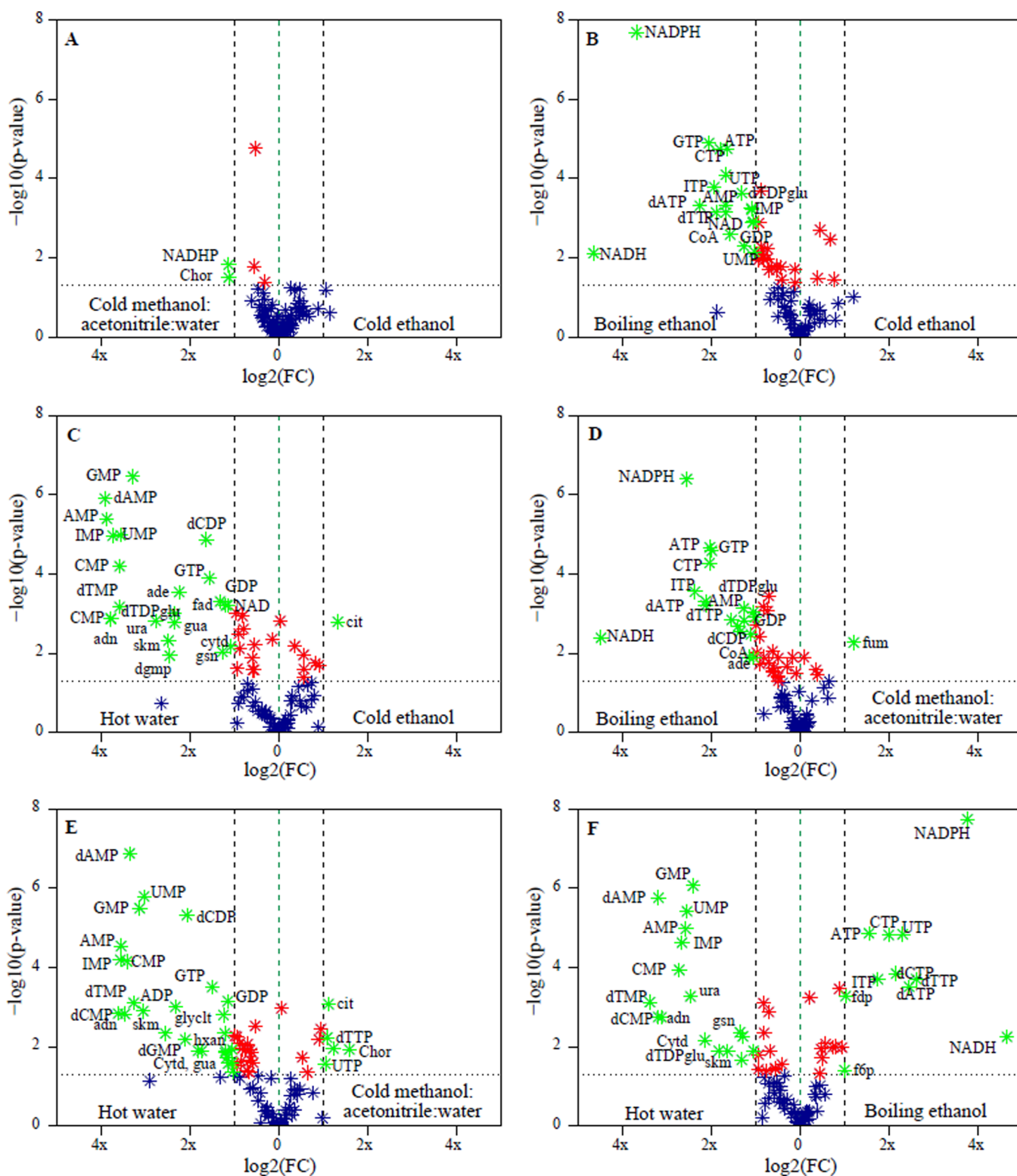


Figure 4. Volcano plots of quantitative metabolome data for the comparison of different quenching/extraction techniques: (A) cold methanol/acetonitrile/water and cold ethanol; (B) boiling ethanol and cold ethanol; (C) hot water and cold ethanol; (D) boiling ethanol and cold methanol/acetonitrile/water; (E) hot water and cold methanol/acetonitrile/water; (F) hot water and boiling ethanol. The x-axis is the mean ratio fold change (plotted on a \log_2 scale) of the relative abundance of each metabolite between the two extraction methods. The y-axis represents the statistical significance p -value (plotted on \log_{10} scale) of the ratio fold change for each metabolite. Metabolites that have both significant p -value ($p \leq 0.05$) and high fold change (more than 2-fold) are marked with green on both sides of the x-axis and metabolites that have only significant statistical p -value ($p \leq 0.05$) represented with red. Metabolites whose abundance is unchanged between the two extraction methods were plotted at the x-axis origin (green vertical line; ratio fold change = 1). Each point represents a different metabolite. Some of the metabolites were not labeled in the figure due to constraints of the volcano plot.

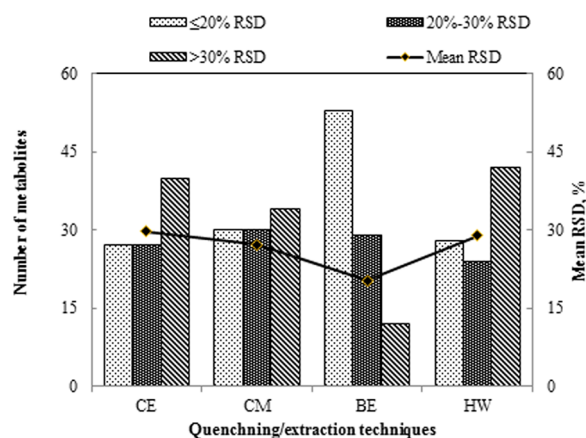


Figure 5. Comparison of the reproducibility (% RSD) of several quenching/extraction techniques. The bars show the total number of metabolites that have a RSD below 20%, between 20% and 30%, and above 30%; the solid line represents the mean RSD (%) of all quantified metabolites for each quenching/extraction technique. Abbreviations: CE, cold ethanol/water (75:25, v/v); CM, cold methanol/acetonitrile/water (40:40:20, v/v); BE, boiling ethanol/water (75:25, v/v); HW, hot water; RSD, relative standard deviation ($n = 5$, biological replicates).

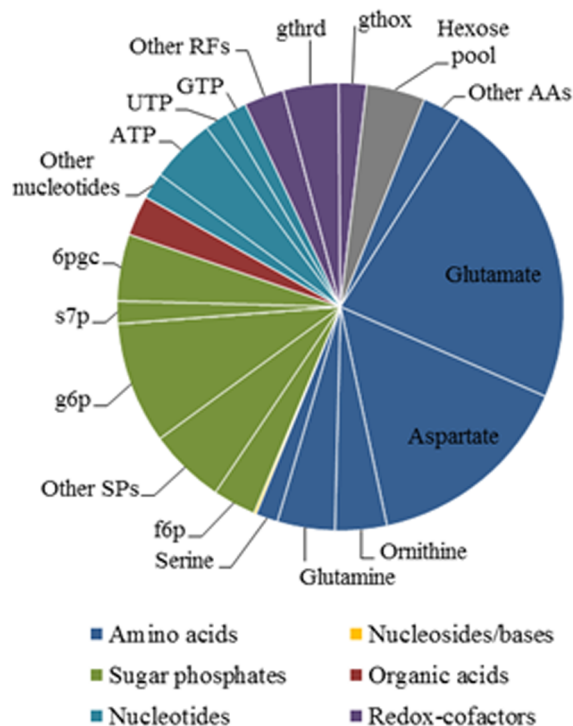


Figure 6. Composition of quantified metabolites of glucose-fed *P. taiwanensis* VLB120 applying the BE method. The top 15 abundant [$\mu\text{mol}/(\text{g}$ of CDW)] metabolites were labeled including aspartate, glutamate, ornithine, 6-phosphogluconate (6pgc), glucose 6-phosphate (g6p), reduced glutathione (gthrd), adenosine triphosphate (ATP), hexose pool (fructose and glucose-D), glutamine, fructose 6-phosphate (f6p), oxidized glutathione (gthox), uridine triphosphate (UTP), sedoheptulose 7-phosphate (s7p), serine, and guanosine triphosphate (GTP). Abbreviations: AAs, amino acids; SPs, sugar phosphates; RFs, redox factors. Aspartate and glutamate concentrations are extrapolated above the calibration curve.

Besides, reduced peak heights were observed for ATP in the ^{13}C -labeled internal standard in both hot extraction/quenching

procedures compared to the two cold ones while both ADP and AMP increased during the hot extraction process. This suggests degradation of ATP to lower grade phosphorylated compounds during hot quenching/extraction process. However, this thermal degradation has no contribution to the overall results presented here as the added ^{13}C -labeled IS accounts for all possible losses including thermal degradation.

In general, the different outcome seen with different quenching/extraction techniques indicates that there is no universal technique that is suitable for all types of metabolites. This underlines the importance of specifically developed protocols.

Experimental Repeatability. The robustness of each extraction method was evaluated based on their reproducibility assessed on percent relative standard deviation (% RSD). The mean % RSDs of the quantified metabolites for CE, CM, BE, and HW were 30, 27, 20, and 28%, respectively, implying the highest reproducibility for BE (Figure 5). The majority of extracted classes of metabolite by BE have low % RSDs (below 20%) compared to the other three quenching/extraction methods applied. Based on those findings, BE is the most robust method applied among the used quenching/extraction techniques which is likely due to a more complete extraction of metabolites.

On the basis of the three evaluation criteria, quenching efficiency, intracellular metabolite concentrations (extraction yield), and experimental repeatability, the pressure driven fast filtration system followed by a boiling ethanol/water (75:25, v/v) at 75 °C is the most adequate quenching/extraction technique for *P. taiwanensis* VLB120 metabolome analysis among the investigated methods.

On the other hand, the findings of this work focusing on a proper procedure to sample the *P. taiwanensis* VLB120 metabolome differed remarkably from that of other Gram-negative bacteria such as *E. coli*^{33,45} and *Klebsiella oxytoca*,³² in which boiling ethanol was not the favorable extraction technique compared to hot water, cold ethanol, cold methanol, methanol/chloroform combinations, perchloric acid, and potassium hydroxide. These differences might be due to the inherent differences in cell wall structure and membrane composition for these organisms,^{31,46,47} and hence it is important to carefully assess a metabolome sampling methodology for the specific organism of interest.

Composition of the *P. taiwanensis* VLB120 Metabolome Extracted with Boiling Ethanol. In total 107 metabolites were identified, and 94 of them were quantified from the Embden–Meyerhof–Parnas (EMP) pathway, the pentose phosphate pathway (PPP), and the tricarboxylic acid cycle (TCA). These metabolites may not be representative of the entire metabolome of *P. taiwanensis* VLB120 as the total number of metabolites present in *Pseudomonas* is estimated to be around 305 (according to genome scale modeling). However, the quantified metabolites cover most highly abundant metabolites on a molar base and they have an essential role in central metabolism. This is comparable to other organisms such as *E. coli*.^{48,49} Among the quantified intracellular metabolites, most are related to the central carbon, energy, and redox metabolism as well as amino acid metabolism.

The metabolome of *P. taiwanensis* VLB120 was dominated by a small number of abundant compound classes on a concentration basis: amino acids (52%), central carbon intermediates including sugar phosphates and organic acids

Table 2. Boiling Ethanol Extracted Intracellular Metabolite Concentrations of *P. taiwanensis* VLB120 Grown on Glucose

metabolite	$\mu\text{mol (g of CDW)}^{-1}$	metabolite	$\mu\text{mol (g of CDW)}^{-1}$	metabolite	$\mu\text{mol (g of CDW)}^{-1}$
L-arginine	0.211	succinate	0.360	GMP	0.438
L-histidine	0.308	L-malate	0.081	IMP	0.107
L-glutamine	5.643	citrate	0.534	UMP	0.106
L-threonine	0.937	isocitrate	0.023	dAMP	0.006
L-methionine	0.098	phenylpyruvate	0.012	cAMP	0.0001
L-tyrosine	0.195	methylmalonate	0.016	dCMP	0.011
L-phenylalanine	0.180	oxalate	0.647	dUMP	0.005
L-aspartate	23.577	chorismate	0.069	dGMP	0.015
L-glutamate	30.60	cis-aconitate	0.114	NADH	0.045
L-tryptophan	0.034	fumarate	0.030	NADP	0.323
L-ornithine	5.077	urate	0.338	NADPH	0.055
L-serine	2.178	ATP	6.385	oxidized glutathione	2.722
L-alanine	0.508	dATP	0.525	reduced glutathione	5.420
L-threonine	0.937	dCTP	0.322	coenzyme A	0.738
L-asparagine	0.069	CTP	0.654	acetyl-coenzyme A	1.094
L-citrulline	0.416	ITP	1.041	D-glucose 6-phosphate	11.94
uracil	0.007	dITP	0.246	D-fructose 6-phosphate	4.227
cytidine	0.061	dTTP	0.355	D-glucose 1-phosphate	0.767
inosine	0.010	GTP	2.023	D-fructose 1,6-bisphosphate	0.771
guanosine	0.017	UTP	2.327	alpha-D-ribose 5-phosphate	0.374
adenosine	0.015	ADP	0.157	sedoheptulose 7-phosphate	2.218
guanine	0.005	UDP	0.329	D-ribulose 5-phosphate	1.858
xanthine	0.013	GDP	0.697	phosphoenolpyruvate	0.414
thymine	0.001	dCDP	0.095	glycerol 3-phosphate	0.179
adenine	0.012	dADP	0.063	dihydroxyacetone phosphate	1.772
uridine	0.087	UDPglucose	0.772	D-glucosamine 6-phosphate	0.638
hypoxanthine	0.003	UDP-glucuronate	0.005	pool 2pg_3pg	0.715
2-oxoglutarate	0.159	dTDPglucose	0.008	6-phospho-D-gluconate	6.528
shikimate	0.002	AMP	0.399	hexose pool ^a	5.736
glycolate	0.340	CMP	0.138	flavin adenine dinucleotide	0.153
5-oxoproline	0.162	dTMP	0.007		
pyruvate	1.070	NAD	1.510		

^aHexose pool denotes the combined pools of fructose and glucose.

(22%), nucleotides (13%), and redox cofactors (9%), as shown in Figure 6. The 15 most abundant compounds comprised 81% of the total content of the quantified metabolome, whereas the less abundant half of the quantified metabolites which includes metabolites of all classes together comprised only 2.5%.

Comparison with metabolome data from *E. coli* indicates clear differences for aerobic growth on glucose due to differences in the glucose catabolic pathways in both organisms. The F6P/G6P and the 6PGC/G6P ratios in *E. coli* are 0.10 and 0.11, respectively.²⁰ The corresponding ratios determined for *P. taiwanensis* VLB120 were 0.35 and 0.55 for F6P/G6P and 6PGC/G6P. Those findings are in agreement with the postulated way of glucose catabolism under aerobic batch conditions. Under those conditions the oxidative pathway with 6PGC being the substrate entry point is supposed to be the main catabolic pathway in contrast to glucose-6-phosphate in *E. coli*.³⁹

The concentration of metabolites extracted from *P. taiwanensis* VLB120 with boiling ethanol is shown in Table 2. For error estimates and comparable data from cold ethanol, cold methanol/acetonitrile/water, and hot water quenching/extraction, see Supporting Information Table S1.

CONCLUSION

The present study conducted a comprehensive examination of different hot and cold combined quenching/extraction

approaches to extract and quantify the metabolome of *P. taiwanensis* VLB120 for the first time. The overall result and performance of intracellular metabolite profiling is significantly affected by the specific method applied during the sampling. Pressure driven fast filtration followed by boiling ethanol quenching/extraction technique was sufficiently fast to provide an accurate snapshot of intracellular metabolism of the cells while also allowing for the most complete and reproducible extraction of intracellular metabolites. On the other hand, hot-water-based quenching/extraction technique is not suitable for *P. taiwanensis* VLB120 metabolome analysis due to incomplete quenching of metabolism, but good extraction results could be obtained for some of metabolites such as amino acids, nucleosides, and bases.

In general, this study showed that each extraction method has its advantage and disadvantage for extraction of metabolites, depending on their physical properties. Thus, sampling, quenching, and extraction protocols need to be validated and adjusted for the specific questions they should help to answer. This is important in metabolomics studies since analytical techniques such as LC-MS will not produce a relevant result from poorly prepared biological samples due to detector response and matrix effects. Thus, accurate sample preparation techniques are required to ensure the analytical method maintains essential elements of robustness and consistency that are expected in any bioanalytical assay. The focus has to be

on the compound class or classes of interest as well as the organism itself that is investigated to decide for a reasonable sample preparation strategy.

■ ASSOCIATED CONTENT

Supporting Information

The Supporting Information is available free of charge on the ACS Publications website at DOI: [10.1021/acs.analchem.7b00793](https://doi.org/10.1021/acs.analchem.7b00793).

Extracted intracellular metabolite concentrations, plot of measured intracellular concentrations, and relative differences between the two quenching/extraction methods (PDF)

■ AUTHOR INFORMATION

Corresponding Author

*Phone: +45 3056 9850. E-mail: kosc@biosustain.dtu.dk.

ORCID

Gossa G. Wordofa: 0000-0002-3218-7821

Konstantin Schneider: 0000-0001-9595-324X

Notes

The authors declare no competing financial interest.

■ ACKNOWLEDGMENTS

We thank Prof. Dr. Andreas Schmid (Department of Solar Materials, The Helmholtz-Center for Environmental Research, UFZ, Germany) for supplying *P. taiwanensis* VLB120. This research was funded by the ERA-NET SynBio/Innovationsfonden and the Novo Nordisk Foundation.

■ REFERENCES

- (1) Volmer, J.; Neumann, C.; Bühler, B.; Schmid, A. *Appl. Environ. Microbiol.* **2014**, *80* (20), 6539–6548.
- (2) Lang, K.; Zierow, J.; Buehler, K.; Schmid, A. *Microb. Cell Fact.* **2014**, *13* (1), 2.
- (3) Köhler, K. A. K.; Blank, L. M.; Frick, O.; Schmid, A. *Environ. Microbiol.* **2015**, *17* (1), 156–170.
- (4) Köhler, K. A. K.; Rückert, C.; Schatschneider, S.; Vorhölder, F. J.; Szczepanowski, R.; Blank, L. M.; Niehaus, K.; Goesmann, A.; Pühler, A.; Kalinowski, J.; Schmid, A. *J. Biotechnol.* **2013**, *168* (4), 729–730.
- (5) Halan, B.; Vassilev, I.; Lang, K.; Schmid, A.; Buehler, K. *Microb. Biotechnol.* **2017**, *10*, 745–755.
- (6) Pei, D.; Xu, J.; Zhuang, Q.; Tse, H.-F.; Esteban, M. A. *Adv. Biochem. Eng. Biotechnol.* **2010**, *123*, 127–141.
- (7) Bennett, B. D.; Yuan, J.; Kimball, E. H.; Rabinowitz, J. D. *Nat. Protoc.* **2008**, *3* (8), 1299–1311.
- (8) Villas-Bôas, S. G.; Højer-Pedersen, J.; Åkesson, M.; Smedsgaard, J.; Nielsen, J. *Yeast* **2005**, *22* (14), 1155–1169.
- (9) de Koning, W.; van Dam, K. *Anal. Biochem.* **1992**, *204* (1), 118–123.
- (10) Buchholz, A.; Takors, R.; Wandrey, C. *Anal. Biochem.* **2001**, *295* (2), 129–137.
- (11) Jensen, N. B.; Jokumsen, K. V.; Villadsen, J. *Biotechnol. Bioeng.* **1999**, *63* (3), 356–362.
- (12) Chen, M.; Li, A.; Sun, M.; Feng, Z.; Meng, X.; Wang, Y. *J. Zhejiang Univ., Sci., B* **2014**, *15* (4), 333–342.
- (13) de Jonge, L. P.; Douma, R. D.; Heijnen, J. J.; van Gulik, W. M. *Metabolomics* **2012**, *8* (4), 727–735.
- (14) Ruijter, G. J. G.; Visser, J. *J. Microbiol. Methods* **1996**, *25*, 295–302.
- (15) Letisse, F.; Lindley, N. D. *Biotechnol. Lett.* **2000**, *22* (21), 1673–1677.
- (16) Link, H.; Anselment, B.; Weuster-Botz, D. *Metabolomics* **2008**, *4* (3), 240–247.
- (17) Wittmann, C.; Krömer, J. O.; Kiefer, P.; Binz, T.; Heinzle, E. *Anal. Biochem.* **2004**, *327* (1), 135–139.
- (18) Wu, L.; Mashego, M. R.; Van Dam, J. C.; Proell, A. M.; Vinke, J. L.; Ras, C.; Van Winden, W. A.; Van Gulik, W. M.; Heijnen, J. J. *Anal. Biochem.* **2005**, *336* (2), 164–171.
- (19) Meyer, H.; Liebecke, M.; Lalk, M. *Anal. Biochem.* **2010**, *401* (2), 250–259.
- (20) McCloskey, D.; Utrilla, J.; Naviaux, R. K.; Palsson, B. O.; Feist, A. M. *Metabolomics* **2015**, *11*, 198–209.
- (21) Canelas, A. B.; Ten Pierick, A.; Ras, C.; Seifar, R. M.; Van Dam, J. C.; Van Gulik, W. M.; Heijnen, J. J. *Anal. Chem.* **2009**, *81* (17), 7379–7389.
- (22) Shryock, J. C.; Rubio, R.; Berne, R. M. *Anal. Biochem.* **1986**, *159* (1), 73–81.
- (23) Gonzalez, B.; François, J.; Renaud, M. *Yeast* **1997**, *13* (14), 1347–1356.
- (24) Hajjaj, H.; Blanc, P. J.; Goma, G.; François, J. *FEMS Microbiol. Lett.* **1998**, *164*, 195–200.
- (25) Visser, D.; Van Zuylen, G. A.; Van Dam, J. C.; Oudshoorn, A.; Eman, M. R.; Ras, C.; Van Gulik, W. M.; Frank, J.; Van Dedem, G. W. K.; Heijnen, J. J. *Biotechnol. Bioeng.* **2002**, *79* (6), 674–681.
- (26) Chassagnole, C.; Noisommit-Rizzi, N.; Schmid, J. W.; Mauch, K.; Reuss, M. *Biotechnol. Bioeng.* **2002**, *79* (1), 53–73.
- (27) Oldiges, M.; Kunze, M.; Degenring, D.; Sprenger, G. A.; Takors, R. *Biotechnol. Prog.* **2004**, *20*, 1623–1633.
- (28) Theobald, U.; Mailinger, W.; Reuss, M.; Rizzi, M. *Anal. Biochem.* **1993**, *214*, 31–37.
- (29) Bhattacharya, M.; Fuhrman, L.; Ingram, A.; Nickerson, K. W.; Conway, T. *Anal. Biochem.* **1995**, *232* (1), 98–106.
- (30) Mashego, M. R.; Wu, L.; Van Dam, J. C.; Ras, C.; Vinke, J. L.; Van Winden, W. A.; Van Gulik, W. M.; Heijnen, J. J. *Biotechnol. Bioeng.* **2004**, *85* (6), 620–628.
- (31) Meyer, H.; Weidmann, H.; Lalk, M. *Microb. Cell Fact.* **2013**, *12* (1), 69.
- (32) Park, C.; Yun, S.; Lee, S. Y.; Park, K.; Lee, J. *Appl. Biochem. Biotechnol.* **2012**, *167* (3), 425–438.
- (33) Hiller, J.; Franco-Lara, E.; Weuster-Botz, D. *Biotechnol. Lett.* **2007**, *29* (8), 1169–1178.
- (34) Fajjes, M.; Mars, A. E.; Smid, E. J. *Microb. Cell Fact.* **2007**, *6*, 27.
- (35) Hartmans, S.; Smits, J. P.; van der Werf, M. J.; Volkering, F.; de Bont, J. A. M. *Appl. Environ. Microbiol.* **1989**, *55* (11), 2850–2855.
- (36) Rabinowitz, J. D.; Kimball, E. *Anal. Chem.* **2007**, *79* (16), 6167–6173.
- (37) dos Santos, V. A. P. M.; Heim, S.; Moore, E. R. B.; Strätz, M.; Timmis, K. N. *Environ. Microbiol.* **2004**, *6* (12), 1264–1286.
- (38) Lessie, T. G.; Phibbs, P. V. *Annu. Rev. Microbiol.* **1984**, *38*, 359–387.
- (39) Latrach Tlemçani, L.; Corroler, D.; Barillier, D.; Mosrati, R. *Arch. Microbiol.* **2008**, *190* (2), 141–150.
- (40) Atkinson, D. E.; Walton, G. M. *J. Biol. Chem.* **1967**, *242* (13), 3239–3241.
- (41) Talwalkar, R. T.; Lester, R. L. *Biochim. Biophys. Acta, Lipids Lipid Metab.* **1973**, *306*, 412–421.
- (42) Poolman, B.; Konings, W. N. *J. Bacteriol.* **1988**, *170* (2), 700–707.
- (43) Coulier, L.; Bas, R.; Jespersen, S.; Verheij, E.; Van Der Werf, M. J.; Hankemeier, T. *Anal. Chem.* **2006**, *78* (18), 6573–6582.
- (44) Prasad Maharjan, R.; Ferenci, T. *Anal. Biochem.* **2003**, *313* (1), 145–154.
- (45) Winder, C. L.; Dunn, W. B.; Schuler, S.; Broadhurst, D.; Jarvis, R.; Stephens, G. M.; Goodacre, R. *Anal. Chem.* **2008**, *80* (8), 2939–2948.
- (46) Zakhartsev, M.; Vielhauer, O.; Horn, T.; Yang, X.; Reuss, M. *Metabolomics* **2015**, *11* (2), 286–301.
- (47) Mashego, M. R.; Rumbold, K.; De Mey, M.; Vandamme, E.; Soetaert, W.; Heijnen, J. J. *Biotechnol. Lett.* **2007**, *29* (1), 1–16.
- (48) Kim, D. H.; Achcar, F.; Breitling, R.; Burgess, K. E.; Barrett, M. P. *Metabolomics* **2015**, *11* (6), 1721–1732.

(49) Park, J. O.; Rubin, S. A.; Xu, Y.-F.; Amador-Noguez, D.; Fan, J.; Shlomi, T.; Rabinowitz, J. D. *Nat. Chem. Biol.* **2016**, *12* (7), 482–489.

Supporting Information for Publication

Quantifying the metabolome of *Pseudomonas taiwanensis* VLB120: Evaluation of hot and cold combined quenching/extraction approaches

Gossa G. Wordofa[†], Mette Kristensen[†], Lars Schrübbers[†], Douglas McCloskey[‡], Jochen Forster[†] and Konstantin Schneider^{*†}

[†] Novo Nordisk Foundation Center for Biosustainability, Technical University of Denmark, DK-2800 Lyngby, Denmark

[‡] Department of Bioengineering, University of California, San Diego, 9500 Gilman Drive, La Jolla, CA 92093-0412, USA

Corresponding Author

*Phone: +45 30569850. Email: kosc@biosustain.dtu.dk

Table S1. Intracellular metabolite concentrations ($\mu\text{mol/gCDW}$) of glucose-fed, exponentially growing *P. taiwanensis* VLB120 cells that were extracted with different techniques.

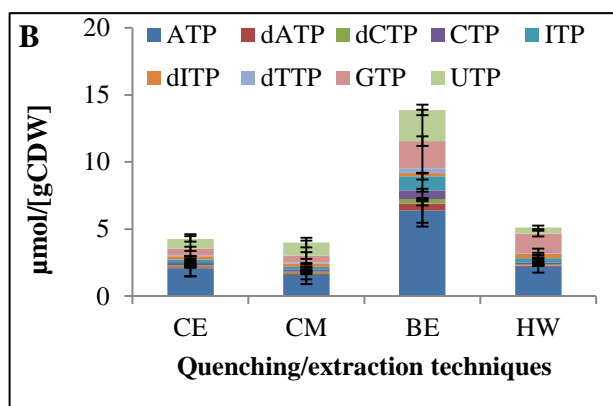
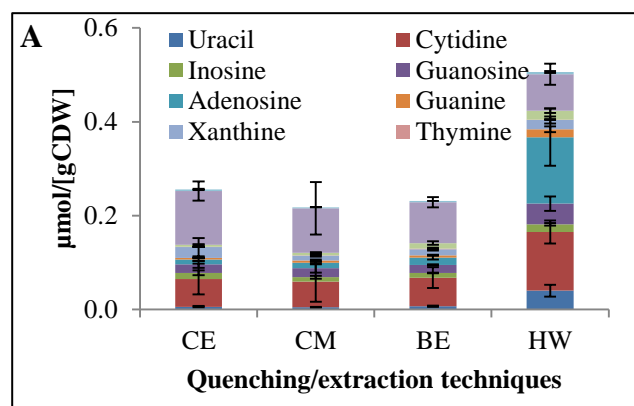
Metabolite	CE		CM		BE		HW	
	$\mu\text{mol/gCDW}$	RSD (%)	$\mu\text{mol/gCDW}$	RSD (%)	$\mu\text{mol/gCDW}$	RSD (%)	$\mu\text{mol/gCDW}$	RSD (%)
L-Arginine	0.204	43.85	0.213	30.82	0.211	16.82	0.257	24.31
L-Histidine	0.314	47.65	0.286	34.01	0.308	12.04	0.453	27.14
L-Glutamine	5.668	22.24	5.991	9.08	5.643	15.70	3.210	42.21
L-Threonine	0.898	39.66	0.901	12.97	0.937	10.13	0.941	25.57
L-Methionine	0.077	28.42	0.074	28.17	0.098	19.67	0.143	24.63
L-Tyrosine	0.214	46.81	0.179	14.91	0.195	16.61	0.372	41.45
L-Phenylalanine	0.229	28.35	0.165	26.06	0.180	29.58	0.249	37.84
L-Aspartate	21.052	9.02	26.481	26.89	23.577	17.57	23.041	24.71
L-Glutamate	35.484	15.17	33.937	15.75	30.596	17.74	32.821	23.94
L-Tryptophan	0.050	73.37	0.032	12.59	0.034	20.00	0.057	35.01
L-Ornithine	7.216	31.67	4.630	26.53	5.077	13.46	6.174	26.83
L-Serine	2.747	54.94	1.783	21.59	2.178	20.65	2.765	36.91
L-Alanine	0.697	53.04	0.571	23.29	0.508	41.26	1.260	43.58
L-Threonine	0.898	39.65	0.901	12.97	0.937	10.13	0.941	25.57
L-Asparagine	0.062	25.30	0.065	13.03	0.069	33.60	0.120	43.41
L-Citrulline	0.570	41.40	0.390	40.05	0.416	19.38	0.305	44.33
Uracil	0.006	31.49	0.005	20.83	0.007	19.64	0.040	30.70
Cytidine	0.059	54.89	0.054	77.94	0.061	36.66	0.125	19.60
Inosine	0.013	40.04	0.010	32.95	0.010	10.05	0.016	16.71
Guanosine	0.018	41.87	0.019	50.48	0.017	7.88	0.044	34.32
Adenosine	0.010	35.73	0.012	24.39	0.015	28.24	0.141	43.19
Guanine	0.003	12.96	0.005	43.48	0.005	20.48	0.017	36.97
Xanthine	0.023	85.30	0.010	22.92	0.013	21.23	0.020	37.54
Thymine	0.001	21.69	0.001	20.62	0.001	18.62	0.001	27.19
Adenine	0.004	41.50	0.005	23.71	0.012	31.36	0.019	24.97
Uridine	0.115	17.73	0.095	58.82	0.087	12.52	0.078	28.89
Hypoxanthine	0.003	37.24	0.002	25.41	0.003	7.09	0.005	41.84
D-Glucose 6-phosphate	10.452	3.43	10.613	11.74	11.937	7.68	10.214	12.33

D-Fructose 6-phosphate	3.899	10.93	4.163	4.92	4.227	10.57	2.106	34.98
D-Glucose 1-phosphate	0.795	10.72	0.818	19.29	0.767	14.57	0.994	42.04
D-Fructose 1,6-bisphosphate	0.553	28.03	0.726	25.62	0.771	19.62	0.377	12.11
alpha-D-Ribose 5-phosphate	0.368	19.01	0.400	8.52	0.374	25.93	0.330	25.58
Sedoheptulose 7-phosphate	2.537	17.38	2.415	26.22	2.218	8.79	2.050	21.69
D-Ribulose 5-phosphate	1.831	8.12	1.792	10.75	1.858	13.06	1.245	25.01
Phosphoenolpyruvate	0.408	15.55	0.422	17.32	0.414	25.11	0.415	10.26
Glycerol 3-phosphate	0.208	23.07	0.198	17.47	0.179	15.82	0.312	22.67
Dihydroxyacetone phosphate	1.880	17.84	1.723	33.13	1.772	29.18	1.529	25.18
D-Glucosamine 6-phosphate	0.443	32.95	0.564	38.99	0.638	10.33	0.580	45.12
Pool 2pg+3pg	0.980	9.06	0.920	14.06	0.715	10.18	0.764	12.91
6-Phospho-D-gluconate	6.921	41.22	7.359	62.95	6.528	30.98	5.253	43.64
Hexose pool	5.689	19.23	5.738	13.59	5.736	20.56	7.926	45.89
2-Oxoglutarate	0.147	19.98	0.148	26.61	0.159	20.68	0.146	35.33
Shikimate	0.002	23.53	0.001	28.92	0.002	26.26	0.009	47.37
Glycolate	0.255	14.22	0.210	10.81	0.340	12.90	0.488	32.34
5-Oxoproline	0.293	61.24	0.160	16.37	0.162	12.43	0.308	34.07
Pyruvate	0.918	47.49	0.699	27.47	1.070	13.72	1.731	59.61
Succinate	0.327	7.85	0.257	23.32	0.360	4.40	0.534	33.76
L-Malate	0.084	51.00	0.058	22.57	0.081	20.38	0.049	29.41
Citrate	0.909	26.56	0.784	19.22	0.534	42.10	0.362	28.25
Isocitrate	0.020	13.79	0.027	22.76	0.023	9.68	0.030	18.88
Phenylpyruvate	0.015	21.77	0.016	16.27	0.012	12.61	0.012	35.67
Methylmalonate	0.012	24.23	0.009	20.55	0.016	10.77	0.020	41.32
Oxalate	0.487	23.13	0.527	7.80	0.647	11.07	0.635	35.75
Chorismate	0.049	24.18	0.107	38.77	0.069	26.04	0.036	5.52
cis-Aconitate	0.129	37.53	0.095	20.24	0.114	19.97	0.156	28.65
Fumarate	0.068	58.07	0.069	27.49	0.030	16.86	0.044	30.16
Urate	0.090	41.60	0.078	20.70	0.338	24.53	0.585	79.19
ATP	2.051	27.75	1.567	21.00	6.385	14.20	2.171	19.90
dATP	0.110	46.21	0.121	47.84	0.525	29.75	0.095	30.04
dCTP	0.101	39.06	0.122	51.95	0.322	24.07	0.072	40.41

CTP	0.188	26.79	0.160	30.26	0.654	15.88	0.163	35.12
ITP	0.273	29.53	0.202	12.41	1.041	23.65	0.308	19.66
dITP	0.239	10.73	0.232	20.82	0.246	11.02	0.335	22.91
dTTP	0.076	38.54	0.101	31.08	0.355	28.86	0.057	13.75
GTP	0.489	32.48	0.512	49.23	2.023	17.22	1.450	14.73
UTP	0.735	28.59	0.966	37.05	2.327	16.95	0.467	28.37
ADP	0.097	24.89	0.080	38.33	0.157	21.38	0.143	17.37
UDP	0.213	23.95	0.241	56.71	0.329	17.91	0.232	19.02
GDP	0.337	40.98	0.325	55.66	0.697	12.90	0.772	14.64
dCDP	0.054	29.60	0.040	37.27	0.095	22.61	0.168	9.32
dADP	0.045	49.30	0.036	72.25	0.063	48.19	0.048	48.50
UDPglucose	0.467	29.11	0.506	36.72	0.772	15.92	0.824	10.73
UDP-D-glucuronate	0.002	37.80	0.002	45.41	0.005	25.85	0.005	14.66
dTDPglucose	0.004	35.58	0.004	30.47	0.008	17.02	0.019	32.87
AMP	0.161	17.23	0.201	8.36	0.399	19.93	2.366	18.85
CMP	0.076	26.20	0.085	29.13	0.138	22.58	0.909	26.93
GMP	0.238	13.52	0.264	1.77	0.438	14.06	2.322	13.14
IMP	0.050	11.89	0.057	12.89	0.107	20.98	0.676	21.34
UMP	0.052	9.13	0.075	2.18	0.106	26.36	0.619	13.60
dAMP	0.003	23.32	0.005	14.71	0.006	16.49	0.052	9.57
cAMP	0.0001	13.34	0.0001	9.72	0.000	22.35	0.0001	33.88
dCMP	0.007	18.44	0.009	20.15	0.011	32.08	0.097	42.96
dUMP	0.004	20.73	0.005	45.60	0.005	22.84	0.005	34.61
dGMP	0.009	10.24	0.011	18.87	0.015	23.94	0.048	45.49
dTMP	0.006	30.38	0.008	21.50	0.007	32.71	0.075	38.13
Nicotinamide adenine dinucleotide	0.798	24.16	0.992	34.73	1.510	17.75	1.551	17.42
Nicotinamide adenine dinucleotide - reduced	0.002	44.63	0.001	30.65	0.045	47.49	0.001	38.17
Nicotinamide adenine dinucleotide phosphate	0.185	38.01	0.185	39.57	0.323	19.27	0.410	14.61
Nicotinamide adenine dinucleotide phosphate- reduced	0.004	21.34	0.009	38.08	0.055	7.33	0.004	18.52
Oxidized glutathione	2.590	28.79	3.177	20.79	2.722	48.76	2.368	40.83
Reduced glutathione	5.351	18.83	5.614	10.96	5.420	22.50	5.102	24.44

Coenzyme A	0.309	32.91	0.359	36.84	0.738	31.16	0.536	10.77
Acetyl-CoA	0.514	33.47	0.542	36.23	1.094	14.69	0.591	16.87
Flavin adenine dinucleotide oxidized	0.048	35.04	0.061	43.87	0.153	26.64	0.120	19.31
Below or above quantification limit								
D-Fructose 1-phosphate	<0.015		<0.015		<0.015		<0.015	
cGMP	<1.22E-05		<1.22E-05		<1.22E-05		<1.22E-05	
Riboflavin	<0.004		<0.004		<0.004		<0.004	
Biotin	<0.002		<0.002		<0.002		<0.002	
L-Cystine	<0.001		<0.001		<0.001		<0.001	
Acetyl phosphate	<0.043		<0.043		<0.043		<0.043	
Oxaloacetate	<0.027		<0.027		<0.027		<0.027	
Folate	<0.0002		<0.0002		<0.0002		<0.0002	
dUTP	<0.039		<0.039		<0.039		<0.039	
dIMP	<0.006		<0.006		<0.006		<0.006	
dGDP	>0.260		>0.260		>0.260		>0.260	
Lactate	>0.531		>0.531		>0.531		>0.531	
Glutaconate	>10.19		>10.19		>10.19		>10.19	

Abbreviations: CE, cold ethanol/water (75/25, v/v); CM, cold methanol/acetonitrile/water (40:40:20, v/v); BE, boiling ethanol/water (75/25, v/v); HW, hot water; RSD, relative standard deviation (n=5).



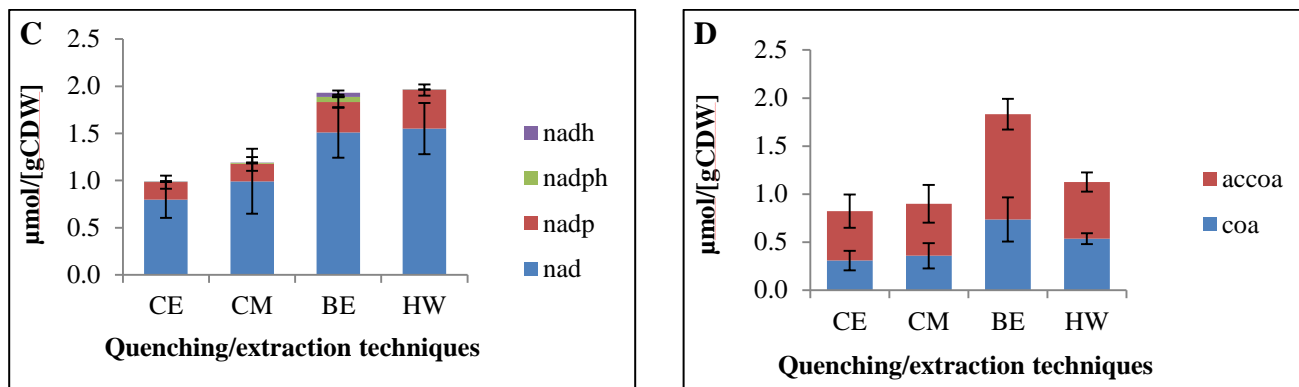


Figure S1. Measured intracellular concentrations of nucleosides and bases (A), nucleotide triphosphates (B), NAD(P)(H) (C) and cofactors (D) extracted from glucose-fed *P. taiwanensis* VLB120. Abbreviations: CE, cold ethanol/water (75/25, v/v); CM, cold methanol/acetonitrile/water (40:40:20, v/v); BE, boiling ethanol/water (75/25, v/v); HW, hot water. The error bars indicate standard deviations from five biological replicates.

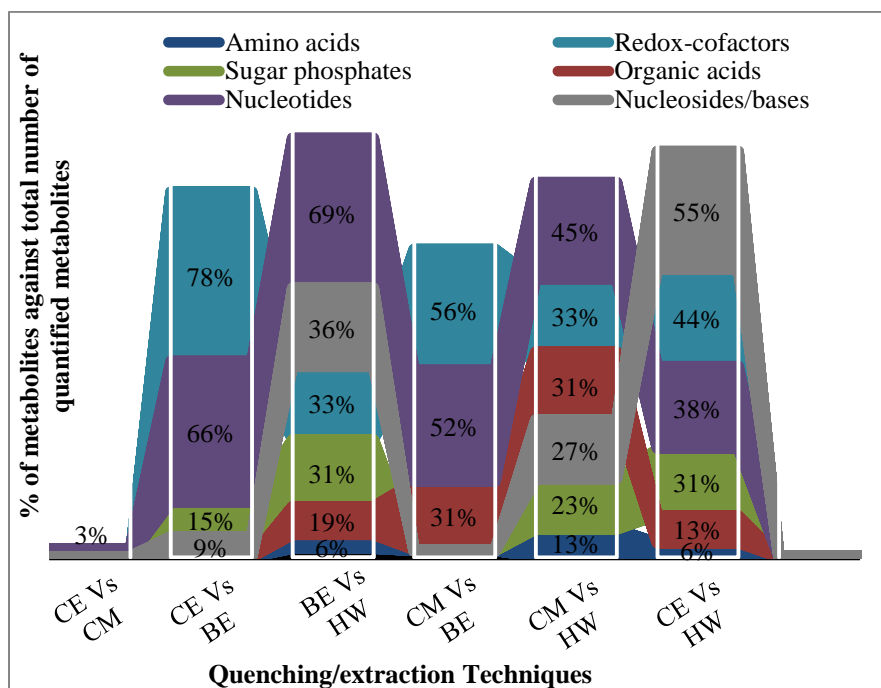


Figure S2. Relative difference between the two quenching/extraction methods. Abbreviations: CE, cold ethanol/water (75/25, v/v); CM, cold methanol/acetonitrile/water (40:40:20, v/v); BE, boiling ethanol/water (75/25, v/v); HW, hot water.

PAPER II

**Tolerance and Metabolic Response of *Pseudomonas taiwanensis* VLB120 towards
Biomass Hydrolysate Derived Inhibitors**

1 **Tolerance and Metabolic Response of *Pseudomonas taiwanensis* VLB120 towards**
2 **Biomass Hydrolysate Derived Inhibitors**

3 Gossa G. Wordofa¹, Mette Kristensen¹ and Konstantin Schneider^{1*}

4 ¹ Novo Nordisk Foundation Center for Biosustainability, Technical University of Denmark, DK-2800
5 Lyngby, Denmark

6 Gossa G. Wordofa: gowor@biosustain.dtu.dk

7 Mette Kristensen: metk@biosustain.dtu.dk

8 Konstantin Schneider: kosc@biosustain.dtu.dk

9 *Corresponding Author

10

11

12

13

14

15

16

17

18

19

20

21

22

23

24 **ABSTRACT**

25 **Background**

26 Bio-conversions of lignocellulosic biomass to high value products offers numerous benefits;
27 however, their development is hampered by chemical inhibitors generated during the pre-
28 treatment process. A better understanding of how microbes naturally respond to those
29 inhibitors is valuable in the process of designing microorganisms with improved tolerance.
30 *Pseudomonas taiwanensis* VLB120 is a natively tolerant strain that utilizes a wide range of
31 carbon sources including pentose and hexose sugars. To this end, we investigated the
32 tolerance and metabolic response of *P. taiwanensis* VLB120 towards biomass hydrolysate
33 derived inhibitors including organic acids (acetic acid, formic acid, levulinic acid), furans
34 (furfural, 5-hydroxymethylfurfural) and phenols (vanillin).

35 **Results**

36 The inhibitory effect of the tested compounds varied with respect to lag-phase, specific
37 growth rate, and biomass yield compared to the control cultures grown under the same
38 conditions without addition of inhibitors. However, *P. taiwanensis* was able to oxidize
39 vanillin and furfural to vanillic acid and 2-furoic acid, respectively. Vanillic acid was further
40 metabolized, whereas 2-furoic acid was secreted outside the cells and remained in the
41 fermentation broth without further conversion. Acetic acid and formic acid was completely
42 consumed from the fermentation broth while concentration of levulinic acid remained
43 constant throughout the fermentation process. Analysis of free intracellular metabolites
44 revealed varying levels when *P. taiwanensis* VLB120 was exposed to inhibitory compounds.

45 This resulted in increased levels of ATP to potentially export inhibitors from the cell and an
46 increased NADPH/NADP ratio that provides reducing power to deal with the oxidative stress
47 caused by the inhibitors. Thus, adequate supply of these metabolites is essential for the
48 survival and reproduction of *P. taiwanensis* in the presence of biomass derived inhibitors.

49 **Conclusions**

50 In this study, the tolerance and metabolic response of *P. taiwanensis* VLB120 to biomass
51 hydrolysate derived inhibitors was investigated. *P. taiwanensis* VLB120 showed high
52 tolerance towards biomass hydrolysate derived inhibitors compared to most wildtype
53 microbes reported in the literature. It adopt different resistance mechanisms, including
54 detoxification, efflux and repair, which require additional energy and resources. Thus,
55 targeting redox and energy metabolism in strain engineering may be a successful strategy to
56 overcome inhibition during biomass hydrolysate conversion and lead to development of more
57 robust strains.

58

59 **KEYWORDS**

60 Biomass Hydrolysate Inhibitors – Inhibitor Tolerance – Metabolomics – *Pseudomonas*
61 *taiwanensis*

62

63

64 **BACKGROUND**

65 Lignocellulosic biomass is the most abundant and bio-renewable feedstock available on earth
66 with an annual production that has been estimated around $150\text{--}170 \times 10^9$ metric tons
67 worldwide [1–3]. The majority of lignocellulosic biomass is generated from agricultural,
68 industrial and municipal waste streams, as well as forestry residues. It consists of three types
69 of polymers including cellulose, hemicellulose and lignin that are strongly bonded by non-
70 covalent forces as well as by covalent cross-links [4, 5]. Cellulose is the major structural
71 component of lignocellulosic biomass, which is responsible for mechanical strength while,
72 hemicellulose is a macromolecules with repeated polymers of pentoses and hexoses. Lignin
73 mainly contains three aromatic alcohols including coniferyl alcohol, sinapyl alcohol and *p*-
74 coumaryl alcohol and forms a protective layer around cellulose and hemicelluloses [6, 7].
75 Cellulose is located within a lignin shell, while the hemicellulose is located within the
76 cellulose and between cellulose and lignin [8].

77 The biological conversion of lignocellulosic biomass to valuable chemicals and polymers
78 offers numerous benefits but its development is still hampered due to low production levels
79 with unsatisfactory titers, yields, and productivities [9–13]. One of the main reasons for the
80 low production level is the rigidity and complexity of the biomass structure [14]. In this
81 context, pretreatment and hydrolysis steps are required to break down the biomass structure
82 to form monomeric sugars, such as glucose, xylose, galactose, mannose, arabinose and
83 rhamnose which can be utilized by microorganisms for biotechnological production
84 processes [15, 16].

85 During the past years various pretreatment techniques have been developed, including
86 acid/alkali treatment, hydrothermal processing, oxidative methods, ammonia explosion, and
87 others [17]. Many of these methods have proven to result in high yields of free sugars. More
88 than 90% of the theoretical yield were achieved for hydrolyzation of woods, grasses, and
89 corn [18]. However, during pretreatment of lignocellulosic biomass a wide range of
90 compounds which are inhibitory to microbial growth are formed [19]. They mainly include
91 furan derivatives, weak acids, phenolic compounds and other aromatic compounds [20–22].

92 During the pretreatment processes, pentoses resulting from hydrolysis of hemicellulose
93 can undergo dehydration to form furfural, while hexoses can be dehydrated to 5-
94 hydroxymethylfurfural (5-HMF). In addition, furfural and 5-HMF can be further degraded
95 to levulinic acid and formic acid, respectively, depending on the conditions applied during
96 the pretreatment process. Acetic acid is released from the acetyl groups bonded to
97 hemicellulose, while a large number of phenolic compounds, such as 4-hydroxybenzoic
98 acid, 4-hydroxybenzaldehyde, vanillin, dihydro-coniferyl alcohol, coniferyl aldehyde,
99 syringaldehyde, syringic acid and ferulic acid can be produced from lignin degradation
100 [23–25].

101 Since the composition and concentration of these compounds present in different biomass
102 hydrolysates vary depending on the feedstock as well as the pretreatment process, they
103 influence the growth of microorganisms in various ways, including DNA mutation,
104 membrane disruption, intracellular pH drop, and other cellular targets [17, 25]. To overcome
105 this, various physical and chemical detoxification methods including dilution, adsorption,
106 and precipitation have been developed. However, these techniques have substantial

107 drawbacks in terms of cost, waste generation and loss of fermentable sugars [2]. In order to
108 achieve high fermentation efficiency with no or minimum detoxification steps, one
109 potential solution is the use of microbes that are highly resistant to the inhibitors in
110 processes where biomass hydrolysates are applied [20].

111 Recently, a number of strategies such as adaptive laboratory evolution, genetic manipulation,
112 and evolutionary engineering have been used to develop more tolerant strains with improved
113 growth characteristics on lignocellulosic biomass hydrolysates without additional
114 detoxification steps [26]. However, since these techniques are time-consuming and
115 technically demanding, understanding how naturally occurring toxic tolerant microbes
116 metabolically respond to inhibitors and identifying which metabolic pathways and
117 metabolites are involved may hasten the process.

118 Metabolites are the end products of cellular regulatory processes, and their levels are highly
119 affected by genetic or environmental changes [27]. Thus, detailed examination of metabolites
120 and associated metabolic pathways related to the phenotype provide relevant information
121 complementary to those obtained by e.g. transcriptomics [28]. The main aim of this work
122 was to determine the tolerance and metabolic response of *Pseudomonas taiwanensis* VLB120
123 toward inhibitory compounds present in lignocellulosic biomass hydrolysates including
124 acetic acid, formic acid, levulinic acid, furfural, 5HMF and vanillin.

125 *P. taiwanensis* VLB120 was chosen as a model strain for two reasons: (i) its capability to
126 naturally grow on both hexose and pentose sugars which are the main component of
127 lignocellulosic biomass hydrolysates, and (ii) due to its native tolerance toward toxic

128 compounds such as toluene and styrene [12, 29, 30] Hence, this strain is a promising host
129 for the biotechnological production of chemicals and biofuels from low-cost renewable
130 feedstocks.

131

132

133 **MATERIALS AND METHODS**

134 **Strain and Culture Mediums**

135 *P. taiwanensis* VLB120 was obtained from the Institute of Applied Microbiology, RWTH
136 Aachen, Germany. The cell culture medium used on this study consisted of (L^{-1}): 2.12 g
137 $NaH_2PO_4 \cdot 2H_2O$, 2 g $(NH_4)_2SO_4$, 10 mg EDTA, 0.1 g $MgCl_2 \cdot 6H_2O$, 2 mg $ZnSO_4 \cdot 7H_2O$, 1 mg
138 $CaCl_2 \cdot 2H_2O$, 5 mg $FeSO_4 \cdot 7H_2O$, 0.2 mg $Na_2MoO_4 \cdot 2H_2O$, 0.2mg $CuSO_4 \cdot 5H_2O$, 0.4 mg
139 $CoCl_2 \cdot 6H_2O$, 1 mg $MnCl_2 \cdot 2H_2O$ and 4.5 g glucose as a carbon source.[31] Unless stated
140 otherwise, all chemicals and reagents used in this study were purchased from Sigma-Aldrich
141 (Chemical Co, USA).

142 **Inhibitors threshold concentration test**

143 The inhibitor threshold concentration affecting growth was evaluated using the Growth
144 Profiler 960 (EnzyScreen, Heemstede, The Netherlands). The inhibitory compounds were
145 added into minimal medium supplemented with 4.5 g L^{-1} of glucose in different concentration

146 level. The media pH was adjusted to 7.0 ± 0.03 with 5M of sodium hydroxide before
147 inoculation. The same medium without inhibitory compounds was used as control.

148 Aerobic cultivations were carried out in 24-well clear bottom microplate (EnzyScreen,
149 Heemstede, The Netherlands) working volume 750 μ L at 30 °C, 225 rpm. The Growth
150 Profiler was set to generate a scan of the plate every 20 minutes. Based on this scan, the
151 Growth Profiler software was used to calculate the density of the cultures in each single well
152 of a plate (green value; G-value). A calibration curve was generated in order to convert the
153 G-values into optical density (OD) values. The following equation was obtained from the
154 calibration curve, and used throughout the study:

$$155 \quad \text{OD}_{600\text{nm}} \text{ equivalent} = 0.0158 \times \text{G-value}^{1.304}$$

156 **Bioreactor batch growth experiment**

157 Bioreactor batch cultivations were performed to characterize the metabolic response of *P.*
158 *taiwanensis* VLB120 under stress conditions. The experiments were performed in 1.3-L
159 bioreactors (SARTORIOUS ®) with 0.5 L working volume. Cultures were inoculated at an
160 OD of approx. 0.05 and fermentation temperature, stirrer speed and pH were set at 30 °C,
161 800 rpm and 7.0, respectively. Cultures were supplied with air at a flow rate of 1 slpm, and
162 the minimum dissolved oxygen saturation level was 40%. The whole fermentation process
163 was monitored by continuously measuring the CO₂ percentage in the off-gas. All cultures
164 were performed in triplicates and batch cultures were run for 24 hours.

165 **Sample preparation for metabolome analysis**

166 During bioreactor batch growth experiments, supernatants were collected along the
167 cultivation to quantify optical density at 600 nm (Spectrophotometer VWR UV-1600PC,
168 USA) as well as extracellular metabolites. Samples for extracellular metabolite analysis were
169 spun down at 10 000 g for 5 min and stored at $-20\text{ }^{\circ}\text{C}$ for further use. Samples for intra-
170 cellular metabolite measurement were rapidly harvested (3 mL) with an electronic pipette at
171 optical density of 0.4 to 0.6 ($\text{OD}_{600\text{nm}}$), and filtered with a fast filtration system as described
172 previously [32]. Immediately after the filtration process, quenching and extraction of
173 metabolites was performed by adding 2 mL of 75% (v/v) boiling ethanol ($70\text{ }^{\circ}\text{C}$) and 25 μL
174 of fully labeled ^{13}C cell extract as internal standard (IS) to the filtered cells and heated for 1
175 min. The cells were re-extracted by adding additional 1.5 mL of boiling ethanol at $70\text{ }^{\circ}\text{C}$.
176 Samples were concentrated by evaporating the organic solvent for 5 h at $25\text{ }^{\circ}\text{C}$ using a
177 vacuum concentrator (SAVANT, SpeedVac, Thermo Fisher Scientific, San Diego, CA,
178 USA) followed by lyophilization (LABCONCO, FreeZone, Kansas City, MO, USA)
179 overnight at $-40\text{ }^{\circ}\text{C}$. All dried extracts were re-suspended in 250 μL of LC-MS grade water,
180 which is compatible with the initial mobile phase of the LC-MS method and stored at -80
181 $^{\circ}\text{C}$ until analysis.

182 **Quantification of inhibitors and extracellular metabolites**

183 The concentration of inhibitors and extracellular metabolites was quantified by high-
184 performance liquid chromatography (HPLC). More specifically, quantification of furfural, 5-
185 HMF, vanillin and their corresponding acid in media was performed using a Dionex Ultimate
186 3000 HPLC equipped with a Supelco Discovery HS F5-3 HPLC column (150 x 2.1 mm x 3
187 μm) and a UV detector (260, 277, 304 and 210 nm). Samples (1 μL) were analyzed using a

188 gradient method with mobile-phase A: 10 mM ammonium formate, pH 3 and B: acetonitrile.
189 A flow rate of 0.7 mL min⁻¹ was used and the column oven temperature was controlled at 30
190 °C. The program started with 5% of solvent B for 0.5 min and increased linearly to 60% over
191 5 min. The gradient was thereafter increased to 90% B over 0.5 min and kept at this condition
192 for 2 min. Finally, returned to 5% B and equilibrated for 10 min.

193 Concentrations of glucose, gluconate, acetic acid, formic acid and levulinic acid were
194 determined using a Dionex Ultimate 3000 HPLC with an Aminex® HPX-87X Ion Exclusion
195 (300 x 7.8mm) column (BioRad, Hercules, CA) and RI-150 refractive index detector.
196 Gluconate was measured by UV monitoring at 210 nm. The mobile phase consisted of 5 mM
197 H₂SO₄, the flow rate was 0.6 mL min⁻¹ and the temperature of the column oven was controlled
198 at 60 °C. Samples were cooled to 5 °C and 20 µL sample volume was injected.

199

200 **Quantification of intracellular metabolites**

201 Intracellular metabolite quantification was performed using an AB SCIEX Qtrap1 5500 mass
202 spectrometer (AB SCIEX, Framingham, MA, USA) ion-pairing techniques operated in
203 negative mode as previously described [33]. A sample of 20 µL was injected on to an
204 XSELECT HSS XP (150 × 2.1 mm × 2.5 µm) (Waters, Milford, MA, USA) column, which
205 was equilibrated for 10 min before injecting with 100% eluent A (10 mM tributylamine, 10
206 mM acetic acid (pH 6.86), 5% methanol, and 2% 2-propanol). Gradient elution was set to
207 0% of eluent B (2-propanol) for the first 5 min and increased to: 2% (5–9 min), 6% (9–12
208 min), 11% (12–13.5 min), 28% (13.5–15.5 min), 53% (15.5–22.5 min) and returned back to

209 0% (22.5–23 min) and equilibrated for 10min (23–33 min) with 100% eluent A. The flow
210 rate was 0.4 mL min⁻¹(0–15.5 min), 0.15 mL min⁻¹ (16.5–23 min), and 0.4 mL min⁻¹ (27–33
211 min), oven temperature was set to 40 °C. The mass spectrometer was operated in multiple-
212 reaction-monitoring (MRM) mode. The optimized parameters for 0.4 mL min⁻¹flow rate were
213 as follows: ion-spray voltage, -4.5 kV; curtain gas and CAD gas, 40 and 12, respectively.
214 The capillary temperature was 500 °C.

215 **Data Processing**

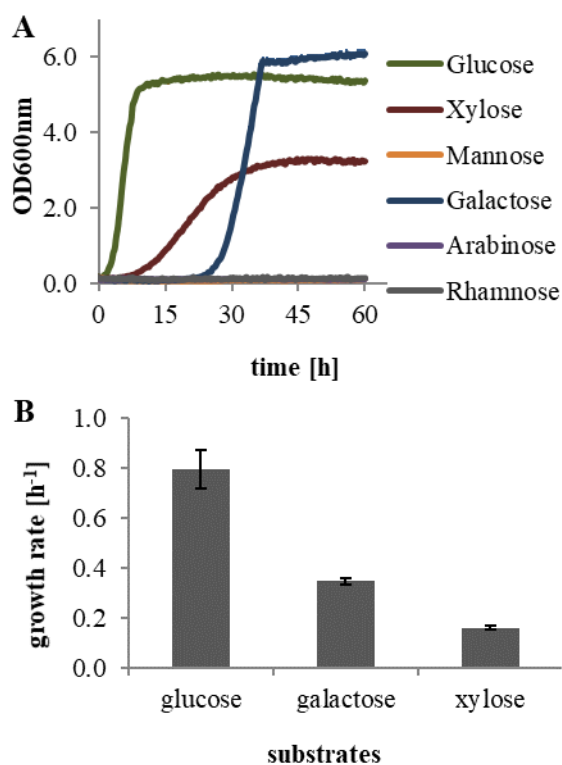
216 HPLC and LC-MS data were processed using Chromeleon™ 7.1.3 (Thermo Scientific™)
217 and Multi-Quant™ 3.0.2 (AB SCIEX™), respectively. For absolute quantification of
218 intracellular metabolites, isotope-ratio based approach was used as previously described.[34,
219 35] This technique was performed using cell extracts grown in fully U-¹³C-labeled glucose
220 as internal standard for quantifying the intracellular metabolites of *P. taiwanensis* VLB120
221 grown on naturally labeled glucose. All statistical analyses were done using R (R
222 Development Core Team[36]) and SIMCA (Umetrics, Umea, Sweden).

223

224 **RESULTS AND DISCUSSION**

225 **Utilization of biomass hydrolysate sugars by *P. taiwanensis* VLB120**

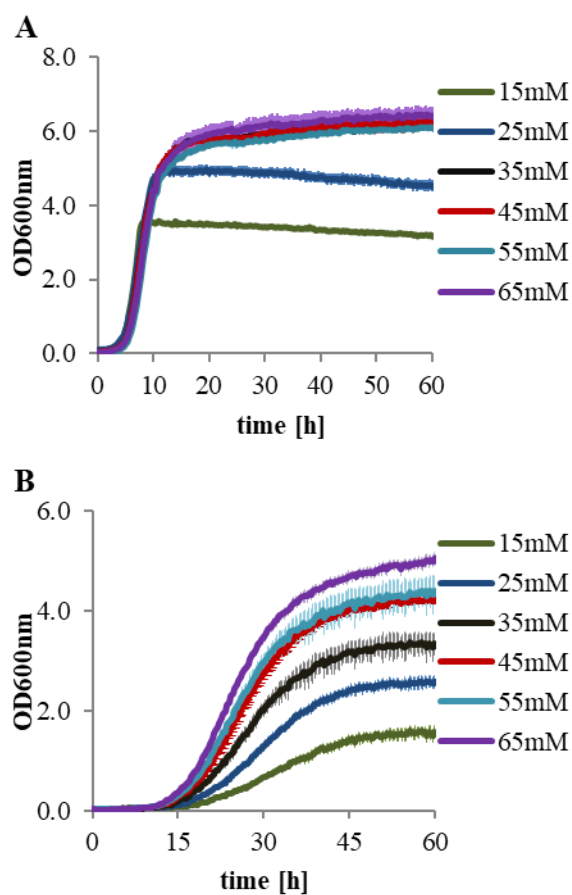
226 Hydrolysis of lignocellulosic biomass results in a mixture of sugars including the hexoses
227 glucose, galactose, and mannose, and the pentoses xylose and arabinose [37]. In most cases,
228 these mixtures can only be metabolized partly or sequentially, with glucose being the
229 preferred carbon source [38–42].



230

231 **Fig. 1** Growth profile of *P. taiwanensis* VLB120 on different lignocellulosic biomass
232 hydrolysate derived sugars A) growth curve, B) specific growth rate. Cells were inoculated
233 in minimal media supplemented with 4.5 g L⁻¹ of each carbon source. Error bars correspond
234 to the standard deviation of three biological replicate cultures.

235 As shown in Figure 1A, *P. taiwanensis* VLB120 is able to efficiently utilize glucose, xylose
236 and galactose despite exhibiting a prolonged lag phase in when grown with galactose as
237 carbon source, which lasted for up to 21 hours. The strain converts glucose and xylose to
238 their respective sugar acids, gluconate and xylonate, respectively, in the periplasmic space
239 by glucose dehydrogenase activity, and the products are further transported to the cytoplasm
240 [12]. No growth of *P. taiwanensis* VLB120 was observed when using mannose, arabinose
241 and rhamnose as sole carbon source.



242

243 **Fig. 2** Growth curves of *P. taiwanensis* VLB120 on minimal medium with glucose (A) or
244 xylose (B) supplied at different concentration levels. Growth was quantified by optical

245 density (OD) measurement at 600 nm. Error bars correspond to the standard deviation of
246 three biological replicate cultures.

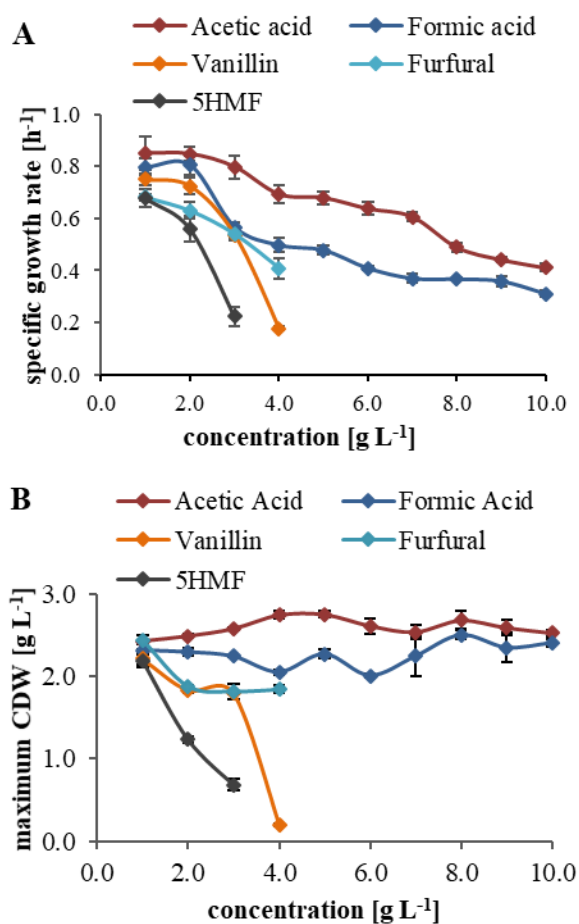
247 Growth of *P. taiwanensis* VLB120 was also assessed on other carbon sources including
248 sodium acetic acid, sodium benzoate, glycerol and mixture of different carbon sources. The
249 results (Additional file 1 Fig. S1) indicate that *P. taiwanensis* VLB120 was able to grow on
250 these compounds as sole source of carbon and energy.

251 Since the initial concentration of sugars in biomass hydrolysates varies among different
252 biomass sources, the effect of initial glucose and xylose concentration on the growth of *P.*
253 *taiwanensis* VLB120 was also examined at different concentration levels (15, 25, 35, 45, 55
254 and 65 mM) (Fig. 2). The results indicate that the specific growth rate of *P. taiwanensis*
255 VLB120 did not change significantly with varying initial concentrations of glucose (Fig. 2A).
256 In contrast, the initial specific growth rate of *P. taiwanensis* VLB120 was increased with
257 increasing xylose concentrations (Fig. 2B). This is directly related to the affinity xylose
258 transporter which control xylose utilization. The degree to which the transporter controls the
259 xylose uptake rate is dependent on the substrate concentration in the medium [43].

260 **Effect of biomass hydrolysate inhibitors on *P. taiwanensis* VLB120 growth**

261 The growth inhibitory effect of acetic acid, formic acid, vanillin, furfural and 5HMF on
262 growth of *P. taiwanensis* VLB120 was evaluated at different concentration levels using the
263 Growth Profiler 960 (EnzyScreen, Heemstede, The Netherlands). The results showed that the
264 inhibitory effect of the tested compounds varied with respect to lag-phase, specific growth
265 rate, and biomass yield compared to the control cultures grown under the same conditions

266 without addition of inhibitory compounds. Presence of furfural and 5-HMF in the media
 267 resulted in a prolonged lag-phase and low cell density, respectively. The lag-phase expanded
 268 from 1 to 24 hours as the concentration of furfural in the fermentation broth increased from
 269 0 to 3 g L⁻¹ (Table 1). 5-HMF reduced the final cell density by 73% (Fig. 3B) at a
 270 concentration level of 3 g L⁻¹. It was also observed that both furfural and 5-HMF reduced the
 271 specific growth rate (Fig. 3A) compared to the reference medium not containing any
 272 inhibitory compounds.



273

274 **Fig. 3** Inhibitory effects of acetic acid, formic acid, levulinic acid, vanillin, furfural and
 275 5HMF on specific growth rate (A), and final biomass (B) of *P. taiwanensis* VLB120 grown

276 on minimal medium supplemented with 4.5 g L⁻¹ of glucose. Error bars correspond to the
 277 standard deviation of three biological replicates. CDW, cell dry weight.

278 The effect of vanillin was comparable to that of furfural and 5-HMF. The lag-phase was
 279 prolonged by 15 hours, while the specific growth rate was reduced by 38% and the final
 280 biomass titer was decreased by 18% at a concentration level of 3 g L⁻¹ of the corresponding
 281 inhibitory compounds. By increasing the concentration of vanillin to 4 g L⁻¹, the final biomass
 282 titer was reduced by 90% and the lag-phase was prolonged to 33 hours (Table 1). A complete
 283 inhibition of growth of *P. taiwanensis* was observed when the concentration of 5HMF,
 284 furfural and vanillin exceeded 3, 4 and 4 g L⁻¹, respectively (Additional file 1: Fig. S2). This
 285 might be caused by the pH drop due to the formation of the corresponding acid form of the
 286 added inhibitors.

287 **Table 1** Effects of hydrolysis derived inhibitors on the lag phase of *P. taiwanensis* VLB120

Concentration [g L ⁻¹]	Lag-phase (h)*					
	Acetic Acid	Formic Acid	Levulinic Acid	Furfural	5HMF	Vanillin
0	0.98	0.98	0.98	0.98	0.98	0.98
1	2.32	2.98	2.32	2.32	6.97	1.98
2	2.32	2.98	2.32	7.58	13.99	5.98
3	2.98	2.98	2.32	24.42	21.92	15.65
4	2.98	3.65	2.65	42.80	n/a	32.63
6	2.98	5.32	2.98	n/a	n/a	n/a

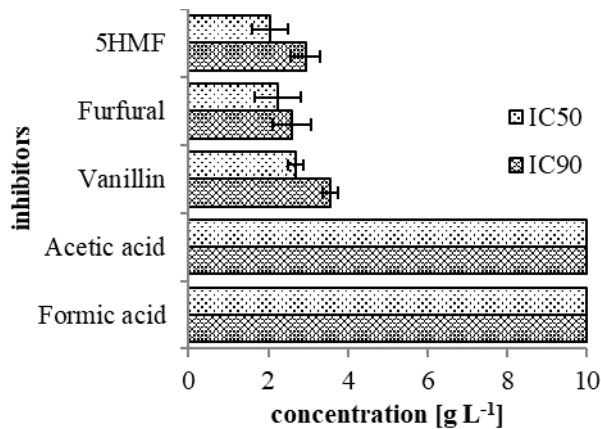
8	11.32	5.32	3.32	n/a	n/a	n/a
10	16.65	5.32	3.65	n/a	n/a	n/a
*lag-phase is defined as the time needed to reach 2% of the maximum cell dry weight [44]; n/a: no growth in 60h						

288 Acetic acid and formic acid showed a similar inhibitory effect on cell growth. Both
289 compounds slightly increased the final biomass of *P. taiwanensis* VLB120 as shown in
290 Additional file 1: Fig. S2, but reduced the growth rate as their concentration increased (Fig.
291 3). The main difference of these two inhibitors was observed as the concentration of acetic
292 acid exceeded 6 g L⁻¹. This caused a prolonged lag-phase compared to formic acid (Table 1),
293 similar as described previously for yeast [44].

294 **Determination of inhibitory threshold concentrations affecting *P. taiwanensis***

295 **VLB120 growth**

296 The inhibitory threshold concentration values of acetic acid, formic acid, furfural, 5HMF and
297 vanillin that reduced the growth of *P. taiwanensis* VLB120 by 50% and 90% (IC50 and IC90)
298 were estimated after 24 hours of cultivation (Fig. 4). The IC50 and IC90 values of each of
299 the inhibitory compounds were determined from inhibition curves for each inhibitor [45, 46].



300

301 **Fig. 4** IC50 and IC90 values of lignocellulose-derived inhibitors for *P. taiwanensis* VLB120
 302 after 24 hours of cultivation. Abbreviations: IC50 and IC90 indicate inhibitory concentrations
 303 that reduce growth of *P. taiwanensis* VLB120 with 50% and 90%, respectively. Error bars
 304 indicate standard deviations of three independent cultures.

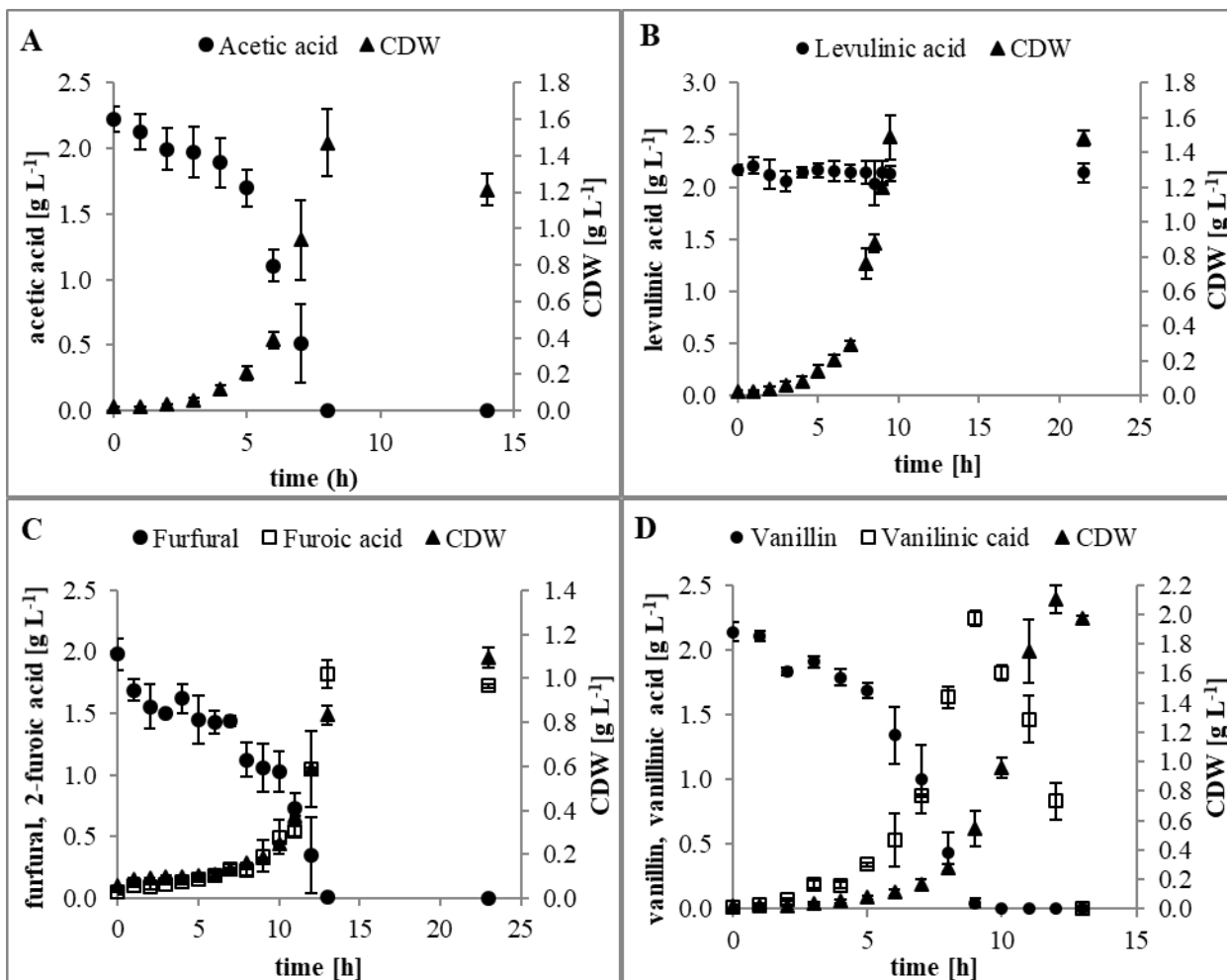
305 The concentrations resulting in a 50% reduction of the specific growth rate of *P. taiwanensis*
 306 VLB120 (IC50) for 5-HMF and furfural are highly comparable with reported values for
 307 *Thermoanaerobacter pseudethanolicus* 39E [47], *Bacillus coagulans* MXL-9 [48], *S.*
 308 *cerevisiae* CBS1200 [49] and *Zymomonas mobilis* ATCC 10988 [49]. Based on IC50 values,
 309 5-HMF provided the strongest inhibition followed by furfural and vanillin, respectively.
 310 These results are in line with previous reports which confirmed that furfural and 5HMF were
 311 identified as main inhibitors in biomass hydrolysates [19, 45, 50, 51]. In contrast, IC50 values
 312 for acetic acid and formic acid were above the highest tested concentration (10 g L⁻¹). These
 313 values are higher compared to well-known production strains such as *E.coli* (IC50: 2.5 g L⁻¹
 314 formic acid, 9.0 g L⁻¹ acetic acid) [52]. This indicates that *P. taiwanensis* VLB120 is highly
 315 tolerant to acetic acid and formic acid when glucose is used as a sole carbon source.

316 **Degradation capacity of lignocellulosic biomass derived inhibitors by *P. taiwanensis***

317 **VLB 120**

318 A number of microorganisms have evolved different strategies including reduction and
319 oxidation processes to detoxify inhibitory compounds [53–56]. For instance,
320 *Gluconacetobacter xylinus* oxidizes furfural and 5-HMF directly to furoic acid and 5-
321 hydroxymethyl-2-furoic acid, respectively [57]. Microorganisms such as *E. coli* and *S.*
322 *cerevisiae* not possessing specific oxidative degradation pathways for furan aldehydes [38],
323 use their native oxidoreductases to reduce furan aldehydes to furan alcohols under anaerobic
324 conditions [52, 58].

325 In this study, the metabolic response and degradation potential of lignocellulosic biomass
326 derived inhibitory compounds by *P. taiwanensis* VLB 120 was investigated using a targeted
327 metabolomics approach. Since some of these inhibitors have structural similarity and share
328 the common degradation pathway, only acetic acid, levulinic acid, furfural and vanillin were
329 considered for the metabolomics study. For a reliable quantitative metabolomics analysis, 2
330 g L⁻¹ of each inhibitory compound was chosen based on half maximal inhibitor concentration
331 (IC50) values assuming this concentration level is sufficiently high to affect cellular
332 physiology and metabolism without being lethal.



333

334 **Fig. 5** Conversion capacity of acetic acid (A), levulinic acid (B), furfural (C) and vanillin (D)
 335 by *P. taiwanensis* VLB120 grown on minimal medium supplemented with 4.5 g L⁻¹ of
 336 glucose at a temperature of 30 °C and pH 7. Error bars indicate standard deviations of three
 337 independent cultures. CDW, cell dry weight.

338 As shown in Figure 5, the concentration of acetic acid, formic acid, furfural, 5HMF and
 339 vanillin were decreased during the cultivation process, suggesting their conversion or
 340 consumption, while the concentration of levulinic acid remained constant throughout the
 341 cultivation process.

342 Based on the supernatant analysis, *P. taiwanensis* VLB120 is able to oxidize vanillin and
343 furfural to vanillic acid and 2-furoic acid, respectively (Fig. 5 C and D). Vanillic acid was
344 further metabolized to protocatechuic acid and eventually entered the central carbon
345 metabolism via the β -keto adipate route [59, 60], whereas the conversion of furfural to 2-
346 furoic acid carried out on the outer surface of the cells [61] and remained in the fermentation
347 broth without further transformation.

348 There was no significant growth observed until the majority of furfural and vanillin in the
349 medium were converted to their corresponding acid, which also explains the prolonged lag-
350 phase. This indicates that the presence of these inhibitors in the media obstructed the growth
351 of *P. taiwanensis* VLB120. However, their corresponding acids had a less toxic effect and
352 therefor allowed growth of *P. taiwanensis* VLB120. These findings are in good agreement
353 with previous studies that proved the aldehyde form as the most toxic one of several aromatic
354 inhibitory compounds, whereas the corresponding acids were less toxic while the alcohol
355 form was the least toxic one [44, 62–64].

356 Acetic acid was completely consumed from the fermentation broth after 8 hours of cultivation
357 (Fig. 5A). This indicates that acetate was activated to acetyl-CoA and completely
358 metabolized from the fermentation broth via the TCA cycle to carbon dioxide, which agrees
359 with findings of Matano *et al* [65].

360 Furthermore, vanillin and furfural appeared to cause a pronounced stress response, resulting
361 in a substantial reduction in specific glucose uptake and specific growth rates during the
362 oxidation process. In contrast, when growing *P. taiwanensis* VLB120 under acetic acid and

363 levulinic acid conditions, the specific glucose uptake rate was increased approx. by 40% and
 364 9% (Table 2), respectively, compared to the control condition. The decreased specific growth
 365 rates and increased specific glucose uptake rates observed for *P. taiwanensis* VLB120 reflect
 366 the additional energy required either for the efflux of inhibitory compound from the cell or
 367 to transport proton through the plasma membrane in order to adjust the intracellular pH to a
 368 threshold at which essential enzymes can function [66, 67]. *P. taiwanensis* VLB120
 369 completely metabolized glucose to gluconate in the presence of acetic acid. This can be
 370 related to the direct utilization of acetic acid as an additional carbon and energy source.

371 **Table 2** Physiological parameters of *P. taiwanensis* VLB120 during growth on glucose in
 372 the presence of inhibitory compounds

Physiological parameters	Unit	Acetic acid	Levulinic acid	Furfural	Vanillin	Control
Specific growth rate	h ⁻¹	0.58 ± 0.02	0.45 ± 0.06	0.19 ± 0.01	0.33 ± 0.04	0.69 ± 0.03
Specific glucose uptake	g g ⁻¹ CDW h ⁻¹	10.45 ± 0.58	8.13 ± 1.69	1.72 ± 0.12	4.25 ± 1.70	7.44 ± 0.42
Specific gluconate production rate	g g ⁻¹ CDW h ⁻¹	10.70 ± 0.39	7.72 ± 1.72	1.49 ± 0.10	3.74 ± 1.52	6.04 ± 0.88
Biomass yield on glucose	g g ⁻¹ CDW	0.05 ± 0.00	0.06 ± 0.00	0.10 ± 0.00	0.12 ± 0.02	0.09 ± 0.01

Note: Since *P. taiwanensis* VLB120 exhibits biphasic growth (glucose and gluconate phase), only glucose phase was considered for determination of specific growth rate, specific glucose uptake/gluconate production rate and biomass yield (Additional file 1: Fig. S4).

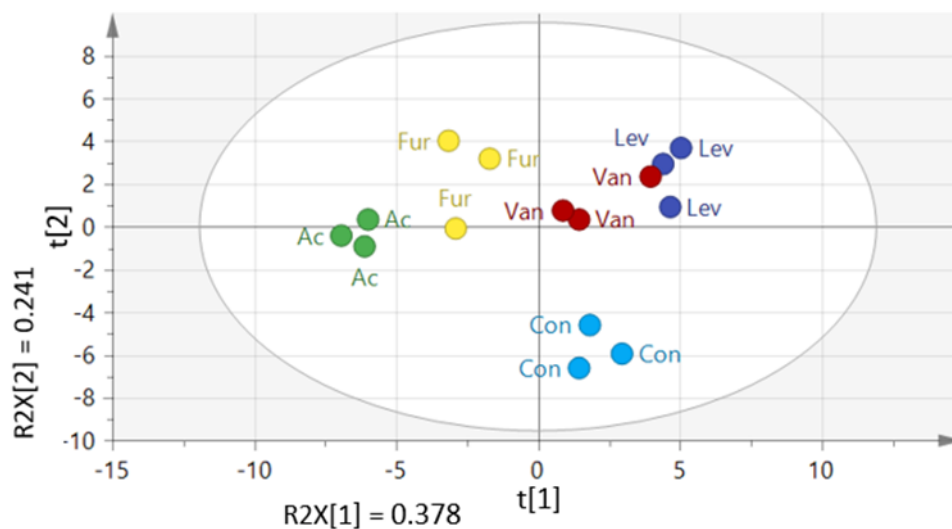
373 **Effect of inhibitory compounds on the metabolome composition of *P. taiwanensis***
 374 **VLB120**

375 Comparative analyses of the primary and key intermediate metabolites were considered to
376 investigate the metabolic response of *P. taiwanensis* VLB120 to lignocellulose derived
377 inhibitors. For each tested inhibitor, intracellular metabolites were extracted with boiling
378 ethanol from exponentially growing *P. taiwanensis* VLB120 cultures at an optical density
379 (OD_{600 nm}) of 0.4 to 0.6.

380 In total, 80 metabolites from different classes, including sugars phosphates, amino acids,
381 organic acids, redox cofactors, nucleosides/bases and nucleotides were quantified across all
382 conditions. These metabolites do not cover the entire metabolome of *P. taiwanensis* VLB120,
383 however, they possess an essential role in central metabolism. In order to provide
384 comparative information regarding the differences in intracellular metabolite levels among
385 each group, a principal component analysis (PCA) was performed.

386 Approximately, 62% of the total variance in the data was represented by the first two
387 principal components (Fig. 6). Samples from different treatments clearly separated from
388 control sample, indicating an adjustment of intracellular metabolism of the *P. taiwanensis*
389 strain in response to the exposure to the different inhibitors. Metabolites including
390 nucleotides, redox-cofactors and sugar phosphates particularly contributed to separate the
391 groups (Additional file 1: Fig. S6). Samples treated with vanillin, furfural and levulinic acid
392 were moved to the upper part of PC(1), indicating relative similarity of their effect on the
393 concentration of several metabolites including, ATP, ADP and NADPH. This is corroborated
394 by heat map cluster analysis based on the degree of similarity of metabolite abundance
395 profiles (Additional file 1: Fig. S7). Levulinic acid and vanillin treated samples were

396 positioned close to each other, indicating that these compounds effected the intracellular
397 metabolome composition in a similar way.



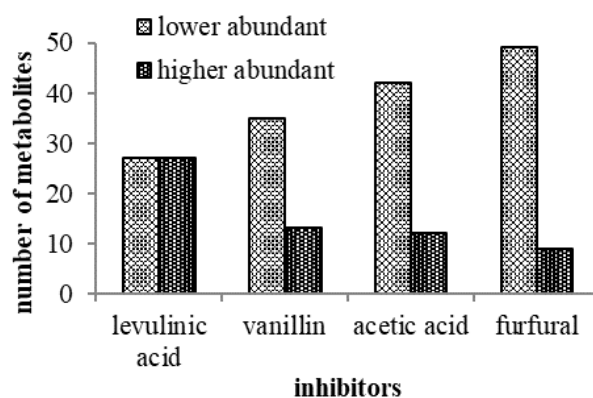
398

399 **Fig. 6** Principal component analysis (PCA) score plots of metabolic profiles in *P. taiwanensis*
400 VLB120 under the treatment of multiple inhibitors. Abbreviations: furfural (Fur), vanillin
401 (Van), levulinic acid (Lev), acetic acid (Ac) and control (Con).

402 Nucleotide monophosphates (e.g. AMP) had high impact on separating the samples treated
403 with acetic acid from the remaining groups. This can be attributed to the requirement of ATP
404 to convert acetate to acetyl-CoA which results in production of AMP. The observed low
405 intracellular concentration of acetyl-CoA might be mainly related to its utilization via the
406 TCA cycle to regenerate ATP [68, 69].

407 As shown in Fig. 7, the number of metabolites that showed significantly increased or
408 decreased levels during cultivation with levulinic acid was identical. However, the majority
409 of quantified metabolites exhibited lower concentrations compared to the control samples in

410 the presence of furfural, acetic acid and vanillin (Fig. 7). The concentration of some of the
411 metabolites were decreased more than two-fold in the presence of acetic acid (e.g. fructose
412 1,6-bisphosphate, 6-phospho gluconate and acetyl-CoA), furfural (e.g. adenine, inosine and
413 glutathione, oxidized), levulinic acid (e.g. AMP, IMP and adenine) and vanillin (e.g. AMP
414 and UDP glucuronate) in comparison to the control samples. This indicates that there was no
415 unique pattern of metabolic rearrangement in *P. taiwanensis* VLB120 to cope with the
416 exposure to inhibitory compounds.



417

418 **Fig. 7** Total number of metabolites that exhibited more than 20% change in abundance
419 compared to the control samples.

420 The mechanisms that lead to the observed change of intracellular concentrations of other
421 classes of metabolite (e.g. sugar phosphates, organic acids and amino acids) could be the
422 consequence of changes in cellular energetics and redox state of the cell. Metabolites
423 including ATP and NADPH are generally reported to have key functions in the survival of
424 any organism in a stressful environment [70, 71]. This is due to the fact that microorganisms
425 require both NADPH dependent detoxification and ATP-dependent efflux to cope with

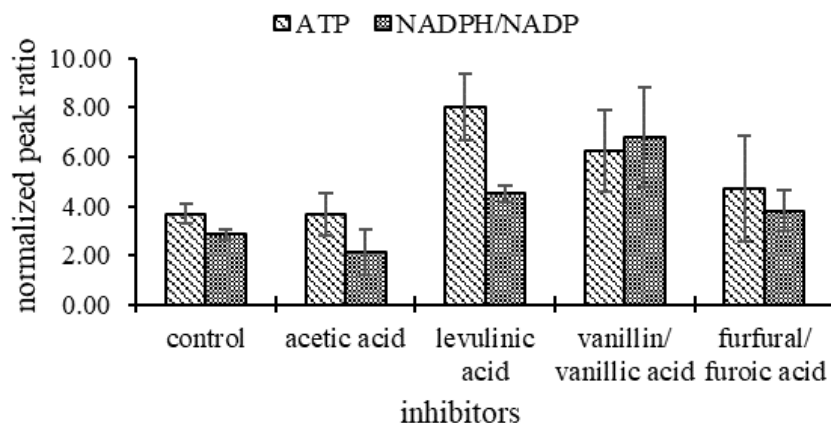
426 inhibitors [72]. Since those metabolites are a fundamental requirement for the maintenance
427 of metabolism, energy generation, and growth, their perturbations may induce widespread
428 changes in metabolism [70, 71, 73–79].

429 In order to investigate the role of cellular energetics and redox carrier metabolites in *P.*
430 *taiwanensis* VLB120 during growth with inhibitory compounds, the level of ATP and
431 NADPH/NADP ratio were determined in both control sample and samples treated with
432 inhibitors. Since several enzymes are regulated by the ratio between reduced and oxidized
433 co-factors [70], NADPH/NADP ratio was rather considered instead of absolute concentration
434 of NADPH.

435 At the time of sampling, the oxidation of vanillin and furfural to their corresponding acids
436 was still ongoing, while acetic acid was still being consumed from the medium. The
437 concentration of levulinic acid remained constant throughout the entire fermentation process.

438 As indicated in Fig. 8, the levels of ATP and the NADPH/NADP ratio (which was directly
439 correlated to the absolute concentration of NADPH) were markedly increased in the cells
440 treated with levulinic acid, vanillin and furfural compared to that of the control. The increased
441 level of ATP could be related to the bacterial cells generating more ATP in order to cope
442 with the efflux of inhibitors from the cell, especially in the case of levulinic acid which is not
443 converted and therefore remains present in the supernatant during cultivation. This indicates
444 that levulinic acid can enter the cytoplasm, and therefore cells treated with this inhibitory
445 compound might require more ATP than the cells treated with other inhibitors in order to
446 fuel the efflux pumps to remove the inhibitory compounds from the cytosol.

447 Similarly, the increased NADPH/NADP ratio provides reducing power to deal with the
 448 oxidative stress caused by the inhibitors[80]. This observation is in agreement with a previous
 449 study showing that *Pseudomonas fluorescens* produced high NADPH in order to cope with
 450 oxidative stress [79]. NADPH diminishes oxidative stress and provides the reductive
 451 environment necessary for cellular activities.[79] For instance, the production of ATP via
 452 oxidative phosphorylation cannot be effective in aerobic organisms growing under stress
 453 conditions unless there is a sufficient supply of NADPH providing a reductive environment
 454 [74, 75, 79]. In the presence of acetic acid, the NADPH/NADP ratio was slightly reduced,
 455 while the concentration of ATP remained unchanged, which was also in reasonable
 456 agreement with a previous study [81]. The observed minimal effect of acetic acid on those
 457 metabolites could be related to the direct utilization of acetate by *P. taiwanensis* as an
 458 additional carbon and energy source.



459

460 **Fig. 8** Effect of inhibitors on energy state and redox-carrier ratio of glucose-utilizing *P.*
 461 *taiwanensis* VLB120. The bars indicate the intracellular levels of ATP and the ratios of

462 NADPH/NADP based on normalized peak ratios (peak ratio is the height ratio between the
463 U ¹³C and ¹²C metabolites normalized to biomass).

464 Overall, there appeared to be a metabolic shift in *P. taiwanensis* to enhance the levels of ATP
465 and NADPH/NADP ratio in order to cope with the stress imposed by inhibitory compounds.
466 Thus, adequate supply of these metabolites are essential for the survival and reproduction of
467 *P. taiwanensis* in the presence of biomass derived inhibitors.

468 Cells grown with vanillin and furfural also exhibited increased ATP levels and an increased
469 NADPH/NADP ratio compared to the strain grown under control conditions without
470 inhibitory compounds added (Fig. 8).

471

472 **CONCLUSIONS**

473 In this study, the tolerance and metabolic responses of *P. taiwanensis* VLB120 to biomass
474 hydrolysate derived inhibitors was investigated. The overall results suggest that the tested
475 inhibitors affect *P. taiwanensis* VLB120 physiology in various ways with respect to lag-
476 phase, specific growth rate, and biomass yield. In order to overcome these effects,
477 *P. taiwanensis* VLB120 adopt different resistance mechanisms, including detoxification,
478 efflux and repair, which require additional cellular energy and resources. *P. taiwanensis*
479 VLB120 went through metabolic rearrangement to generate more ATP and NADPH to
480 mitigate the stress imposed by inhibitors.

481 In general, efficiently use of biomass hydrolysate as fermentation media requires
482 microorganism that can utilize both C6 and C5 sugars and are able to tolerate the inhibitory
483 compounds formed during the biomass pretreatment process. *P. taiwanensis* VLB120
484 showed high tolerance towards biomass hydrolysate derived inhibitors and efficiently utilizes
485 glucose, xylose and galactose as a carbon and energy source. This indicates that the
486 physiology of *P. taiwanensis* VLB120 matches the aforementioned basic requirements for
487 growth on biomass hydrolysates.

488

489 **DECLARATIONS**

490 **Ethics approval and consent to participate**

491 Not applicable

492 **Consent for publication**

493 Not applicable

494 **Availability of data and materials**

495 All data generated or analyzed during this study are included within the article and additional file.

496 **Competing interests**

497 The authors declare that they have no competing interests.

498 **Funding**

499 This research was funded by the ERA-NET SynBio/Innovations fonden and the Novo Nordisk
500 Foundation.

501 **Authors' contributions**

502 MK and KS supervised and guided the study, and were involved in scientific discussions.
503 GW and KS designed experiments and interpreted the data. GW carried out and analyzed the
504 experiments. GW, MK and KS wrote the manuscript. All authors read and approved the final
505 manuscript.

506 **Acknowledgements**

507 We thank Prof. Dr. Andreas Schmid (Department of Solar Materials, The Helmholtz-Center
508 for Environmental Research, UFZ, Germany) for supplying *P. taiwanensis* VLB120 strain.
509 We also thank Yasin Yildiz Dastan for his help during fermentation setup.

510 **Authors' information**

511 ¹Novo Nordisk Foundation Center for Biosustainability, Technical University of Denmark, DK-2800
512 Lyngby, Denmark

513

514 **REFERENCES**

- 515 1. Sánchez C. Lignocellulosic residues: Biodegradation and bioconversion by fungi. *Biotechnol*
516 *Adv.* 2009;27:185–94. doi:10.1016/j.biotechadv.2008.11.001.
- 517 2. Almeida JRM, Modig T, Petersson A, Hähn-Hägerdal B, Lidén G, Gorwa-Grauslund MF.
518 Increased tolerance and conversion of inhibitors in lignocellulosic hydrolysates by *Saccharomyces*
519 *cerevisiae*. *J Chem Technol Biotechnol.* 2007;82:340–9.
- 520 3. Lieth H. Primary Production of the Major Vegetation Units of the World. 1975;;10–1.
- 521 4. Pérez J, Muñoz-Dorado J, De La Rubia T, Martínez J. Biodegradation and biological treatments
522 of cellulose, hemicellulose and lignin: An overview. *Int Microbiol.* 2002;5:53–63.
- 523 5. Kumar A, Gautam A, Dutt D. Biotechnological Transformation of Lignocellulosic Biomass in to
524 Industrial Products: An Overview. *Adv Biosci Biotechnol.* 2016;7:149–68.
525 doi:10.4236/abb.2016.73014.
- 526 6. Anwar Z, Gulfraz M, Irshad M. Agro-industrial lignocellulosic biomass a key to unlock the
527 future bio-energy: A brief review. *J Radiat Res Appl Sci.* 2014;7:163–73.
528 doi:10.1016/j.jrras.2014.02.003.
- 529 7. E. AA, D. M-C. Oyster mushrooms (*Pleurotus*) are useful for utilizing lignocellulosic biomass.
530 *African J Biotechnol.* 2015;14:52–67. doi:10.5897/AJB2014.14249.
- 531 8. Zhang J, Choi YS, Yoo CG, Kim TH, Brown RC, Shanks BH. Cellulose – Hemicellulose and
532 Cellulose – Lignin Interactions during Fast Pyrolysis. 2015.
- 533 9. Weber C, Farwick A, Benisch F, Brat D, Dietz H, Subtil T, et al. Trends and challenges in the

- 534 microbial production of lignocellulosic bioalcohol fuels. *Appl Microbiol Biotechnol*.
535 2010;87:1303–15.
- 536 10. Khattab SMR, Saimura M, Kodaki T. Boost in bioethanol production using recombinant
537 *Saccharomyces cerevisiae* with mutated strictly NADPH-dependent xylose reductase and NADP+-
538 dependent xylitol dehydrogenase. *J Biotechnol*. 2013;165:153–6. doi:10.1016/j.jbiotec.2013.03.009.
- 539 11. Svetlitchnyi VA, Kensch O, Falkenhan DA, Korseska SG, Lippert N, Prinz M, et al. Single-step
540 ethanol production from lignocellulose using novel extremely thermophilic bacteria. *Biotechnol*
541 *Biofuels*. 2013;6:31. doi:10.1186/1754-6834-6-31.
- 542 12. Köhler KAK, Blank LM, Frick O, Schmid A. D-Xylose assimilation via the Weimberg pathway
543 by solvent-tolerant *Pseudomonas taiwanensis* VLB120. *Environ Microbiol*. 2015;17:156–70.
- 544 13. Isikgor FH, Becer CR. Lignocellulosic biomass: a sustainable platform for the production of
545 bio-based chemicals and polymers. *Polym Chem*. 2015;6:4497–559. doi:10.1039/C5PY00263J.
- 546 14. Wordofa G. Effect of thermal pretreatment on chemical composition and biogas production
547 from kitchen waste. 2014;:37.
- 548 15. Alvira P, Tomas-Pejo E, Ballesteros M, Negro MJ. Pretreatment technologies for an efficient
549 bioethanol production process based on enzymatic hydrolysis: A review. *Bioresour Technol*.
550 2010;101:4851–61. doi:10.1016/j.biortech.2009.11.093.
- 551 16. Sun Y, Cheng J. Hydrolysis of lignocellulosic materials for ethanol production : a review q.
552 *Bioresour Technol*. 2002;83:1–11. doi:10.1016/S0960-8524(01)00212-7.
- 553 17. Jansson LJ, Martin C. Pretreatment of lignocellulose: Formation of inhibitory by-products and
554 strategies for minimizing their effects. *Bioresour Technol*. 2016;199:103–12.

- 555 18. Galbe M, Zacchi G. Pretreatment of lignocellulosic materials for efficient bioethanol
556 production. *Adv Biochem Eng Biotechnol.* 2007;108 July:41–65.
- 557 19. Palmqvist E, Hahn-Hägerdal B. Fermentation of lignocellulosic hydrolysates. I: Inhibition and
558 detoxification. *Bioresour Technol.* 2000;74:17–24.
- 559 20. Liu X, Xu W, Mao L, Zhang C, Yan P, Xu Z, et al. Lignocellulosic ethanol production by
560 starch-base industrial yeast under PEG detoxification. *Sci Rep.* 2016;6:20361.
561 doi:10.1038/srep20361.
- 562 21. Fillat Ú, Ibarra D, Eugenio M, Moreno A, Tomás-Pejó E, Martín-Sampedro R. Laccases as a
563 Potential Tool for the Efficient Conversion of Lignocellulosic Biomass: A Review. *Fermentation.*
564 2017;3:17. doi:10.3390/fermentation3020017.
- 565 22. Moreno AD, Alvira P, Ibarra D, Tomás-pejó E. Production of Platform Chemicals from
566 Sustainable Resources. 2017. doi:10.1007/978-981-10-4172-3.
- 567 23. Dunlop A.P. Furfural formation and behaviour. *Ind Eng Chem.* 1948;40:204–9.
- 568 24. Ulbricht RJ, Northup SJ, Thomas JA. A review of 5-hydroxymethylfurfural (HMF) in parenteral
569 solutions. *Toxicol Sci.* 1984;4:843–53.
- 570 25. Mills TY, Sandoval NR, Gill RT. Cellulosic hydrolysate toxicity and tolerance mechanisms in
571 *Escherichia coli*. *Biotechnol Biofuels.* 2009;2:26. doi:10.1186/1754-6834-2-26.
- 572 26. Nichols NN, Sharma LN, Mowery RA, Chambliss CK, van Walsum GP, Dien BS, et al. Fungal
573 metabolism of fermentation inhibitors present in corn stover dilute acid hydrolysate. *Enzyme*
574 *Microb Technol.* 2008;42:624–30.

- 575 27. Fiehn O. Metabolomics - The link between genotypes and phenotypes. *Plant Mol Biol.*
576 2002;48:155–71.
- 577 28. Teoh ST, Putri S, Mukai Y, Bamba T, Fukusaki E. A metabolomics-based strategy for
578 identification of gene targets for phenotype improvement and its application to 1-butanol tolerance
579 in *Saccharomyces cerevisiae*. *Biotechnol Biofuels.* 2015;8:144. doi:10.1186/s13068-015-0330-z.
- 580 29. López MJ, Moreno J, Nichols NN, Dien BS, Bothast RJ. Isolation of microorganisms for
581 biological detoxification of lignocellulosic hydrolysates. *Appl Microbiol Biotechnol.* 2004;64:125–
582 31.
- 583 30. Volmer J, Neumann C, Bühler B, Schmid A. Engineering of *Pseudomonas taiwanensis* VLB120
584 for constitutive solvent tolerance and increased specific styrene epoxidation activity. *Appl Environ*
585 *Microbiol.* 2014;80:6539–48.
- 586 31. Hartmans S, Smits JP, Van der Werf MJ, Volkering F, De Bont JAM. Metabolism of styrene
587 oxide and 2-phenylethanol in the styrene-degrading *Xanthobacter* strain 124X. *Appl Environ*
588 *Microbiol.* 1989;55:2850–5.
- 589 32. Wordofa GG, Kristensen M, Schrübbers L, McCloskey D, Forster J, Schneider K. Quantifying
590 the metabolome of *Pseudomonas taiwanensis* VLB120: Evaluation of hot and cold combined
591 quenching/extraction approaches. *Anal Chem.* 2017;;:acs.analchem.7b00793.
592 doi:10.1021/acs.analchem.7b00793.
- 593 33. McCloskey D, Utrilla J, Naviaux RK, Palsson BO, Feist AM. Fast Swinnex filtration (FSF): a
594 fast and robust sampling and extraction method suitable for metabolomics analysis of cultures
595 grown in complex media. *Metabolomics.* 2014;:198–209.

- 596 34. Wu L, Mashego MR, Van Dam JC, Proell AM, Vinke JL, Ras C, et al. Quantitative analysis of
597 the microbial metabolome by isotope dilution mass spectrometry using uniformly ¹³C-labeled cell
598 extracts as internal standards. *Anal Biochem.* 2005;336:164–71.
- 599 35. Mashego MR, Wu L, Van Dam JC, Ras C, Vinke JL, Van Winden WA, et al. MIRACLE: Mass
600 Isotopomer Ratio Analysis of U-¹³C-Labeled Extracts. A New Method for Accurate Quantification
601 of Changes in Concentrations of Intracellular Metabolites. *Biotechnol Bioeng.* 2004;85:620–8.
- 602 36. R Development Core Team R. R: A Language and Environment for Statistical Computing.
603 2011. doi:10.1007/978-3-540-74686-7.
- 604 37. Zaldivar J, Nielsen J, Olsson L. Fuel ethanol production from lignocellulose: A challenge for
605 metabolic engineering and process integration. *Appl Microbiol Biotechnol.* 2001;56:17–34.
- 606 38. Nieves LM, Panyon LA, Wang X. Engineering Sugar Utilization and Microbial Tolerance
607 toward Lignocellulose Conversion. *Front Bioeng Biotechnol.* 2015;3 February:17.
608 doi:10.3389/fbioe.2015.00017.
- 609 39. Dien BS, Iten L, Bothast RJ. Conversion of corn fiber to ethanol by recombinant *E. coli* strain
610 FBR3. *J Ind Microbiol Biotechnol.* 1999;22:575–81. doi:10.1038/sj.jim.2900628.
- 611 40. Han JH, Park JY, Yoo KS, Kang HW, Choi GW, Chung BW, et al. Effect of glucose on xylose
612 utilization in *Saccharomyces cerevisiae* harboring the xylose reductase gene. *Arch Microbiol.*
613 2011;193:335–40.
- 614 41. Yanase H, Miyawaki H, Sakurai M, Kawakami A, Matsumoto M, Haga K, et al. Ethanol
615 production from wood hydrolysate using genetically engineered *Zymomonas mobilis*. *Appl*
616 *Microbiol Biotechnol.* 2012;94:1667–78.

- 617 42. Xia T, Eiteman MA, Altman E. Simultaneous utilization of glucose, xylose and arabinose in the
618 presence of acetate by a consortium of *Escherichia coli* strains. *Microb Cell Fact.* 2012;11:77.
619 doi:10.1186/1475-2859-11-77.
- 620 43. Runquist D, Hahn-Hägerdal B, Rådström P. Comparison of heterologous xylose transporters in
621 recombinant *Saccharomyces cerevisiae*. *Biotechnol Biofuels.* 2010;3:5. doi:10.1186/1754-6834-3-
622 5.
- 623 44. Zha Y, Muilwijk B, Coulier L. Inhibitory Compounds in Lignocellulosic Biomass Hydrolysates
624 during Hydrolysate Fermentation Processes. *J Bioprocess Biotech.* 2012;2:1–11.
- 625 45. Wang W, Yang S, Hunsinger GB, Pienkos PT, Johnson DK. Connecting lignin-degradation
626 pathway with pre-treatment inhibitor sensitivity of *Cupriavidus necator*. *Front Microbiol.* 2014;5
627 MAY:1–10.
- 628 46. Franden MA, Pilath HM, Mohagheghi A, Pienkos PT, Zhang M. Inhibition of growth of
629 *Zymomonas mobilis* by model compounds found in lignocellulosic hydrolysates. *Biotechnol*
630 *Biofuels.* 2013;6:1. doi:10.1186/1754-6834-6-99.
- 631 47. Clarkson SM, Hamilton-Brehm SD, Giannone RJ, Engle NL, Tschapinski TJ, Hettich RL, et al.
632 A comparative multidimensional LC-MS proteomic analysis reveals mechanisms for furan aldehyde
633 detoxification in *Thermoanaerobacter pseudethanolicus* 39E. *Biotechnol Biofuels.* 2014;7:165.
634 doi:10.1186/s13068-014-0165-z.
- 635 48. Bischoff KM, Liu S, Hughes SR, Rich JO. Fermentation of corn fiber hydrolysate to lactic acid
636 by the moderate *thermophile Bacillus coagulans*. *Biotechnol Lett.* 2010;32:823–8.
- 637 49. Delgenes JP, Moletta R, Navarro JM. Effects of lignocellulose degradation products on ethanol

638 fermentations of glucose and xylose by *Saccharomyces cerevisiae*, *Zymomonas mobilis*, *Pichia*
639 *stipitis*, and *Candida shehatae*. *Enzyme Microb Technol.* 1996;19:220–5.

640 50. Klinke HB, Thomsen AB, Ahring BK. Inhibition of ethanol-producing yeast and bacteria by
641 degradation products produced during pre-treatment of biomass. *Appl Microbiol Biotechnol.*
642 2004;66:10–26.

643 51. Wierckx N, Koopman F, Bandounas L, De Winde JH, Ruijsenaars HJ. Isolation and
644 characterization of *Cupriavidus basilensis* HMF14 for biological removal of inhibitors from
645 lignocellulosic hydrolysate. *Microb Biotechnol.* 2010;3:336–43.

646 52. Zaldivar J, Martinez A, Ingram LO. Effect of selected aldehydes on the growth and
647 fermentation of ethanologenic *Escherichia coli*. *Biotechnol Bioeng.* 1999;65:24–33.

648 53. Booth IR, Ferguson GP, Miller S, Li C, Gunasekera B, Kinghorn S. Bacterial production of
649 methylglyoxal: a survival strategy or death by misadventure? *Biochem Soc Trans.* 2003;31 Pt
650 6:1406–8.

651 54. Herring CD, Blattner FR. Global transcriptional effects of a suppressor tRNA and the
652 inactivation of the regulator frmR. *J Bacteriol.* 2004;186:6714–20.

653 55. Marx CJ, Miller J a, Lidstrom ME, Chistoserdova L. Multiple Formaldehyde Oxidation /
654 Detoxification Pathways in *Burkholderia fungorum* LB400 Multiple Formaldehyde Oxidation /
655 Detoxification Pathways in *Burkholderia fungorum* LB400. 2004;186:2173–8.

656 56. Jarboe LR. YqhD: A broad-substrate range aldehyde reductase with various applications in
657 production of biorenewable fuels and chemicals. *Appl Microbiol Biotechnol.* 2011;89:249–57.

658 57. Zhang S, Winstrand S, Chen L, Li D, Jonsson LJ, Hong F. Tolerance of the nanocellulose-

659 producing bacterium *gluconacetobacter xylinus* to lignocellulose-derived acids and aldehydes. J
660 Agric Food Chem. 2014;62:9792–9.

661 58. Zaldivar J, Martinez A, Ingram LO. Effect of alcohol compounds found in hemicellulose
662 hydrolysate on the growth and fermentation of ethanologenic *Escherichia coli*. Biotechnol Bioeng.
663 2000;68:524–30.

664 59. Mohan K., Phale P. Carbon Source-Dependent Inducible Metabolism of Veratryl Alcohol and
665 Ferulic Acid in *Pseudomonas putida* CSV86. Appl Environ Microbiol. 2017;83:1–12.

666 60. Álvarez-Rodríguez ML, Belloch C, Villa M, Uruburu F, Larriba G, Coque JJR. Degradation of
667 vanillic acid and production of guaiacol by microorganisms isolated from cork samples. FEMS
668 Microbiol Lett. 2003;220:49–55.

669 61. Eilers FI, Sussman AS. Conversion of furfural to furoic acid and furfuryl alcohol by *Neurospora*
670 *ascospores*. Planta. 1970;94:253–64.

671 62. Klinke HB, Olsson L, Thomsen AB, Ahring BK. Potential inhibitors from wet oxidation of
672 wheat straw and their effect on ethanol production of *Saccharomyces cerevisiae*: wet oxidation and
673 fermentation by yeast. Biotechnol Bioeng. 2003;81:738–47. doi:10.1002/bit.10523.

674 63. B. H-H. Detoxification of wood hydrolysate with laccase and peroxidase from the white-rot
675 fungus *T. versicolor*. Appl Microb Biotechnol. 1998;49:691.

676 64. Larsson S, Quintana-Sáinz A, Reimann A, Nilvebrant NO, Jönsson LJ. Influence of
677 lignocellulose-derived aromatic compounds on oxygen-limited growth and ethanolic fermentation
678 by *Saccharomyces cerevisiae*. Appl Biochem Biotechnol. 2000;84–86:617–32.
679 doi:10.1385/ABAB:84-86:1-9:617.

680 65. Matano C, Meiswinkel TM, Wendisch VF. Amino Acid Production from Rice Straw
681 Hydrolyzates. Elsevier; 2014. doi:10.1016/B978-0-12-401716-0.00038-6.

682 66. Suko AV, Bura R. Enhanced Xylitol and Ethanol Yields by Fermentation Inhibitors in Steam-
683 Pretreated Lignocellulosic Biomass. *Ind Biotechnol*. 2016;12:187–94.

684 67. Guo Z, Olsson L. Physiological response of *Saccharomyces cerevisiae* to weak acids present in
685 lignocellulosic hydrolysate. *FEMS Yeast Res*. 2014;14:1234–48.

686 68. Bräsen C, Schönheit P. Regulation of acetate and acetyl-CoA converting enzymes during
687 growth on acetate and/or glucose in the halophilic archaeon *Haloarcula marismortui*. *FEMS*
688 *Microbiol Lett*. 2004;241:21–6.

689 69. Liang M-H, Qv X-Y, Jin H-H, Jiang J-G. Characterization and expression of AMP-forming
690 Acetyl-CoA Synthetase from *Dunaliella tertiolecta* and its response to nitrogen starvation stress.
691 *Sci Rep*. 2016;6:23445. doi:10.1038/srep23445.

692 70. Ask M, Bettiga M, Mapelli V, Olsson L. The influence of HMF and furfural on redox-balance
693 and energy-state of xylose-utilizing *Saccharomyces cerevisiae*. *Biotechnol Biofuels*. 2013;6:22.
694 doi:10.1186/1754-6834-6-22.

695 71. Messaoudi N, Gautier V, Dairou J, Mihoub M, Lelandais G, Bouloc P, et al. Fermentation and
696 alternative respiration compensate for NADH dehydrogenase deficiency in a prokaryotic model of
697 DJ-1-associated Parkinsonism. *Microbiol (United Kingdom)*. 2015;161:2220–31.

698 72. Piotrowski JS, Zhang Y, Bates DM, Keating DH, Sato TK, Ong IM, et al. Death by a thousand
699 cuts: The challenges and diverse landscape of lignocellulosic hydrolysate inhibitors. *Front*
700 *Microbiol*. 2014;5 MAR:1–8.

701 73. Bloem A, Sanchez I, Dequin S, Camarasa C. Metabolic impact of redox cofactor perturbations
702 on the formation of aroma compounds in *Saccharomyces cerevisiae*. Appl Environ Microbiol.
703 2016;82:174–83.

704 74. Jo SH, Son MK, Koh HJ, Lee SM, Song IH, Kim YO, et al. Control of Mitochondrial Redox
705 Balance and Cellular Defense against Oxidative Damage by Mitochondrial NADP⁺-dependent
706 Isocitrate Dehydrogenase. J Biol Chem. 2001;276:16168–76.

707 75. Rydström J. Mitochondrial transhydrogenase - a key enzyme in insulin secretion and,
708 potentially, diabetes. Trends Biochem Sci. 2006;31:355–8.

709 76. Chai MF, Chen QJ, An R, Chen YM, Chen J, Wang XC. NADK2, an *Arabidopsis* chloroplastic
710 NAD kinase, plays a vital role in both chlorophyll synthesis and chloroplast protection. Plant Mol
711 Biol. 2005;59:553–64.

712 77. Grose JH, Joss L, Velick SF, Roth JR. Evidence that feedback inhibition of NAD kinase
713 controls responses to oxidative stress. Proc Natl Acad Sci U S A. 2006;103:7601–6.
714 doi:10.1073/pnas.0602494103.

715 78. Sakuraba H, Kawakami R, Ohshima T. First Archaeal Inorganic Polyphosphate / ATP-
716 Dependent NAD Kinase , from Hyperthermophilic Archaeon *Pyrococcus horikoshii* : Cloning ,
717 Expression , and Characterization. 2005;71:4352–8.

718 79. Singh R, Mailloux RJ, Puiseux-Dao S, Appanna VD. Oxidative stress evokes a metabolic
719 adaptation that favors increased NADPH synthesis and decreased NADH production in
720 *Pseudomonas fluorescens*. J Bacteriol. 2007;189:6665–75.

721 80. Hara M, Matsuura T, Kojima S. Innovative Medicine. 2015. doi:10.1007/978-4-431-55651-0.

722 81. Guo W, Chen Y, Wei N, Feng X. Investigate the metabolic reprogramming of *Saccharomyces*
723 *cerevisiae* for enhanced resistance to mixed fermentation inhibitors via 13C metabolic flux analysis.
724 PLoS One. 2016;11:1–15.

725

Supporting Information for Publication

Tolerance and Metabolic Response of *Pseudomonas taiwanensis* VLB120 towards Biomass Hydrolysate Derived Inhibitors

Gossa G. Wordofa[†], Mette Kristensen[†] and Konstantin Schneider^{*†}

[†] Novo Nordisk Foundation Center for Biosustainability, Technical University of Denmark, DK-2800 Lyngby, Denmark

Corresponding Author

*Phone: +45 30569850. Email: kosc@biosustain.dtu.dk

Additional file 1: Fig. S1

Evaluation of different carbon sources for growth by *P. taiwanensis* VLB120

Additional file 1: Fig. S2

Effect of biomass hydrolysate derived inhibitors on *P. taiwanensis* VLB120

Additional file 1: Fig. S3

Degradation capacity of biomass hydrolysate derived inhibitors by *P. taiwanensis* VLB120

Additional file 1: Fig. S4

Impact of inhibitory compounds on specific glucose uptake rate

Additional file 1: Fig. S5

Venn diagram

Additional file 1: Fig. S6

PCA loading plot

Additional file 1: Fig. S7

Heat map based on intracellular metabolites data

1. Evaluation of different carbon sources for growth by *P. taiwanensis* VLB120

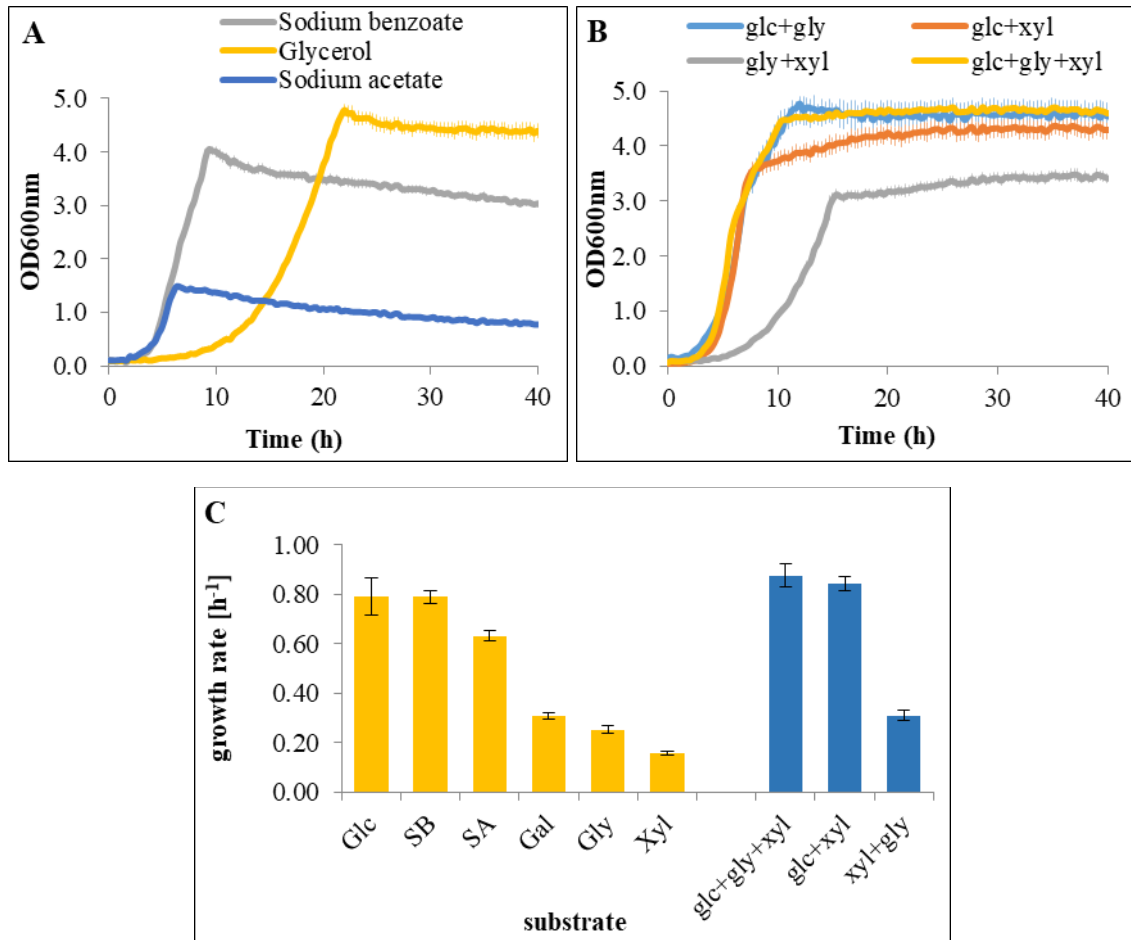


Fig. S1 Growth profile of *P. taiwanensis* VLB120 in different carbon source (A) and mixed carbon sources (B). Growth rate (C) was calculated from growth curves. Aerobic cultivations were carried out in 24-well clear bottom microplate (EnzyScreen, Heemstede, The Netherlands) working volume 750 μL at 30 $^{\circ}\text{C}$, 225 rpm. Error bars are the standard deviation of three biological replicate cultures. Abbreviations: glucose (glc), sodium benzoate (SB), sodium acetate (SA), galactose (gal), glycerol (gly) and xylose (xyl).

2. Effect of biomass hydrolysate derived inhibitors on *P. taiwanensis* VLB120

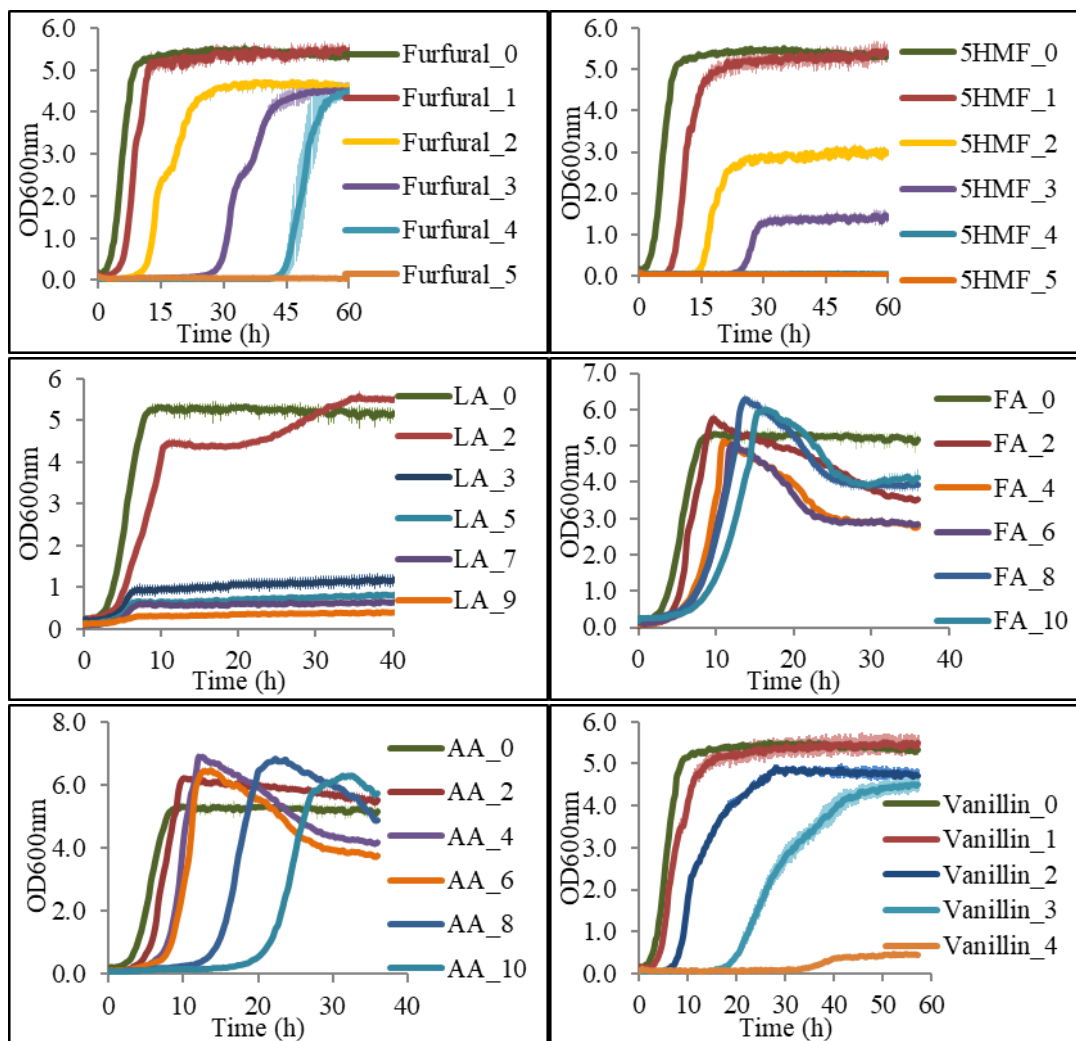


Fig. S2 Growth curve of *P. taiwanensis* VLB120 in the presence of furfural, 5-HMF, levulinic acid, formic acid, acetic acid and vanillin. Aerobic cultivations were carried out in 24-well clear bottom microplate (EnzyScreen, Heemstede, The Netherlands) working volume 750 μL at 30 $^{\circ}\text{C}$, 225 rpm. Concentration: [g L^{-1}]. Error bars are the standard deviation of three biological replicate cultures.

3. Degradation capacity of biomass hydrolysate derived inhibitors by *P. taiwanensis* VLB120

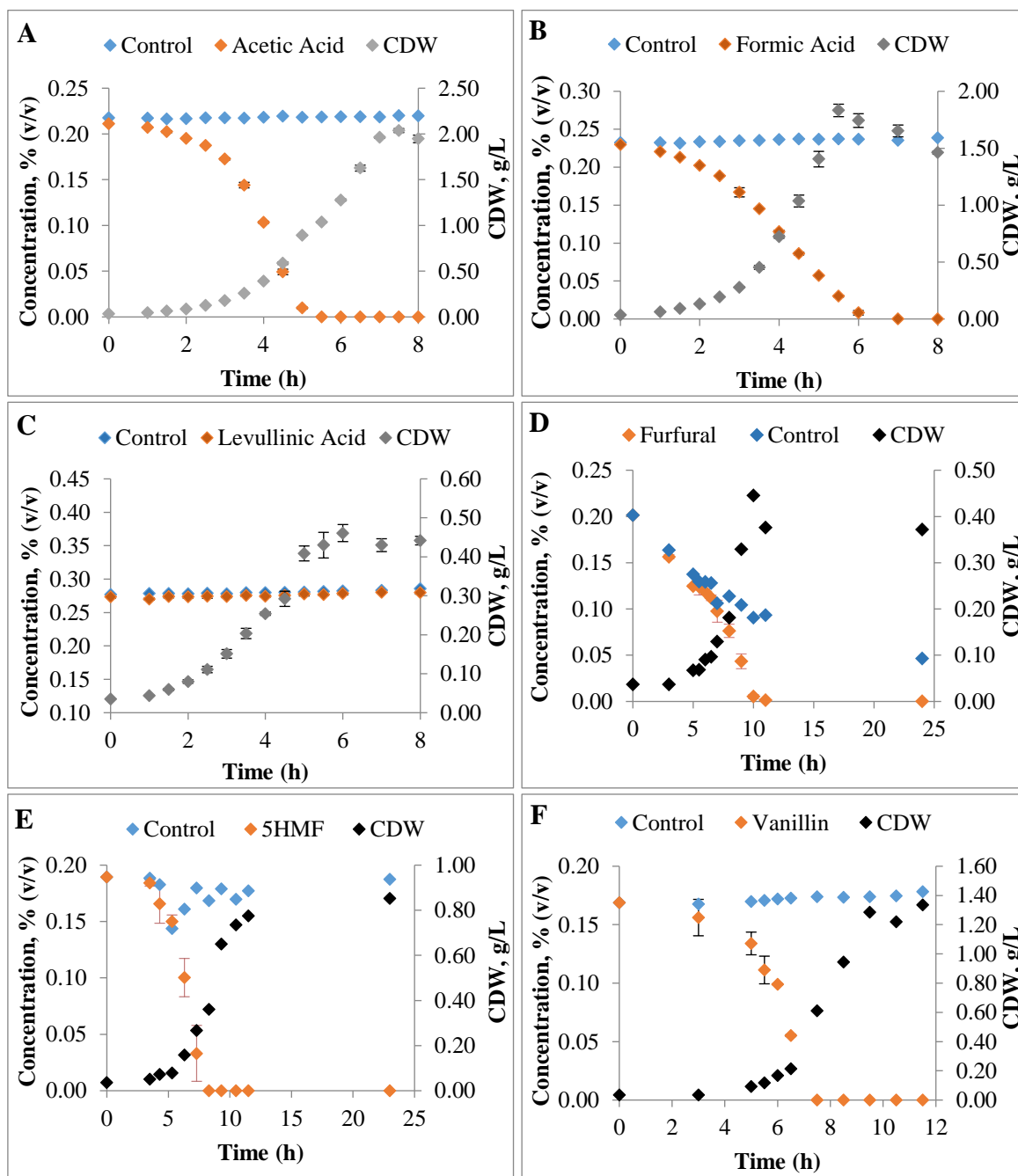


Fig. S3 Degradation capacity of acetic acid (A), formic acid (B), levulinic acid (C), furfural (D), 5-HMF (E) and vanillin (F) by *P. taiwanensis* VLB120 grown on minimal medium supplemented with 4.5 g L⁻¹ of glucose. Cultivations were carried out in 250 mL shake flask (working volume 25 mL) at 30 °C, 250 rpm.

4. Impact of inhibitory compounds on specific glucose uptake rate

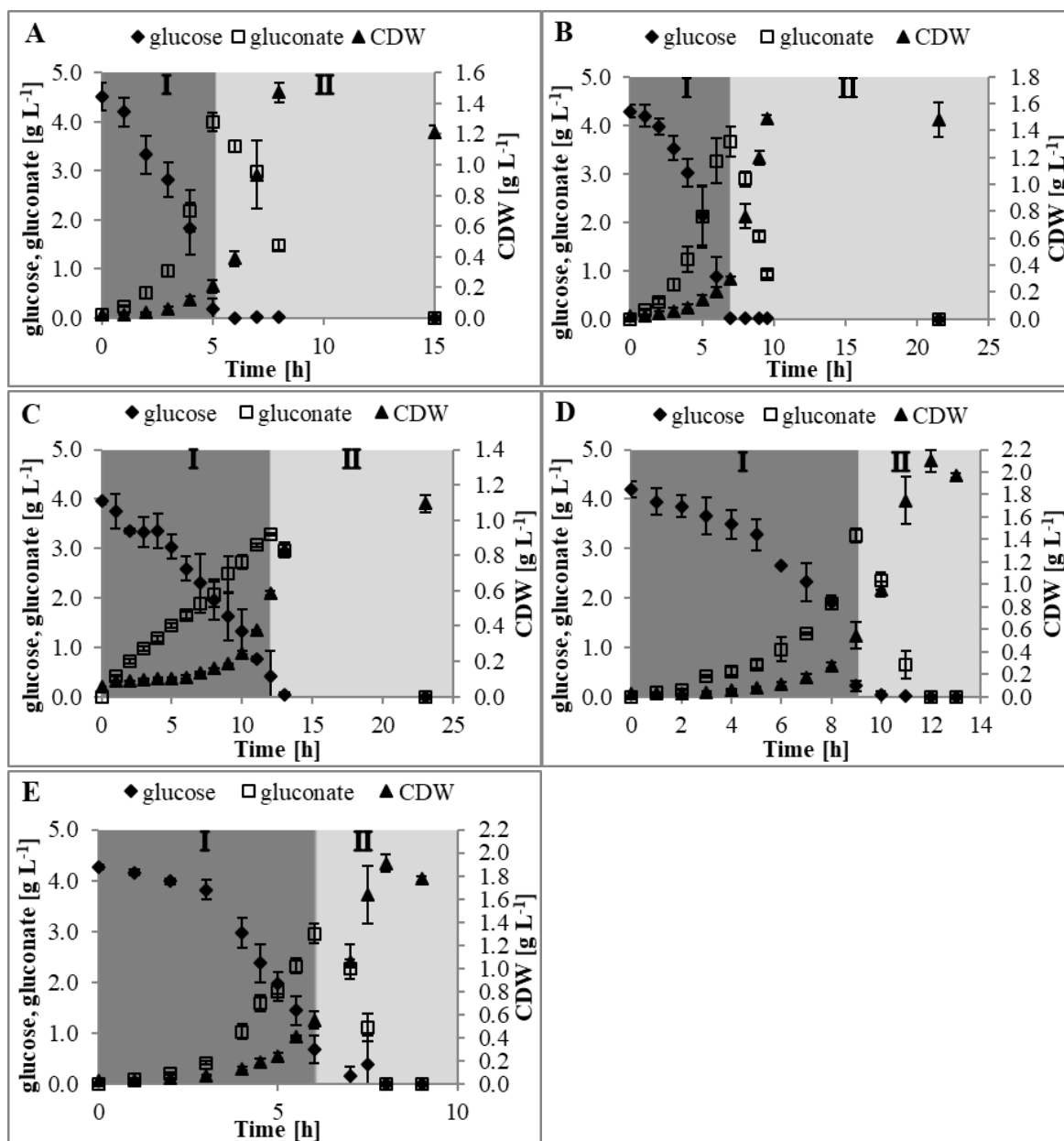


Fig. S4 Growth of *P. taiwanensis* VLB120 in minimal media supplemented with 4 g L⁻¹ of glucose in the presence of 2 g L⁻¹ acetic acid (A), levulinic acid (B), furfural (C), or vanillin (D) and in the absence of inhibitory compound (E). The experiments were performed in 1.3-L bioreactors (SARTORIOUS ®) with 0.5 L working volume. The temperature, stirrer speed and pH were set at 30 °C, 800 rpm and 7.0, respectively. Cultures were supplied with air at a flow rate of 1 slpm, and minimum dissolved oxygen saturation level was 40%. Error bars indicate standard deviations of three independent cultures. CDW, cell dry weight. (I) glucose phase, (II) gluconate phase.

5. Venn diagram

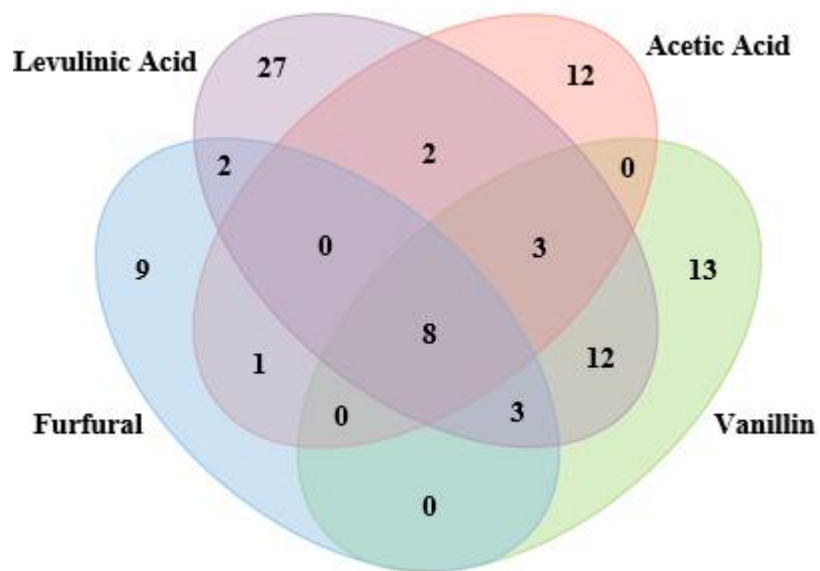


Fig. S5 Venn diagram illustrating number of significantly (>20%) increased metabolites that overlap between different conditions.

6. PCA loading plot

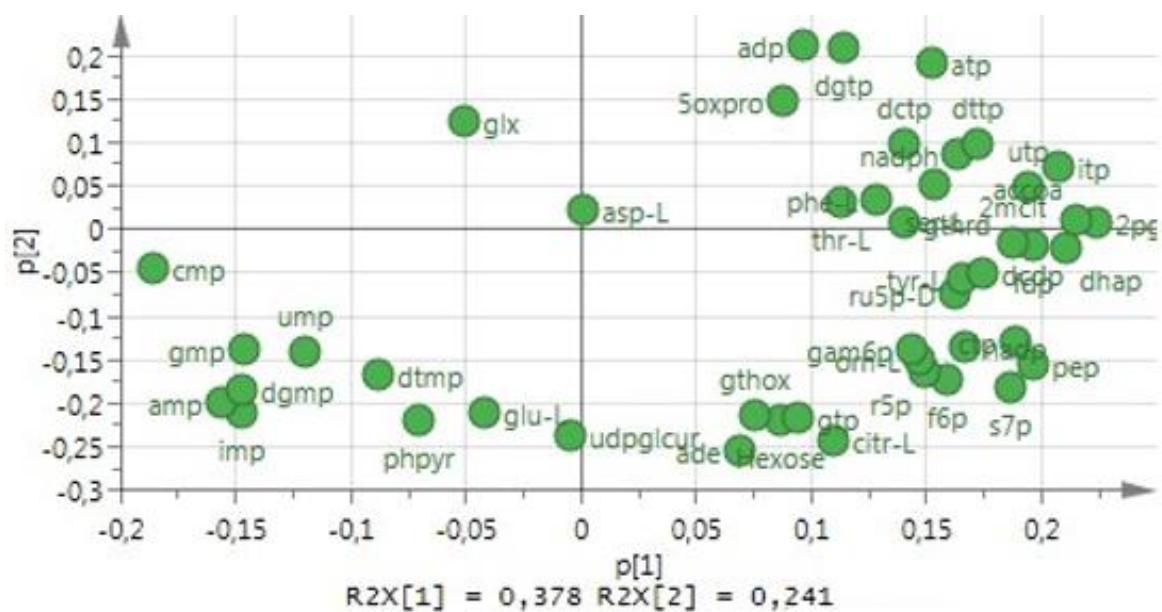


Fig. S6 Score plots of principal component analysis (PCA) of *P. taiwanensis* VLB120 metabolites under various inhibitory test.

7. Heat map based on intracellular metabolites data

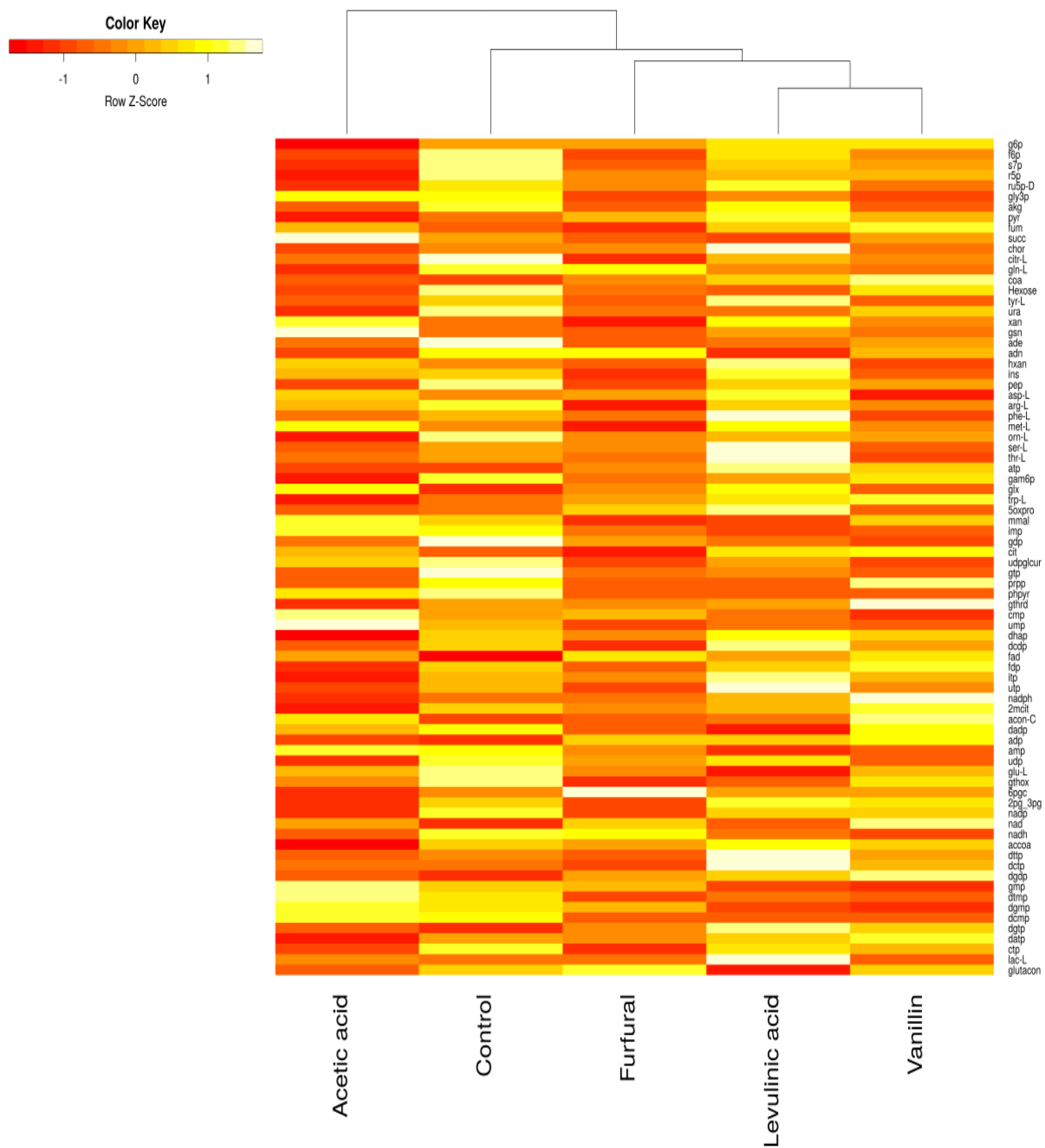


Fig. S7 Heatmap of metabolites extracted from *P. taiwanensis* VLB120 under different stress conditions. Metabolites abundance differences were clustered according to trends measured across all biological replicates (n = 3).